NASA
Technical
Paper
3398

April 1994

Physical and Mechanical Metallurgy of NiAl

Ronald D. Noebe,
Randy R. Bowman,
and Michael V. Nathal

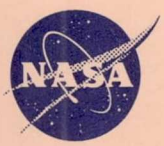

National Aeronautics and
Space Administration

NASA Technical Paper 3398

1994

Physical and Mechanical Metallurgy of NiAl

Ronald D. Noebe, Randy R. Bowman, and Michael V. Nathal
NASA Lewis Research Center
Cleveland, Ohio

National Aeronautics and Space Administration

Office of Management

Scientific and Technical Information Program

Contents

Summary

Considerable research has been performed on NiAl over the last decade, with an exponential increase in effort occurring over the last few years. This is due to interest in this material for electronic, catalytic, coating, and especially high-temperature structural applications. This report uses this wealth of new information to develop a comprehensive description of the properties and processing of NiAl and NiAl-based materials. Emphasis is placed on the controlling fracture and deformation mechanisms of single and polycrystalline NiAl and its alloys over the entire range of temperatures for which data are available. Creep, fatigue, and environmental resistance of this material are discussed. In addition, issues surrounding alloy design, development of NiAl-based composites, and materials processing are addressed.

1. Introduction

As with many intermetallic alloys, NiAl was originally studied as a potential structural material because of its high melting temperature, hardness, and chemical stability. Early investigations were exploratory in nature, designed to determine whether NiAl held promise as a high-temperature refractory compound (Wachtell 1952). These were followed by studies in the early 1960's that concentrated on the effects of processing and other metallurgical variables on mechanical behavior (Wood et al. 1960 to 1964). By the mid-1960's NiAl was identified as a possible leading-edge material for a superalloy turbine vane. However, no solution was found for the low-temperature brittleness of this compound, and by the end of the 1960's government and industrial interest in NiAl had faded. At this point, research shifted primarily to universities; between 1970 and the mid-1980's, there was a very small, but steady, effort to investigate the oxidation behavior, mechanical properties, and deformation mechanisms of NiAl.

Then, in the mid to late 1980's, research on NiAl exploded on several fronts. The physics/surface science community became intrigued with the surface properties and catalytic behavior of NiAl. This work was motivated by the fact that NiAl is one of the few intermetallic systems known to have a stable, well-defined surface structure on an atomic level (Franchy, Wuttig, and Ibach 1987; Castro et al. 1991). Because of NiAl's high melting point, excellent thermal stability, and serendipitous lattice match with GaAs compounds, the electronics industry began to take a serious look at using NiAl as a buried interconnect in electronic components (Sands 1988; Chambers and Loebs 1990; Joo et al. 1992). Also, research on NiAl is again centered on its possible use as a high-temperature structural material. The renewed driving forces for this general application have been generic government aeropropulsion programs (Stephens 1988; Doychak 1992) and industrial development of NiAl as a turbine engine material (Darolia 1991; Darolia et al. 1992).

Current researchers face the same problems that hindered widespread acceptance of NiAl as a structural material in the early 1960's: namely, poor creep resistance and inadequate low-temperature toughness and ductility. However, these barriers are disappearing as the properties of NiAl and our understanding of its behavior improve.

This report reviews the physical and mechanical metallurgy of NiAl-based materials, concentrating on the effects of processing, alloying, and microstructural modification on behavior. Directions for improving low-temperature toughness and ductility are described, and successful strategies for enhancing creep resistance are reviewed. References are made primarily to the most recent studies in each area because in-depth reviews of the NiAl literature have recently been published (Noebe, Bowman, and Nathal 1993; Miracle 1993). All alloy compositions are given in atomic percent.

2. Physical Metallurgy

NiAl is an ordered intermetallic compound that crystallizes in a primitive cubic CsCl structure that exists over the composition range of 45 to almost 60 at.% Ni. Although the phase diagram by Singleton, Murray, and Nash (1986) indicates that stoichiometric Ni-50Al melts congruently at 1911 K, more recent determinations place the melting temperature T_m of binary stoichiometric NiAl closer to 1955 K (Walston and Darolia 1993). The original lower value for T_m could be attributed to the steep dropoff in melting temperature with deviations from stoichiometry or to unintentional additions of ternary elements. NiAl not only has the highest melting temperature of any compound in the Ni-Al system but also is the most stable, as evident from its very large negative heat of formation—a maximum of -72 kJ/mol at the stoichiometric

composition (Henig and Lukas 1975). This high degree of thermodynamic stability and the existence of a wide phase field makes NiAl relatively easy to fabricate in a range of forms from fine homogeneous powders to single crystals.

Properties such as lattice parameter and density have been thoroughly studied as a method to infer the type of defect structure that occurs in the NiAl lattice, and consequently, significant data have been generated for these properties (fig. 1). Because Ni is a smaller, but heavier, atom than Al, increasing the Ni content by substituting Ni on Al sites should decrease the lattice parameter and increase the density, consistent with data for alloys containing greater than 50 at.% Ni (fig. 1). However, the behavior of Al-rich alloys does not continue to follow this trend. Instead, the lattice parameter decreases, and the decrease in density is more rapid than would be expected from the replacement of Ni atoms by Al. Consequently, the deviation in stoichiometry of Al-rich alloys is accommodated by the creation of vacancies on the Ni-lattice sites instead of by substitutional defects as in Ni-rich alloys. This process can result in extremely large numbers of constitutional vacancies. For example, a Ni-55Al intermetallic would contain a constitutional vacancy concentration of almost 10 percent.

Another property that has been extensively studied is the elastic behavior of NiAl. The single-crystal elastic constants for NiAl, which have been determined as a function of temperature, cooling rate (thermal vacancy concentration), and stoichiometry, have been summarized by Rusovic and Warlimont (1977). Overall, the elastic properties of NiAl are anisotropic, A = 3.28 (Wasilewski 1966), and the degree of anisotropy depends mildly on temperature and strongly on stoichiometry. Figure 2(a) shows the dynamic Young's modulus E for near-stoichiometric NiAl as a function of orientation—demonstrating the mild, but linear, dependence of temperature on modulus and the slightly decreasing anisotropy with increasing temperature. Good agreement exists between the temperature dependence of modulus for <100> crystals that was determined by Wasilewski in 1966 and by Walston and Darolia in 1993. Also, minor alloying additions have relatively little effect on the dynamic Young's modulus of <001> single crystals (Walston and Darolia 1993).

The elastic properties of polycrystalline NiAl have also been determined in some detail. Young's modulus is very dependent on processing technique and temperature but relatively insensitive to stoichiometry (Rusovic and Warlimont 1979; Harmouche and Wolfenden 1987; Moose 1991). The effect of processing route on the temperature dependence of the Young's modulus for near-stoichiometric NiAl is demonstrated in figure 2(b). Extrusion produces a material that has a higher modulus and a slightly different temperature dependence compared with materials produced from hot-pressed prealloyed powders or cast and homogenized ingots. By comparison with the single-crystal data, the effect of processing on Young's modulus can be rationalized in terms of crystallographic texture. The extruded material probably exhibits a preferred <111> orientation because this is the most commonly observed texture in extruded NiAl (Khadkikar, Michal, and Vedula 1990; Bieler et al. 1992). Cast or hot-pressed material would not be expected to have a strong preferred orientation and would, therefore, have a lower modulus in comparison to the higher modulus for <111>-oriented materials.

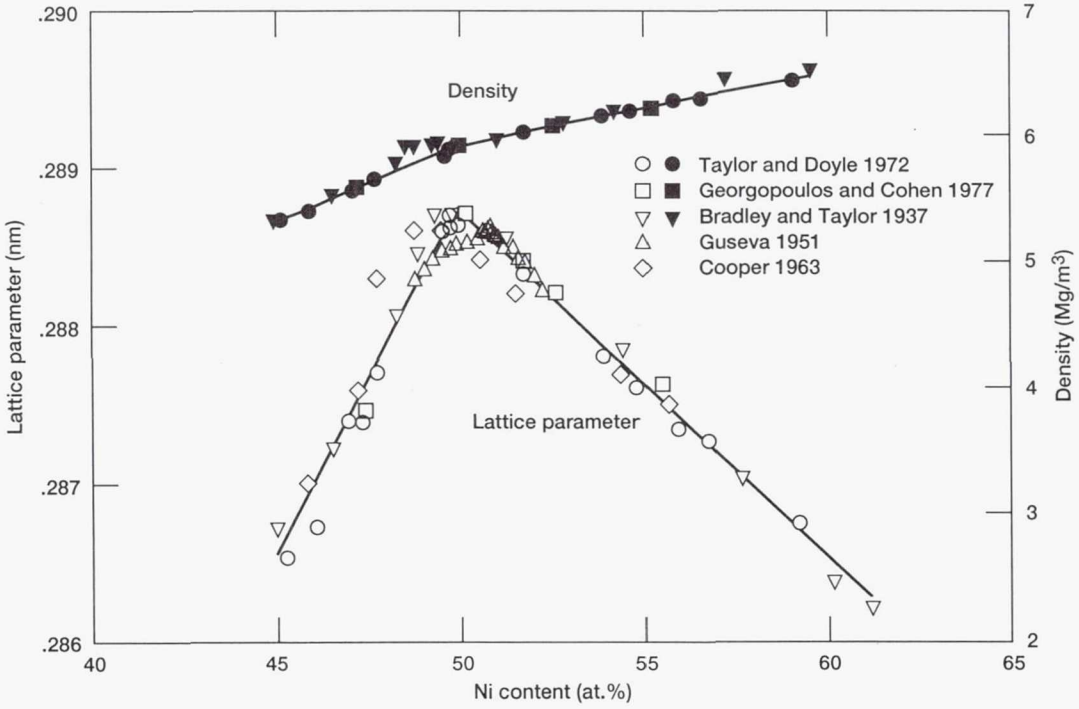

Figure 1.—Room-temperature lattice parameter and density of NiAl as a function of stoichiometry.

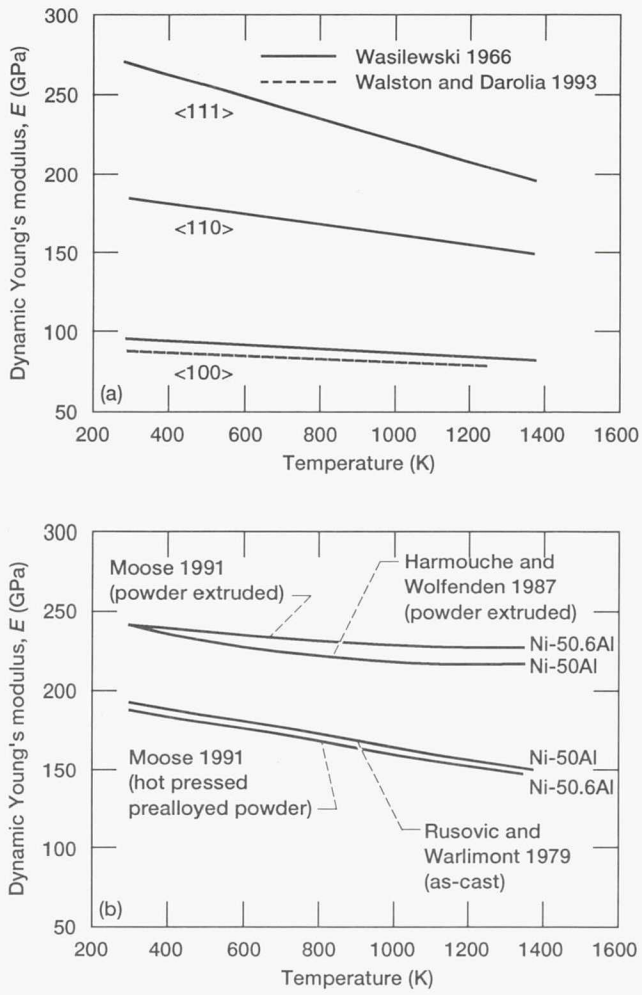

Figure 2.—(a) Dynamic Young's modulus for single-crystal NiAl as a function of orientation and temperature. (b) Effect of processing and temperature on dynamic Young's modulus of polycrystalline NiAl.

Most other physical properties have not been characterized to the same degree as lattice parameter, density, and elastic modulus. Only limited data were available on NiAl's thermal properties until researchers realized that the high thermal conductivity of NiAl is one of its major advantages over superalloys. This realization prompted recent studies to determine the effects of alloying additions on thermal and other physical properties of NiAl. It was found that alloying NiAl with Ti and Re significantly reduced thermal conductivity, whereas 2.5 at.% Hf additions had a minor effect, decreasing the thermal conductivity of single-crystal NiAl by only 15 percent (Walston and Darolia 1993). Minor deviations from stoichiometry were also found to have a significant effect on the thermal diffusivity of NiAl. A 2-at.% deviation in stoichiometry results in a 4-fold decrease in thermal diffusivity (unpublished research by Carl E. Lowell, 1993, NASA Lewis Research Center, Cleveland, OH).

Table I summarizes the physical properties of binary NiAl and creep-resistant NiAl alloys containing Hf, Re, or Ti, and it compares these properties to those of a typical Ni-base superalloy. For high-temperature structural applications, NiAl would have the greatest advantage over superalloys in terms of its thermal conductivity and density. Because of these differences in properties, replacing superalloy high-pressure turbine blades with ones made from NiAl would reduce turbine rotor weight by 40 percent and the "hot spot" temperature by 50 K (Darolia et al. 1992). Direct replacement of superalloy components with a NiAl alloy would be straightforward because the moduli and thermal expansion are similar. But most components would require customized design and special handling to accommodate the lower toughness of NiAl.

3. Flow and Fracture

3.1 Plasticity and Operative Slip Systems

The operative slip systems in NiAl single crystals and polycrystalline material have been rigorously investigated and described in detail (Noebe, Bowman, and Nathal 1993; Miracle 1993). In general, NiAl exhibits two significantly different types of slip behavior depending on crystal orientation. The dominant slip vector for "soft" single-crystal orientations and polycrystalline material is <001>. But, if the loading direction is along [001], known as the "hard" single-crystal orientation, the operative slip vector is <111> at low and intermediate temperatures and a combination of <110> and <100> at elevated temperatures (table II). Soft orientations include all non-<001> loading directions where <100> slip dominates. Test orientations close to [001] are hard orientations because <001> Burgers vectors have a zero or near-zero resolved shear stress.

By all indications, NiAl obeys Schmid's law and deforms by a <001> slip vector in either {100} or {110} planes for all but near-[001] crystal orientations (Lahrman, Field, and Darolia 1993a). Ball and Smallman (1966a and 1966b) were the first researchers to make a complete slip system determination for NiAl by identifying a <001> slip vector and {110} slip plane in all soft orientations and at all temperatures investigated (300 to 1273 K). They also observed cross slip or pencil glide on orthogonal {110} planes. In addition to <001>{110} slip, Wasilewski, Butler, and Hanlon (1967) observed duplex cube slip, <001>{100}, in [110]-oriented single crystals (as have Field, Lahrman, and Darolia 1991a). Cube slip also was seen by Loretto and Wasilewski (1971) in [112] crystals deformed between 77 and 1053 K. In soft-orientation single crystals, only <001> slip is observed because of the nondissociated, compact structure of the <001> dislocation core (Mills and Miracle 1993). Therefore, <001> dislocations are much more mobile than dislocations with any other slip vector.

Consistent with deformation studies on soft-orientation single crystals, investigators have reported the operation of a <001> slip vector in polycrystalline NiAl gliding on either {110} or {100} planes (Bowman et al. 1992; Nagpal and Baker 1992;

TABLE I.—PHYSICAL PROPERTIES OF NiAl, NiAl ALLOYS, AND AN ADVANCED SUPERALLOY
[Walston and Darolia (1993)]

Property	Temperature, K	NiAl	NiAl alloys[a]	Advanced superalloy
Bonding	----	Covalent/metallic	Covalent/metallic	Metallic
Melting Point, K	----	1955[b]	1833 to 1949	1633
Matrix lattice parameter, Å	Room	2.887	2.888 to 2.900	3.580
Matrix/ppt. lattice mismatch, percent		N/A	1 to 6 (β′)	0 to -0.5 (γ′)
Density, g/cm³		5.9	up to 6.30	8.60
Young's modulus, polycrystal, GPa		188	188	205
Young's modulus, <001>, GPa		88	88	130
Anisotropy factor		3.25	3.25	2.72
Shear modulus, polycrystal, GPa		71.5	71.5	74
Poisson's ratio		0.313	0.313	0.380
Thermal expansion, 10^{-6}/K	873	13.2	13.7	13.5
Specific heat, J/g•K		0.64	0.61 to 0.64	0.46
Thermal diffusivity, cm²/sec		0.22	0.10 to 0.22	0.033
Thermal conductivity, W/m•K		76	35 to 76	15
Electrical resistivity, μΩ•cm	Room	8 to 10	10 to 30	120 to 140

[a]NiAl alloys containing primarily β′ precipitates and less than 5 at.% alloying addition.
[b]General Electric Aircraft Engines Differential Thermal Analysis data show that the melting point of NiAl is about 40 K higher than shown in literature data.

Cotton, Noebe, and Kaufman 1993b). Isolated dislocation segments with Burgers vectors other than <001> have been identified in as-extruded NiAl (Lloyd and Loretto 1970; Dollar et al. 1992). However, the presence of non-<001> dislocations in these polycrystalline studies does not indicate the operation of an alternate deformation mechanism. Dislocations such as <110> are probably formed by interactions between <001> dislocations because of the extensive deformation that occurs during the extrusion process (Baker and Schulson 1984). Furthermore, non-<001> dislocations are not observed in as-cast materials or after room-temperature deformation of cast alloys (Cotton, Noebe, and Kaufman 1993b).

The operation of a <100> slip vector on planes other than {001} and {011} has been observed under special conditions of constrained flow. For example, Miracle (1991) observed a (210) slip plane in one of the many deformed bicrystals he analyzed. Also, Wunderlich, Machon, and Sauthoff (1992) observed <100>{310} slip in NiAl within the plastic zone produced by a blunted crack. This crack was initiated in the NiNbAl phase after high-temperature deformation of a NiAl/NiAlNb alloy. Although observations of atypical slip systems are ardently reported, these results need to be tempered by the realization that even in the above studies <100>{011} slip was the dominant deformation mechanism.

TABLE II.—OBSERVED SLIP SYSTEMS IN UNIAXIALLY DEFORMED NiAl

Temperature range, K	Slip vector	Slip plane
Polycrystals		
300 to 1200	<100>	{001},{011}[a]
Single crystals		
"Soft" orientations: non-[001]		
77 to 1300	<100>	{011}, {001}
"Hard" orientations: [001]		
77 to 600	<111>	{112}, {011}, or {123}
600 to 1372	<110>	{011}
300 to 1300	<100>	{011}

[a]Less than five independent slip systems.

Deformation of single crystals oriented along [001] is a special case in terms of operative slip systems because the resolved shear stress for <100> slip approaches zero. As a result, deformation occurs primarily by non-<001> dislocation processes. This gives rise to a high yield stress at low temperatures (Wasilewski, Butler, and Hanlon 1967) as well as enhanced creep strength at elevated temperatures for crystals of this orientation compared with non-[001] crystals (Forbes et al. 1993). Consequently, significant effort has been spent on experimental analyses of the operative deformation mechanisms in hard-orientation crystals.

From 77 K to approximately 600 K, the primary slip vector in hard-orientation crystals is <111>, with the most likely slip plane being {112} (Pascoe and Newey 1968a; Kim and Gibala 1991; Veyssiere and Noebe 1992). Previous reports of deformation by <001> dislocations in [001] crystals over this temperature range (Fraser, Smallman, and Loretto 1973) have been attributed to an unstable sample geometry, which invariably leads to kinking (Bowman, Noebe, and Darolia 1989). At higher temperatures (>600 K, which is above the brittle-to-ductile transition temperature (BDTT) for [001] crystals), the operative slip vector changes, and deformation occurs by nonconservative motion of <001> and <011> dislocations (Kim and Gibala 1991; Field, Lahrman, and Darolia 1991b).

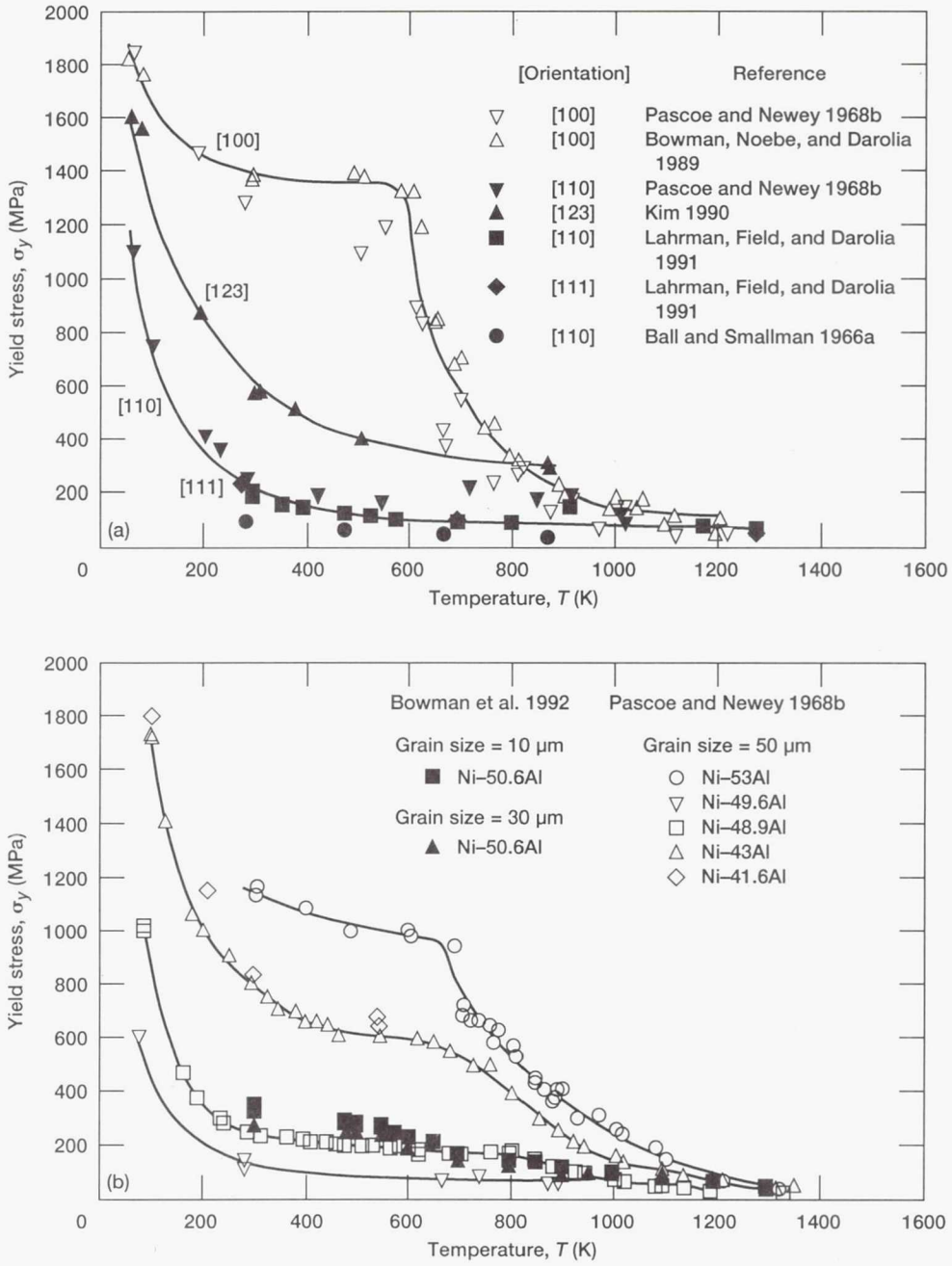

Figure 3.—Yield stress as a function of temperature for (a) several different single-crystal orientations and (b) polycrystalline NiAl as a function of strain rate, stoichiometry, and temperature.

3.2 Yield Strength

Although yield stress is highly sensitive to many metallurgical variables, all studies on single-crystal and polycrystalline material concur that with increasing temperature, yield strength decreases or remains constant over certain temperature regimes (figs. 3(a) and (b)). In general, the flow stress of NiAl is similar to that of body-centered cubic metals, exhibiting a strong temperature dependence at low absolute temperatures that is attributed to a large Peierls stress. At intermediate temperatures, there is a plateau where yield stress is only mildly dependent on temperature; this is followed by a further drop in strength at elevated temperatures.

The yield strength of NiAl single crystals has a very strong dependence on orientation (fig. 3(a)). Single crystals with soft orientations exhibit a yield stress σ_y versus temperature T relation that is distinct from that for [001] crystals but very similar to that for low-yield-strength polycrystalline NiAl. At lower

temperatures, single crystals of NiAl that are loaded along <001> directions exhibit yield stresses several times higher than those for other orientations and are less strongly dependent on temperature than soft orientations are. At temperatures above 600 K, the yield strength of [001] crystals becomes very sensitive to temperature, with a significant reduction in σ_y occurring over a relatively narrow temperature range. Within this temperature regime, the slip vector in hard-orientation crystals begins to change from <111> to <001> and <110> (Kim and Gibala 1991). Above 1000 K, where bulk diffusional processes begin to dominate, hard-orientation single crystals have yield strengths similar to soft-orientation single crystals and polycrystalline NiAl.

Figure 3(b) shows typical polycrystalline NiAl yield stress behavior as a function of temperature, stoichiometry, and grain size. Although the values of the yield stress and the shape of the σ_y versus temperature curves depend on composition and strain rate, in all cases the yield stress decreases with increasing temperature. The behavior of near-stoichiometric polycrystalline NiAl resembles that of the soft-orientation, single-crystal material. With greater deviations from stoichiometry, polycrystalline material has considerably higher strength, comparable to that of stoichiometric [001] crystals, even though slip is expected to occur by <001> dislocations in all polycrystalline NiAl alloys.

Not only is the yield strength for NiAl anisotropic, but the strain rate sensitivity is anisotropic also, with cube-oriented crystals displaying a greater sensitivity to strain rate than soft orientations at intermediate temperatures (500 to 1000 K) (Pascoe and Newey 1968b; Lahrman, Field, and Darolia 1991). The greater sensitivity of [001] crystals to strain rate is due to the decomposed core structure of <110> dislocations, which cannot glide conservatively in hard-orientation crystals, and the zero critical resolved shear stress on <001> dislocations, making it necessary for both types of dislocations to rely on thermal activation to assist their motion (Mills et al. 1993). On the other hand, deformation of soft-orientation single crystals is controlled by <001> dislocations that have a compact core structure. Consequently, the yield stress of soft-orientation single crystals is relatively insensitive to strain rate below the BDTT. Also, the brittle-to-ductile transition temperature itself is only mildly dependent on strain rate for soft-orientation single crystals. (Lahrman, Field, and Darolia 1991).

In polycrystalline NiAl, strain rate has almost no effect on yield strength below 600 K, with a strain rate sensitivity $m < 0.01$. Strain rate has a moderate effect at temperatures between 600 and 1000 K ($m \approx 0.06$) and a significant effect on yield strength above 1000 K in the creep deformation regime ($m \approx 0.18$) (Bowman et al. 1992). However, the BDTT for polycrystalline NiAl is strongly affected by strain rate. A 3 orders of magnitude increase in strain rate results in approximately a 200 K increase in BDTT (Noebe, Cullers, and Bowman 1992). A similar rate dependence of the BDTT is observed in [001] single crystals (Lahrman, Field, and Darolia 1991).

Because σ_y is strongly dependent on temperature, it is useful to represent the yield stress data in an Arrhenius form where the slope of the curve is proportional to the activation energy for deformation. Consequently, changes in slope on an Arrhenius plot usually indicate a change in the deformation mechanism. When the polycrystalline NiAl yield strength data of Bowman et al. (1992) from figure 3(b) are replotted in an Arrhenius form, three distinct deformation regimes are observed (fig. 4). The lower temperature (~550 K) discontinuity in figure 4, or change in deformation mechanism, is of particular interest because it coincides with the BDTT in NiAl. This change in slope in the Arrhenius plot reinforces the concept that additional deformation mechanisms are operating, accounting for the large-scale plasticity in NiAl above the BDTT. The actual deformation mechanisms responsible for this change in behavior are discussed in section 3.3. The change in slope beginning at region III is due to creep deformation processes. Similar to the behavior shown in figure 4, a change in slope of an Arrhenius plot of yield stress is also observed at the BDTT of Zr- and Re-doped polycrystalline NiAl alloys and hard-orientation single crystals (Noebe et al. 1990; Bowman, Noebe, and Darolia 1989).

In NiAl, significant deviations are possible from the stoichiometric composition without altering the basic crystal structure of the intermetallic. This in turn, has a significant effect on mechanical behavior (as reviewed previously by Vedula and Khadkikar 1990). Although an increase in yield stress is observed for both Ni- and Al-rich alloys at low temperatures, the magnitude of the strengthening effect is not equivalent. From a previous compilation of low-temperature data, the average hardening rate for Ni-rich alloys was 120 MPa/at.%, whereas that for Al-rich NiAl was approximately 350 MPa/at.% (Noebe, Bowman, and Nathal 1993). The greater hardening rate for Al-rich alloys suggests that Ni vacancies provide a greater resistance to dislocation motion than antisite atoms. Regardless of whether the material is Ni-rich or Al-rich, the effects of nonstoichiometry on strength become negligible around 1000 K (fig. 3(b)), and a reversal in strength occurs at higher temperatures such that stoichiometric alloys become stronger than nonstoichiometric compositions (Ball and Smallman 1966a; Whittenberger, Noebe, Cullers, Kumar, and Mannan 1991).

Vacancies significantly influence the flow properties of NiAl as evident from the high hardening rates in Al-rich alloys, where constitutional vacancies are formed on the Ni sublattice. Another type of vacancy defect that can exist in NiAl is a thermal vacancy introduced by rapid quenching from elevated temperatures. Therefore, cooling rate becomes another important variable to be considered before testing NiAl. In polycrystals, a 50-fold increase in cooling rate from temperatures above 1000 K can increase the compressive yield stress almost 30 percent for near-stoichiometric binary NiAl. However, when the material is doped with minor alloying additions such as 500 ppm Zr, there is no dependence of cooling rate on strength, though the solute addition itself has a significant effect

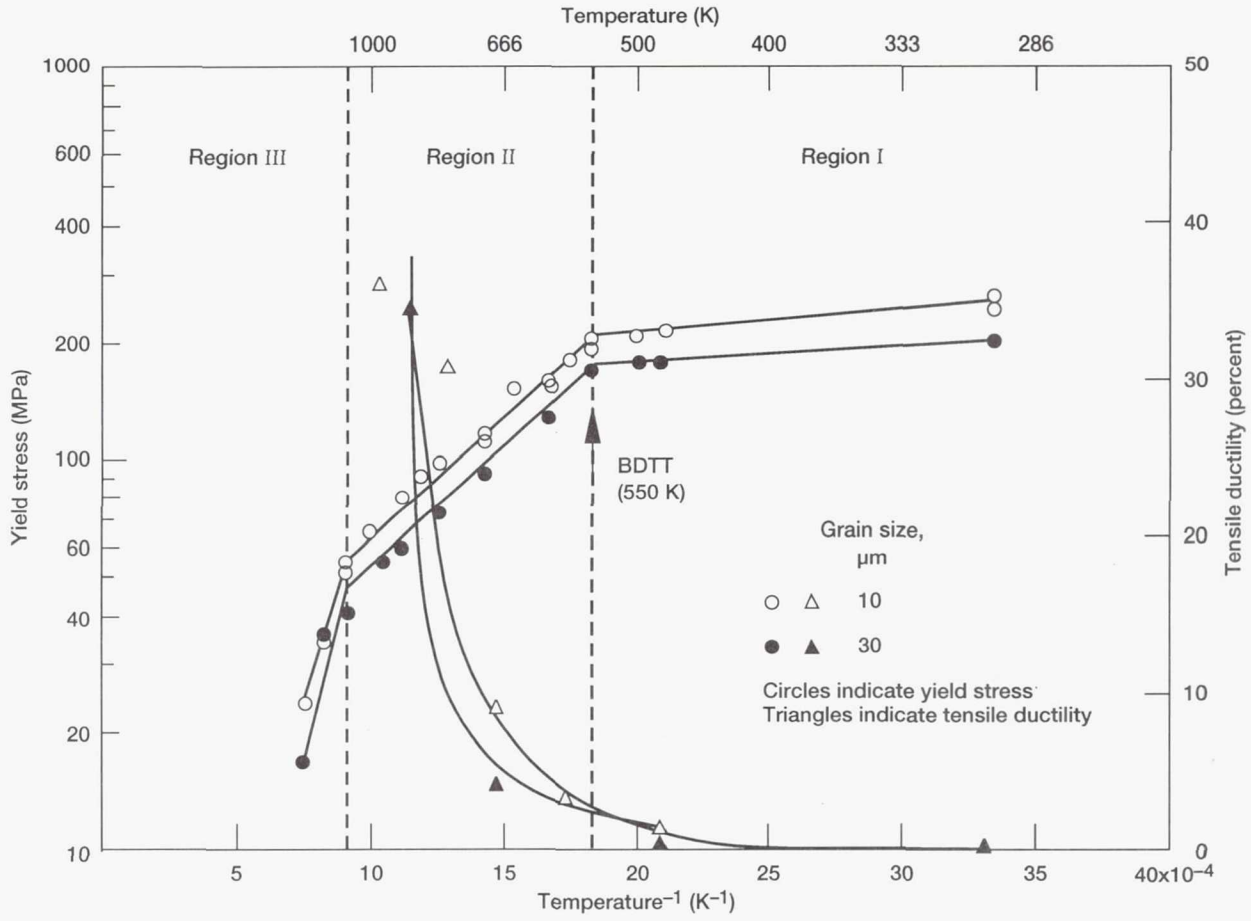

Figure 4.—Yield stress and tensile ductility of polycrystalline NiAl as an inverse function of temperature. The brittle-to-ductile transition temperature (BDTT) defined by the dramatic increase in ductility corresponds to a change in activation energy for plastic flow beginning at region II (Bowman et al. 1992); strain rate, 1.4×10^{-4} s^{-1}.

(Bowman et al. 1992). Similarly, deviations from stoichiometry reduce the sensitivity of binary NiAl to cooling rate effects (Nagpal and Baker 1990a). Cooling rate has a similar effect on the yield strength of NiAl single crystals (Weaver, Kaufman, and Noebe 1993).

Substitutional and interstitial elements also significantly affect the strength of NiAl. However, published single-crystal data are relatively scarce, and much of the available information is for hard orientations. Additions of Cr (Field, Lahrman, and Darolia 1991c), V (Darolia et al. 1989), and Zr (Noebe et al. 1989) do not have any demonstrated hardening effect on [001]-oriented single crystals at low temperatures but do strengthen NiAl at temperatures above 600 to 700 K, where a change in slip mode is known to occur. Systematic study of the influence of Mo, Ga, and Fe on the yield strength of <110>-oriented, single-crystal NiAl revealed a range of strengthening behaviors at room temperature (Darolia, Lahrman, and Field 1992). These researchers determined that Mo is a potent solid-solution hardening agent but that it has a very limited solubility in NiAl. Ga has a mild strengthening effect, whereas Fe, at levels of less than 1 at.%, slightly decreases the yield stress. Preliminary testing of high-purity single crystals also indicates that interstitial levels can significantly influence flow stress (Weaver, Kaufman, and Noebe 1993). The critical resolved shear stress reported for high-purity, low-interstitial, [123]-oriented NiAl is only 57 MPa, in contrast to 79 MPa for a commercial purity material that received an identical thermal treatment.

Solid-solution alloying data for polycrystalline NiAl are more abundant than for single-crystal material. Ternary additions to polycrystalline NiAl have included Be, B, and C (George and Liu 1990); Cr and Cu (Cotton, Noebe, and Kaufman 1993a,d); Y, Mo, and La (Graham 1984); Fe and Ga (Noebe and Behbehani 1992); and Zr (Bowman et al. 1992). Figure 5 shows the relation between the hardening rates of these elements in polycrystalline NiAl and atom size. In all cases the flow strength of NiAl was enhanced by the presence of solutes, and in general the hardening rate was proportional to solute size, though exceptions do exist. For example, Ga and Mo have very similar Goldschmidt or atomic radii but result in significantly different hardening rates when they are added to NiAl.

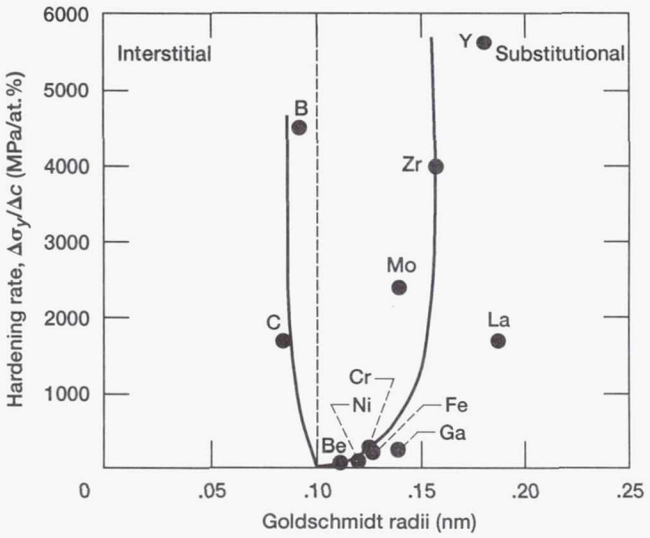

Figure 5.—Relation between hardening rate and element size for various alloying additions in NiAl.

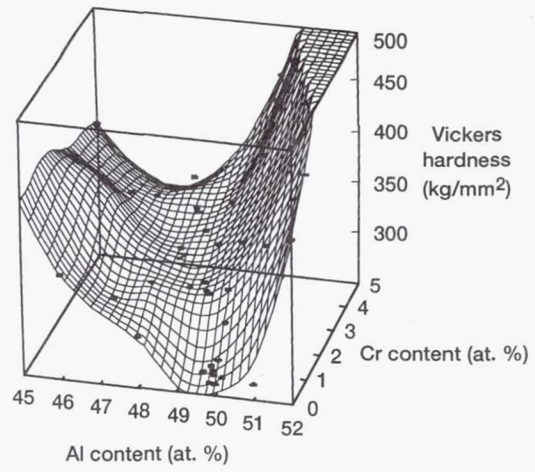

Figure 6.—Combined effect of stoichiometry and Cr additions on the hardness of Cr-doped B2 NiAl alloys (Cotton, Noebe, and Kaufman 1993a).

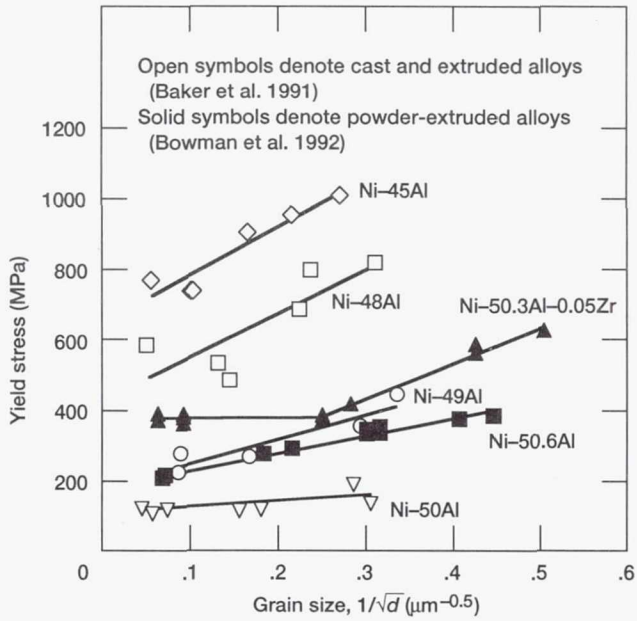

Figure 7.—Effect of grain size, stoichiometry, and alloying additions on the room-temperature yield stress of NiAl alloys.

No acceptable theory of solid-solution strengthening can explain all aspects of hardening in intermetallic alloys, even for the relatively simple B2 compounds (Fleischer 1993). For example, substituting a particular ternary addition such as Cu for Ni in NiAl will result in significantly different hardening characteristics than if the element were substituted for Al (Cotton, Noebe, and Kaufman 1993d). A further complication occurs if the alloying addition changes the overall stoichiometry of the intermetallic or if it is added to a nonstoichiometric base. For example, figure 6 demonstrates the influence of Cr and Al levels on the hardness of NiAl. Chromium has a moderate strengthening effect on near-stoichiometric NiAl up to its solubility limit of about 2 at.%, but even more significant strengthening is observed on either side of stoichiometry because of constitutional defects. Consequently, defect structures in ternary alloys need to be characterized so that addition and cancellation rules for the various defect hardening mechanisms can be defined. The potential for defect pairing or clustering also has to be accounted for if solid-solution hardening models are to be effective (Cotton, Noebe, and Kaufman 1993d).

Finally, grain size also influences the room-temperature yield strength of NiAl, but not in a straightforward manner. Grain size effects are complicated by the additional variables of alloy stoichiometry and third-element additions (fig. 7). The relation between alloy stoichiometry and Hall-Petch parameter (slope of the curves in fig. 7) clearly shows that the influence of grain size on yield stress is more significant with increasing deviation from stoichiometry (Nagpal et al. 1991). Consequently, yield stress is essentially independent of grain size for Ni-50Al, whereas the yield stress of even slightly nonstoichiometric alloys is strongly influenced by grain size.

The effect of grain size on yield strength is further complicated when alloying additions are involved, as demonstrated in figure 7. When NiAl was alloyed with 0.05 at.% Zr, the yield stress was independent of grain size for grain sizes between 16 to 280 μm. However, it was strongly dependent on grain size for grains less than 16 μm because of the enrichment of Zr at the grain boundaries (Zeller, Noebe, and Locci 1990). In the region where the yield stress was independent of grain size, the mean free path of the dislocations was suspected to be less than the average grain diameter because of solid-solution effects.

In summary, many metallurgical parameters influence the flow strength of NiAl. However, the magnitude of the strengthening effect typically depends on other factors in a usually complicated manner. As previously noted, the manner in which temperature affects flow stress is sensitive to alloy composition

and crystal orientation. The sensitivity of yield stress to strain rate depends on the temperature range being investigated and on the orientation for single crystals. The effect of cooling rate (thermal vacancy concentration) is not well understood but is mainly a concern for binary near-stoichiometric NiAl, but not NiAl alloys. Several interstitial and substitutional alloying additions significantly affect flow strength even when they are present at rather low levels. In fact, these elements may have a significant effect on strength at concentrations that are not readily detectable by present analytical techniques. Finally, the amount of strengthening due to grain refinement is sensitive to both stoichiometry and alloying additions. Even with all of these variables accounted for, our present understanding of the flow behavior of NiAl alloys is still suspect because our present knowledge may be clouded by as-of-yet unknown interactions.

3.3 Ductility and Fracture

Cube-oriented, Ni-50Al single crystals exhibit essentially zero plastic strain to failure at room temperature but undergo a sharp brittle-to-ductile transition at temperatures just above 600 K (Bowman, Noebe, and Darolia 1989; Darolia et al. 1992; Takasugi, Watanabe, and Hanada 1992). This BDTT corresponds to the temperature at which [001] crystals begin to undergo a steep decrease in yield stress with increasing temperature (fig. 3(a)) because the deformation mechanism changes from <111> slip to climb of <100> and <110> dislocations. Ni-rich, cube-oriented Ni-40Al crystals undergo a similar brittle-to-ductile transition but at approximately 1000 K (Noebe, Misra, and Gibala 1991).

Previously, it appeared that soft-orientation, single-crystal NiAl also possessed very limited room-temperature tensile ductility. Near-stoichiometric, soft-orientation single crystals have been routinely reported to exhibit room-temperature tensile elongations on the order of 1 percent (Lahrman, Field, and Darolia 1993b; Takasugi, Kishino, and Hanada 1993). On occasion, however, room-temperature tensile ductilities on the order of 5 to 7 percent have been measured in binary NiAl soft-orientation single crystals without any obvious mechanism for the increased tensile ductility (Field, Lahrman, and Darolia 1993; Brzeski et al. 1993). Similarly, an intriguing effect of microalloying additions on the tensile properties of soft-orientation, single-crystal nickel aluminides has been observed (Darolia, Lahrman, and Field 1992). When near-stoichiometric, <110> single crystals were doped with approximately 1000 ppm of Fe, Mo, or Ga, the room-temperature tensile elongation increased from approximately 1 percent to upwards of 6 percent (fig. 8). From figure 8, it is obvious that the peak in ductility occurs at very small alloying additions, and as the level of dopant exceeds 0.5 at.% the benefits to ductility are lost. This ductilizing effect is possibly due to gettering of interstitial contaminants, which would be consistent with the recent observations on the fracture toughness of NiAl discussed below.

Soft-orientation single crystals also undergo a fairly abrupt brittle-to-ductile transition at temperatures slightly below those of polycrystals. Depending on the specific orientations, the BDTT's range from 475 to 525 K (Lahrman, Field, and Darolia 1991; Takasugi, Kishino, and Hanada 1993). Just above the BDTT, anomalously large tensile elongations (greater than 120 percent) were observed for soft-orientation single crystals; ductility decreased to around 50 percent at higher temperatures because of the onset of necking (fig. 9). The anomalously large elongations at intermediate temperatures have been attributed to a balance between work hardening caused by glide and relaxation processes due to climb resulting in a high necking resistance (Takasugi, Kishino, and Hanada 1993).

Originally, the room-temperature fracture toughness of single-crystal NiAl bend samples was reported from 7 to 12 $MPa\sqrt{m}$ when the notch is cut perpendicular to <100>-oriented crystals and from 4 to 6 $MPa\sqrt{m}$ when the notch is cut perpendicular to <110>-oriented crystals (Chang, Darolia, and Lipsitt 1992; Vehoff 1993). The fracture toughness of the soft-orientation single crystals agrees perfectly with fracture toughness values for binary, single-phase, polycrystalline NiAl, which have been measured between 4 and 7 $MPa\sqrt{m}$. Furthermore, the fracture toughness of polycrystalline NiAl is essentially independent of grain size, stoichiometry, or processing technique (Reuss and Vehoff 1990a; Rigney and Lewandowski 1992a; Kumar, Mannan, and Viswanadham 1992).

However, it was recently discovered (Hack, Brzeski, and Darolia 1992) that the fracture toughness of commercial purity, single-crystal NiAl is extremely sensitive to heat treatment and cooling rate, as determined from double cantilever beam specimens with a notch plane perpendicular to <110>. For example, single-crystal samples that were rapidly air cooled to room temperature from 1573 K had a fracture toughness of almost 16 $MPa\sqrt{m}$, but when they were reannealed at 473 K and slowly cooled to room temperature, the fracture toughness dropped to about 3 $MPa\sqrt{m}$ (Hack, Brzeski, and Darolia 1992). Comparable heat treatments had

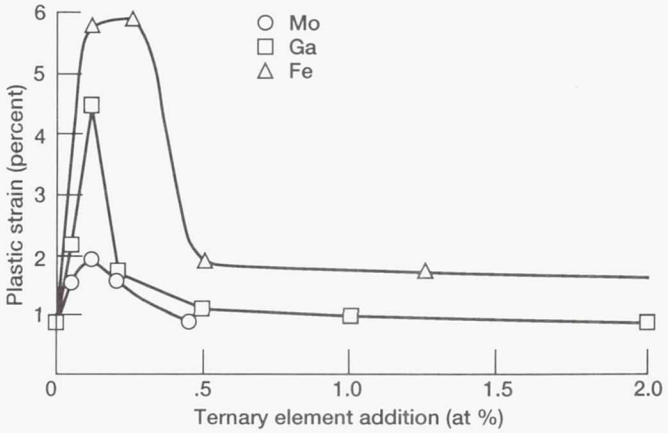

Figure 8.—Room-temperature tensile ductility of <110> single-crystal NiAl microalloyed with Fe, Ga, or Mo, (Darolia, Lahrman, and Field 1992).

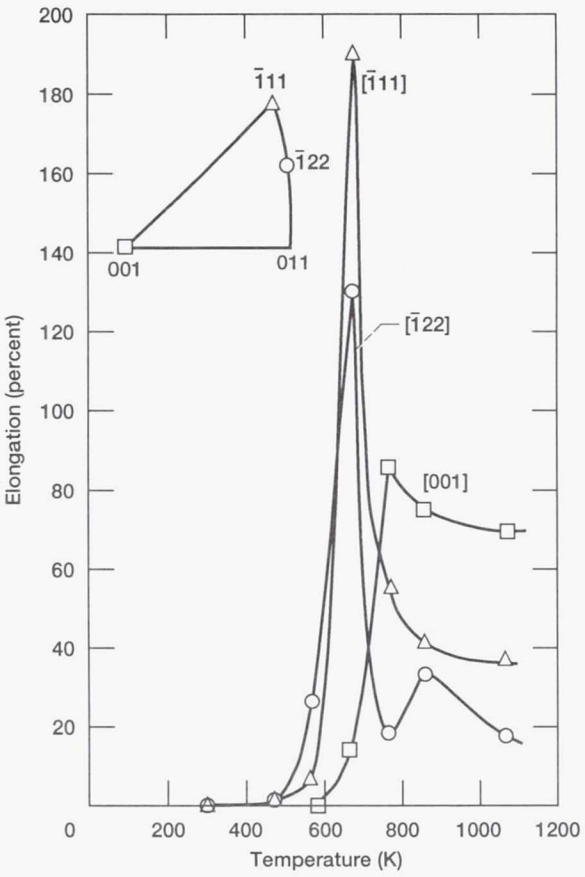

Figure 9.—Effect of temperature on the tensile ductility of NiAl single crystals (Takasugi, Wantanabe, and Hanada 1992).

no effect on the toughness of zone-refined, low-interstitial, single-crystal NiAl when it was tested in four-point bending with the crack plane normal to <100>. The fracture toughness of this high-purity NiAl was 10 to 12 MPa$\sqrt{m}$ independent of heat treatment (Johnson et al. 1993). Furthermore, experiments in biaxial bending and tension indicate that zone-refined, low-interstitial NiAl single crystals have a much greater room-temperature ductility and fracture strength than commercial purity material does (DeMarco and Ardell 1993; Johnson et al. 1993). These observations are consistent with a strain aging phenomenon in NiAl.

This behavior would be similar to that observed in mild steels where carbon is responsible for pinning the mobile dislocation density, causing brittle fracture. Thus, the inherent ductility and fracture toughness of single-crystal NiAl may be much greater than originally determined. However, considerable work is still necessary to understand and sort out the various metallurgical phenomena. For instance, higher toughness values in NiAl are always associated with an increased percentage of transient fracture along higher index planes, such as {511}, before transitioning to {110} planes (Darolia, Chang, and Hack 1993). But the mechanism for this transient fracture behavior and the roles that composition and heat treatment play are still unclear.

Polycrystalline alloys have an additional complicating factor in the presence of grain boundaries. Because NiAl deforms by a <001> slip vector, there are only three independent slip systems available for deformation; no extra independent systems are provided by cross slip (Ball and Smallman 1966b). Because this is less than the five independent deformation modes considered necessary for extensive, uniform, crack-free deformation of a polycrystalline aggregate, polycrystalline NiAl has little potential for significant room-temperature ductility. Experimental evidence to date supports this view. In room-temperature studies of NiAl, the reported tensile ductilities have ranged from zero to a maximum of about 4 percent (Rozner and Wasilewski 1966; Hahn and Vedula 1989). Furthermore, intergranular fracture in both tensile and compression specimens at low temperatures appear to confirm that the limited ductility of binary, near-stoichiometric NiAl is the result of incompatible shape changes of neighboring grains. These incompatible shape changes are due, in turn, to an insufficient number of slip systems (Ball and Smallman 1966a; Noebe et al. 1991).

However, intergranular fracture can result from many different sources. Intergranular fracture of NiAl due to impurity segregation at the grain boundaries has been ruled out through in-situ Auger electron spectroscopy studies (George and Liu 1990; Zeller, Noebe, and Locci 1990). Examination of cast plus extruded alloys and powder-extruded materials after various thermal treatments revealed that the grain boundaries in NiAl were clean and free from measurable impurity contamination including O and C. Intergranular fracture could arise if the grain boundaries were intrinsically weak because of their structure, as was once thought to be the case in Ni_3Al (Chaki 1991). However, grain boundary structure simulations for NiAl indicate that there are no periodic structural defects present at the grain boundaries in near-stoichiometric NiAl that would cause the grain boundaries to be inherently weak (Vitek and Chen 1991). The grain boundary modeling results indicate the possible presence of slight discontinuities in the grain boundary structure of nonstoichiometric alloys; however, nonstoichiometric NiAl fractures in a transgranular manner (Nagpal and Baker 1991). Finally, Ni_3Al has limited ductility in polycrystalline form because of intergranular fracture aggravated by environmental effects when tested in room-temperature air (George, Liu, and Pope 1992). However, in comparable testing of NiAl in air, vacuum, and various gas environments, environment had no impact on the tensile ductility of polycrystalline NiAl (personal communication with C.T. Liu, 1993, Oak Ridge National Laboratory, Oak Ridge, TN) or single-crystal material (Lahrman, Field, and Darolia 1993b). All these results suggest that grain boundary incompatibility due to an insufficient number of independent slip systems is the primary factor responsible for the observed intergranular fracture and limited tensile ductility of near-stoichiometric NiAl.

Both intergranular and transgranular fracture modes have been observed in alloyed NiAl. Intergranular fracture initiation

in NiAl depends on the operation of at least localized plastic flow to nucleate a critical defect for fracture, whereas transgranular fracture initiation and propagation generally occur before yielding. This behavior is summarized in the fracture map shown in figure 10 (Noebe 1994). Low-yield-strength binary NiAl alloys exhibit limited tensile ductility that leads to the formation of intergranular microcracks because of incompatible plastic deformation at the grain boundaries. This results in a fracture mechanism defined as brittle intergranular fracture III (BIF III) by Gandhi and Ashby (1979). In this region, fracture is intergranular or mixed mode in nature, occurring after some measurable plastic deformation, but initiating intergranularly. In higher strength alloys, usually powder-processed material or microalloyed NiAl, fracture occurs at the macroscopic yield strength of the material, but no significant tensile ductility is achieved (BIF II). Localized or microscopic yielding is responsible for initiating fracture in the material; but because the stresses are higher, the critical stress for crack propagation has already been reached, and fracture occurs at the first defect formed in the material. Finally, in some NiAl materials, such as those alloyed with Re, B, C, or Cr, fracture occurs without any prior plasticity in a completely brittle manner. In such cases, fracture almost always initiates and propagates in a transgranular fashion (cleavage I). Similarly, nonstoichiometric binary NiAl alloys do not exhibit room-temperature ductility and fail in a predominantly transgranular manner (Nagpal and Baker 1991).

Consequently, the origin of fracture in polycrystalline NiAl depends significantly on composition. In low-strength, stoichiometric, binary NiAl alloys, grain boundaries become the sites of Griffith defects after slip is activated. In alloyed materials of moderate strength, local yielding is responsible for initiating intergranular fracture. In contrast, high-strength NiAl-based materials fail transgranularly, with fracture originating at some internal or surface defect.

Although limited tensile ductility can be achieved in low-yield-strength NiAl alloys at room temperature, this is not the brittle-to-ductile transition temperature for polycrystalline alloys. Instead, a dramatic increase in ductility corresponding to the BDTT is observed in the range of 550 to 700 K (Noebe, Cullers, and Bowman 1992). Not only is the BDTT defined by a substantial increase in tensile ductility, but a significant and concurrent increase in fracture strength (fig. 11) and fracture toughness (fig. 12) are observed. The fracture toughness of polycrystalline NiAl increases abruptly as temperature increases, with the transition to ductile behavior and high toughness values occurring between 550 and 650 K. In this intermediate temperature regime, the fracture toughness of NiAl ranges from 20 to nearly 50 MPa$\sqrt{m}$ depending on microstructure and grain size (Reuss and Vehoff 1990a). The increasing toughness of NiAl with temperature corresponds to the observed increase in tensile fracture strength with temperature and would be expected because of the linear dependence between the critical stress intensity factor K_{IC} and fracture stress for a constant flaw size.

For polycrystalline material, these changes in behavior have been attributed to the onset of localized dislocation climb processes that occur within the vicinity of the grain boundaries (Noebe 1994). These dislocation climb processes result in five independent deformation mechanisms, permitting the accommodation of strains across the grain boundaries. In-situ annealing studies have verified the onset of significant dislocation climb activity near grain boundaries in NiAl beginning at the BDTT, correlating with the beginning of region II deformation

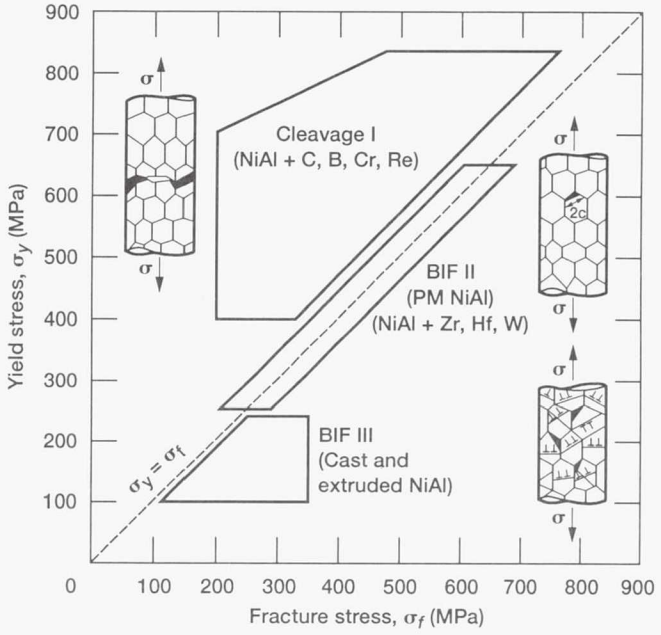

Figure 10.—Relation between alloying additions, room-temperature tensile properties, and fracture initiation mechanisms in NiAl alloys. Brittle intergranular fracture, BIF; powder metallurgy, PM.

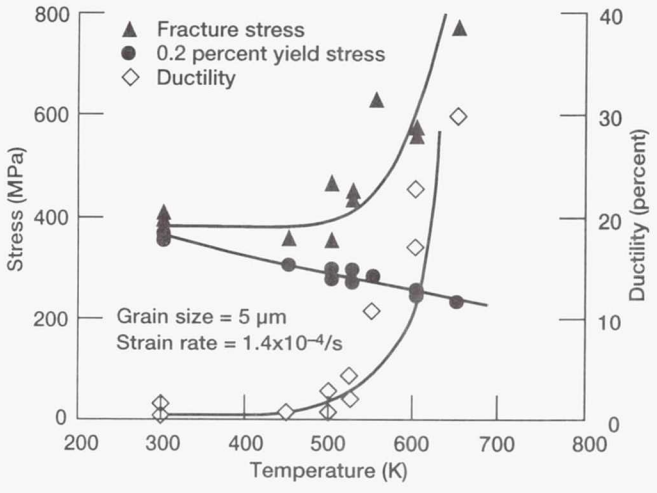

Figure 11.—Effect of test temperature on the yield stress, fracture stress, and tensile elongation of power-extruded NiAl (Noebe et al. 1991).

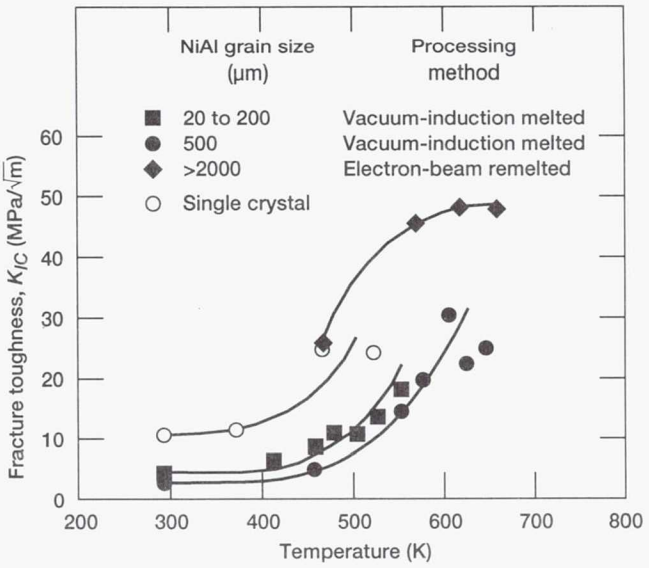

Figure 12.—Fracture toughness of NiAl as a function of temperature. Alloys were produced by several different techniques resulting in materials with a range of grain sizes (Reuss and Vehoff 1990b).

in figure 4 (Bowman et al. 1992). The significance of dislocation climb in a material such as NiAl was demonstrated by Groves and Kelly (1969). They showed that the combination of glide and climb of dislocations with <100> Burgers vectors will result in five independent deformation mechanisms. This condition would satisfy the Von Mises criterion allowing for extensive plasticity in polycrystalline NiAl by relieving stresses at the grain boundaries and other sites of extensive stress concentration. The lowest BDTT observed in polycrystalline NiAl, $\sim 0.30T_m$, falls within the temperature regime for which thermally activated deformation mechanisms occur by short circuit diffusion. For example, climb could be restricted to grain boundary regions and still be very influential in relieving compatibility stresses. Typical dislocation glide processes would continue to dominate the deformation behavior of the grain interiors until temperatures of approximately $0.5T_m$ are reached. This description is consistent with in-situ transmission electron microscope annealing studies on NiAl that have qualitatively determined the temperatures for which dislocation climb by short circuit and bulk diffusion processes becomes significant (Bowman et al. 1992). This description of the deformation behavior of polycrystalline NiAl near the brittle-to-ductile transition is also consistent with the observed effects of strain rate and alloying additions on the BDTT (Noebe, Cullers, and Bowman 1992; Noebe 1994).

Dislocation climb processes driven by short circuit diffusion along dislocation cores could similarly be used to explain the brittle-to-ductile transition in [001]-oriented single crystals. The range of the BDTT for hard-orientation crystals corresponds to the change in deformation mechanism from <111> slip to deformation by <100> and <110> dislocations. Because the resolved shear stress on the <001> dislocations would be small and the <110> dislocations have a decomposed core structure and can only move by nonconservative processes (Mills et al. 1993), a significant amount of thermal activation would be necessary before these dislocations could accommodate imposed strains on [001] crystals.

The mechanism responsible for the brittle-to-ductile transition in soft-orientation single crystals is not obvious. For soft-orientation single crystals, the BDTT occurs as low as $0.25T_m$ and is relatively insensitive to strain rate (Lahrman, Field, and Darolia 1991). This lower BDTT could be due to enhanced cross-slip leading to slip homogenization or due to the unlocking of dislocations from point defects or impurities. This last mechanism is consistent with the strain-aging effects recently observed in single-crystal NiAl (Hack, Brzeski, and Darolia 1992). However, the onset of thermally activated deformation processes may still play an important role in the relaxation of stress concentrations that may occur at surface notches or internal defects such as pores and shrinkage cavities. Dislocation glide alone (generally on a single slip system) would not be sufficient to accommodate the complex stress state near these types of defects in single crystals. Furthermore, single crystals (Takasugi, Kishino, and Hanada 1993), like polycrystalline NiAl, undergo a dramatic change in ductility at intermediate temperatures where thermally activated deformation processes become active.

4. Alloy Design

Figure 13 shows several basic possibilities for alloying NiAl. The first is adding elements with high solubility in NiAl. Because NiAl is isostructural with several other intermetallic compounds and has a wide phase field, Mn, Cu, and group VIII elements are generally quite soluble. This family of elements offers a considerable alloying potential that is mainly unexplored at this time. The refractory metal group VIB elements plus V and Re exhibit very little solubility in NiAl and form no ternary intermetallic phases, with the exception of V in Ni-rich alloys. Instead, these elements form pseudobinary eutectic systems with stoichiometric NiAl and, therefore, may both strengthen NiAl at high temperatures and act as ductile rein-

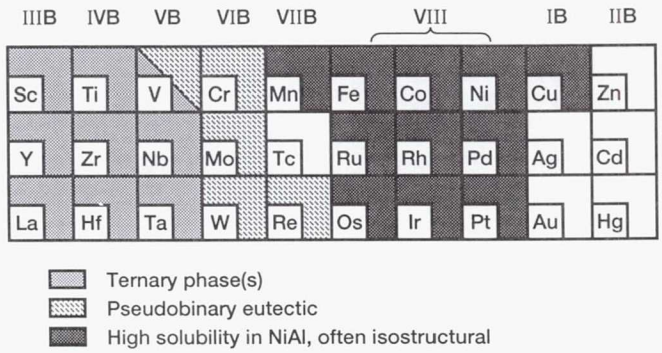

Figure 13.—Portion of the periodic table of elements illustrating general alloying behavior of ternary additions to NiAl (Cotton 1991).

forcing agents at low temperatures (Johnson et al. 1993). Finally, group IIIB, IVB, and VB elements have very limited solubility in NiAl and form at least one ternary-ordered intermetallic compound with Ni and Al. The most common of these intermetallics are the Heusler phases, Ni_2AlX, and the Laves phases, NiAlX. These ordered phases are significantly more brittle than NiAl and would, therefore, preclude the development of a ductile-phase toughened material. Nevertheless, NiAl-Heusler and NiAl-Laves alloys are being actively investigated because of their superior creep resistance. In fact, some of the most creep-resistant NiAl-based alloys produced to date are single-crystal NiAl-Heusler compounds (Darolia et al. 1992; Darolia 1993).

Alloy design for creep strength will be discussed in detail in section 5. The remainder of this passage addresses the most common approaches for increasing the ductility and/or toughness of NiAl at ambient temperatures and presents an overview of their relative success.

4.1 Effect of Microalloying Additions on Properties

As discussed in section 3.3 and demonstrated in figure 8, microalloying additions of Fe, Ga, and Mo at the 0.1 to 0.2 at.% level consistently and significantly increase the room-temperature tensile ductility of soft-orientation, single-crystal NiAl. The mechanism for this increase in ductility has not been determined; however, a change in slip vector or even an obvious modification in dislocation morphology has been ruled out (Darolia, Lahrman, and Field 1992). A similar alloying approach with these elements has been attempted on polycrystalline NiAl without success (Schulson 1982; Noebe and Behbehani 1992; Matsugi, Wenman, and Stoloff 1992). The temperature-dependent tensile properties of polycrystalline NiAl microalloyed with 0.1 at.% Fe, Ga, and Zr are shown in figure 14. At this level, Fe and Ga have no beneficial effect on the tensile properties of NiAl: they nominally decrease the room-temperature tensile ductility and slightly increase the BDTT (by approximately 25 K). At a level of 0.28 at.% Fe, the BDTT of the microalloyed material is increased even further to approximately 730 K (Matsugi, Wenman, and Stoloff 1992). Moreover, additions of up to 1 at.% Fe had no effect on the room-temperature fracture toughness of polycrystalline NiAl (Schneibel, Jenkins, and Maziasz 1993).

Whereas microalloying additions of Fe, Ga, and Mo have not improved the fracture toughness or tensile ductility of polycrystalline NiAl, other additions, such as Zr and B, have had an extremely strong, but detrimental, effect on ductility (Bowman et al. 1992; George and Liu 1990). For example, figure 14 demonstrates the effect of Zr on the tensile properties of NiAl when present at a level of only 0.1 at.%. Zirconium not only has a significant influence on the yield strength, but its presence nearly doubles the BDTT of NiAl. Small additions of Mo, La, Y, Re, and Hf to NiAl have also been observed to increase the yield strength, decrease the ductility, and increase the BDTT (Schulson 1982; Mason et al. 1991). Alloying additions of W

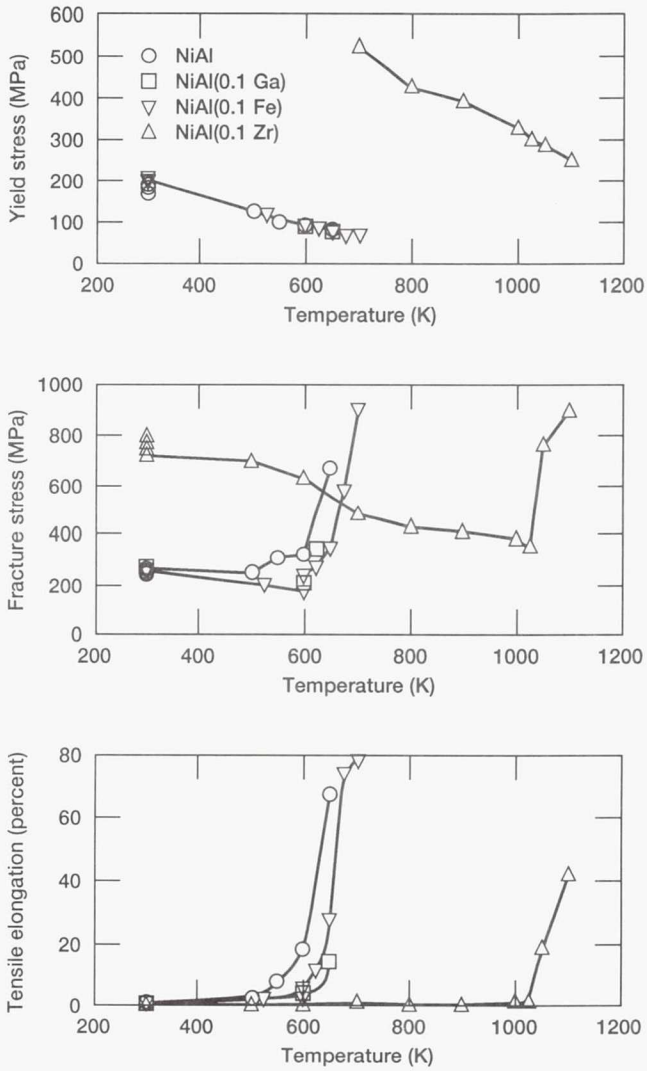

Figure 14.—Effect of test temperature on the 0.2-percent offset yield stress, fracture stress, and tensile elongation of NiAl microalloyed with 0.1 at.% Ga, Fe, or Zr (Noebe and Behbehani 1992).

and Be have no beneficial effect on ductility, though they also do not seem to be detrimental (Mason et al. 1991; George and Liu 1990). This is probably due to the extremely low hardening rate of Be (fig. 5) and the very low solubility of W in NiAl (Locci et al. 1989). Finally, the interstitial element C has an adverse effect on the room-temperature ductility of NiAl (George and Liu 1990), though other interstitial elements such as O and N do not seem to be equally detrimental to tensile properties (Noebe and Garg 1994). Consequently, most alloying elements studied to date seem to reduce the already limited tensile ductility of polycrystalline NiAl, and no additions (except the addition of Mo, Ga, and Fe to single-crystal material) have been identified as being beneficial for ductility.

The major shortcoming in attempting to improve the tensile properties of polycrystalline NiAl through microalloying additions is that the additions are so small that a change in deformation behavior to a slip system that results in five

independent deformation modes is not expected. Therefore, the grain boundary compatibility problem, which is a limiting factor in the low-temperature ductility of polycrystalline NiAl, is not resolved. Conversely, most microalloying additions have had very dramatic, but deleterious, effects on the mechanical properties of polycrystalline NiAl. In single-crystal NiAl, microalloying additions are suspected of acting as gettering agents for some interstitial impurity. Therefore, the alloying addition does not alter the behavior of the single crystal but getters a detrimental impurity in the intermetallic, permitting NiAl to display its inherent properties. The similarity in the room-temperature tensile properties of high-purity, low-interstitial NiAl and microalloyed single crystals supports this idea with both materials exhibiting 4- to 5-percent tensile elongations, in comparison to 1 percent or less for commercially pure NiAl (Lahrman, Field, and Darolia 1993a; Johnson et al. 1993).

4.2 Effect of Macroalloying Additions on Slip Character

Another strategy for improving the ductility and toughness of polycrystalline NiAl is to add ternary macroalloying elements to enhance or modify the slip processes (Law and Blackburn 1987; Cotton, Noebe, and Kaufman 1993b). The general approach has been to identify elements that should lower the ordering energy of NiAl, thus making <111> slip easier. Cr, Mn, and V are reasonable choices for promoting <111> slip in NiAl, based on calculations resulting from interatomic potential models (Hong and Freeman 1991). These models demonstrate that up to 70-percent reductions in antiphase boundary energy are possible when alloying additions of at least 17 at.% are substituted for Ni or Al. In reality, such large alloying additions are not possible. The solubility of Cr in NiAl is approximately 1 to 2 at.% on either sublattice (Cotton, Noebe, and Kaufman 1993c). The solubility of V is about 5 to 12 at.% when substituted for Al and is essentially zero when substituted for Ni (Cotton, Kaufman, and Noebe 1991). According to calculations, V substituted for Ni would be the preferred substitution method for lowering the antiphase boundary energy.

In spite of the low solubility for Cr in NiAl, but in apparent agreement with the concept just presented, <111> slip has been reported in polycrystalline NiAl alloyed with approximately 5 at.% Cr or Mn (Law and Blackburn 1987). Although the operation of <111> slip satisfies the requirement for generalized polycrystalline plasticity, no tensile ductility was reported in these materials at low temperatures. However, a change in fracture mode from intergranular to transgranular cleavage was observed. According to figure 10, a change in fracture mode would not be unexpected because the yield strength of the alloy was greatly affected by the alloying additions.

Nevertheless, this result prompted more detailed work on NiAl(Cr) alloys by Cotton et al. (1993a-c). In this more recent work, analysis of over 2000 dislocation segments in deformed NiAl(Cr) alloys covering 16 different ternary alloy compositions failed to identify any significant <111> dislocation activity. To eliminate any chance that processing or chemistry effects could influence slip behavior, Cotton, Noebe, and Kaufman (1993b) also examined a piece of the original casting studied by Law and Blackburn. Again, no evidence of <111> dislocations was observed in the as-cast or deformed material. Therefore, in spite of Law and Blackburn's contention in 1987, Cr additions to NiAl do not promote <111> slip.

Iron would be another obvious alloying addition for slip alteration because B2 FeAl alloys deform by <111> slip (Crimp and Vedula 1991). However, single-phase ß-Ni-Fe-Al alloys like binary NiAl exhibit only 0- to 2.5-percent tensile ductility at room temperature (Guha, Munroe, and Baker 1991; Russell et al. 1991; Raj, Locci, and Noebe 1992). The observed slip vector in these Ni-Fe-Al alloys was <100> so that the ternary alloys were still slip system limited. The slip behavior of a series of polycrystalline (Ni,Fe)-40Al alloys was also examined by Patrick et al. (1991), who concluded that <100> slip is dominant in these B2-phase alloys containing up to 40 at.% Fe. Despite the lack of tensile ductility, ternary Ni-Fe-Al alloys may exhibit very high toughness levels, approaching 25 MPa$\sqrt{m}$ in fine-grained material (Kostrubanic et al. 1991).

Other studies that are usually referenced to support the operation of <111> slip in NiAl due to Cr or V additions were performed on [001]-oriented single crystals (Field, Lahrman, and Darolia 1991c; Miracle, Russell, and Law 1989). Because <111> is already the preferred slip vector in this crystal orientation, no conclusion about the influence of alloying on slip mode can be drawn from these studies. Therefore, alloying of NiAl to alter the operative slip vector has been unsuccessful to date. Not only is the slip system left unchanged, but the BDTT of NiAl macroalloyed with Cr (Cotton, Noebe, and Kaufman 1993b) and Fe (Raj, Locci, and Noebe 1992) is significantly higher than that of binary NiAl. However, little effort has been expended to date on NiAl(Mn) alloys. Because of the much greater solubility of Mn in NiAl in comparison to either Cr or V (Chakrabarti 1977), more extensive investigation of Mn on the slip behavior of NiAl is warranted.

4.3 Microstructural Modification

Instead of trying to alter the inherent properties of the intermetallic, an alternate approach to improving the ductility and toughness of NiAl is to modify the microstructure of the material. The idea is to improve the mechanical behavior of NiAl through extrinsic toughening mechanisms. This approach includes microstructural variations from fine-grained materials to multiphase microstructures.

Grain refinement is one of the oldest techniques recognized for improving the ductility and toughness of metals (Cottrell 1958). On the basis of this approach, Schulson (1981) suggested that grain refinement could also be used to increase the tensile ductility of brittle intermetallics like NiAl. However, grain size has a critical effect on the ductility of NiAl only within the

550 to 750 K window, which is generally defined as the BDTT for polycrystalline binary NiAl (Schulson and Barker 1983; Schulson 1985). Even though room-temperature tensile ductility was not achieved in these original tests by Schulson and Barker (1983), the results are often quoted to support a critical grain size for room-temperature NiAl ductility. However, further testing of extruded NiAl castings or powder demonstrated that room-temperature tensile ductility is essentially independent of grain size (Nagpal and Baker 1990b; Noebe et al. 1991), at least within the range of grain sizes that can be realistically achieved by conventional processing methods. In addition, the room-temperature fracture toughness of Ni-45Al is independent of grain size in the range of 20 to 2000 μm (Rigney and Lewandowski 1992a).

Chan (1990a) developed a quantitative model based on a critical J-integral approach that accurately predicts the dependence of tensile ductility on grain size for semi-brittle materials. Application of Chan's model to NiAl makes it clear that grain size affects ductility in markedly different ways depending on the temperature range (Noebe et al. 1991). Above the BDTT, there is a strong dependence of tensile ductility on grain size for NiAl because of the higher fracture toughness; however, at room temperature there is very little dependence of ductility on grain size for grain sizes greater than 1 μm. Although room-temperature ductility is predicted to slightly increase when the grain size decreases below 1 μm, tensile ductility is predicted to be only about 5 percent for a grain size of approximately 0.1 μm. Because it would be extremely difficult to keep such a fine grain size from coarsening during processing and service exposure, grain-size refinement alone does not seem to be a practical method for significantly improving the ductility of NiAl at room temperature.

An alternative approach to increasing ductility is to develop two-phase microstructures where toughness is enhanced through crack interactions with a ductile second phase. Toughness would be improved by such processes as crack bridging, crack blunting, or crack deflection. An example of an intermetallic system that has been successfully toughened by such an approach is Ti_3Al, which was toughened by using a Ti-24Al-11Nb or similar alloy composition (Chan 1990b). As yet, a successful counterpart to this system has not been identified for NiAl, though significant work is ongoing in this area. Because the development of two-phase NiAl-based alloys has been reviewed previously (Noebe, Misra, and Gibala 1991), only a brief discussion centering on more recent advances is presented.

One has only to look at the binary Ni-Al phase diagram to find a model system for ductile reinforcement of NiAl. Within the single-phase regime, deviations from stoichiometry have no apparent effect on the toughness of NiAl. However, the fracture toughness of polycrystalline NiAl can be increased by going to two-phase, Ni-rich compositions (fig. 15). There are several possible toughening mechanisms responsible for the increased toughness in this regime. A toughness of approximately 9 $MPa\sqrt{m}$ has been reported for quenched single-phase ß-alloys with 61.5 at.% Ni because of martensitic transformation toughening (Kumar, Mannan, and Viswanadham 1992). However, because of the small volume increase during the NiAl to martensite transformation (Chakravorty and Wayman 1976), only a small increase in toughness results from this mechanism. The toughness and ductility of Ni-rich Ni-Al alloys

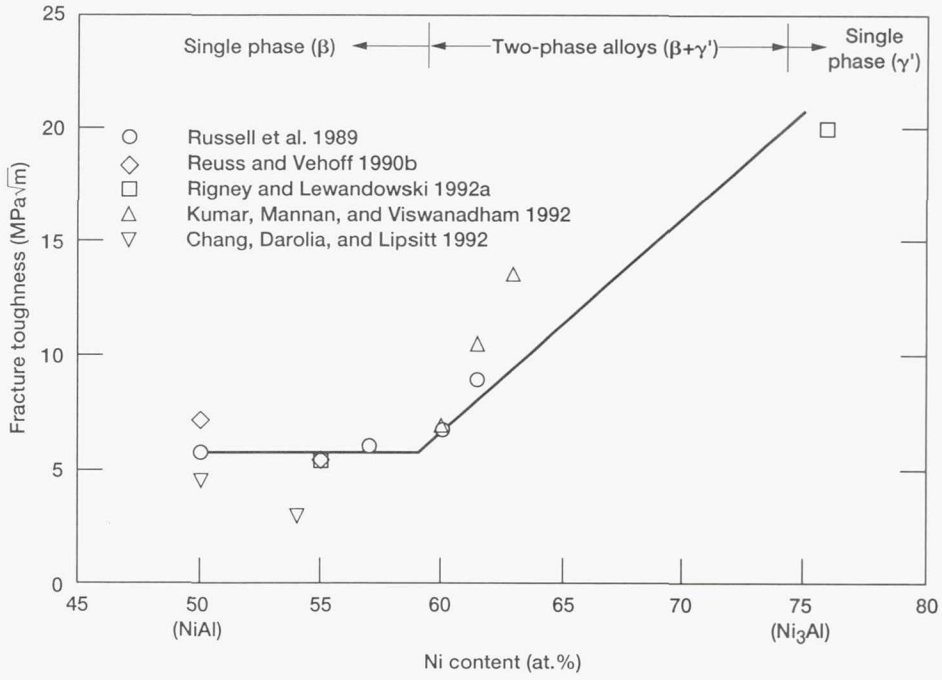

Figure 15.—Room-temperature fracture toughness of Ni-Al alloys as a function of stoichiometry.

can be increased best by the formation of a two-phase microstructure. In directionally solidified materials, room-temperature tensile ductilities of 10 percent have been achieved in a binary Ni-30Al alloy consisting of aligned γ' rods in a NiAl matrix (Noebe, Misra, and Gibala 1991). Conventionally processed, two-phase, polycrystalline Ni-Al alloys consist of a Ni_3Al necklace structure surrounding ß-grains, with fracture toughness increasing roughly proportional to the amount of γ' phase present (fig. 15). Fracture toughness values as high as 25 MPa$\sqrt{m}$ also have been measured in two-phase (γ'+ ß) Ni-Al-Co alloys (Russell et al. 1989). The increased toughness and ductility of these two-phase alloys can be attributed to typical ductile-phase toughening mechanisms such as crack bridging and crack blunting as well as to an additional mechanism known as slip transfer (Misra, Noebe, and Gibala 1993). During this last process, dislocation activity in the ductile phase initiates slip in the ß-phase, thus increasing the plasticity of the overall alloy.

Brittleness in NiAl can be traced to a dislocation initiation problem as opposed to a dislocation mobility problem. This was originally demonstrated in surface film softening studies (Noebe and Gibala 1986). Other studies, including prestrain experiments on single-crystal NiAl (Hack, Brzeski, and Darolia 1992) and pressurization experiments on polycrystalline NiAl (Margevicius and Lewandowski 1993), also illustrate that the lack of tensile ductility in NiAl is, in part, due to dislocation initiation problems. Consequently, slip transfer mechanisms could increase the inherent toughness of NiAl because they directly address the problem of slip initiation.

However, a two-phase alloy can be less tough than NiAl if the reinforcing phase has poor toughness, especially when the brittle second phase is of significant volume fraction and strongly bonded. For example, toughness values similar or less than that of binary NiAl have been observed in two-phase NiAl/NiAlNb alloys (Reuss and Vehoff 1990a) and in NiAl/NiAlTa eutectics (Johnson et al. 1993). In these alloys, cracks run easily through the brittle reinforcing phase and the solid-solution-strengthened NiAl phase.

In certain instances, limited toughening attributed to crack-deflection mechanisms has been observed in NiAl alloys because of the presence of brittle second phases, though this is generally an inefficient way of increasing toughness. Kumar, Mannan, and Viswanadham (1992) found that 1-µm-diameter TiB_2 particulates had essentially no effect on the room-temperature fracture toughness of NiAl but that Al_2O_3 whisker reinforcement increased toughness 50 percent when present in volume fractions of 15 to 25 vol %. Rigney and Lewandowski (1992b) noted that in two out of three heats of NiAl/TiB_2 particulate-reinforced material, no statistically significant increase in toughness was achieved. In one heat, toughness increased 40 percent, but the increase in toughness was attributed to the clustering of TiB_2 particles, leading to a "fiberlike" toughening response.

Fiberlike or semicontinuous reinforcements, if brittle but weakly bonded or tough and strongly bonded, provide greater toughening than particulates because cracks cannot circumvent the reinforcement as easily. Therefore, a natural extension of high-aspect-ratio reinforcements would be continuous-fiber-reinforced NiAl alloys. Somewhat similar, naturally occurring materials can also be produced by eutectic solidification processing. For example, when a NiAl-9Mo eutectic is arc melted it has a fracture toughness of approximately 9 MPa$\sqrt{m}$ (Subramanian et al. 1990). But after directional solidification, the eutectic composite consists of ~11 vol % of 1-µm-diameter rods in a single-crystal NiAl matrix and has a fracture toughness of 15 MPa$\sqrt{m}$ because of crack bridging and the ductile rupture of the Mo ligaments (Darolia et al. 1992). However, increasing the Mo content beyond the eutectic composition does not produce additional toughening (Johnson et al. 1992). Directionally solidified eutectics containing larger volume fractions of a refractory metal phase demonstrate similar or higher levels of toughness. For example, NiAl-Cr eutectics have a toughness of approximately 18 MPa$\sqrt{m}$ (Darolia et al. 1992), whereas a fracture toughness of 31 MPa$\sqrt{m}$ has been measured in a NiAl-V eutectic alloy (Johnson et al. 1992).

5. Creep

Adequate creep resistance is another critical requirement for the extended use of NiAl in elevated-temperature structural applications. Consequently, high-temperature mechanical properties have been studied extensively. This has led to significant progress in developing creep-resistant NiAl alloys in recent years. To help the reader fully appreciate and understand the work performed in this area, the basic creep mechanisms in NiAl are described; then the various strategies used for improving high-temperature strength are analyzed.

5.1 Creep Mechanisms in NiAl

Creep behavior in B2 aluminides, which is analogous to that for metals and alloys, can be analyzed accordingly. The second stage, or steady-state creep rate $\dot{\varepsilon}$, is usually expressed as a form of the Dorn equation:

$$\dot{\varepsilon} = A(\sigma/E)^n \exp(-Q/RT)$$

where σ is the applied stress, E is the Young's modulus, n is the stress exponent, Q is the activation energy for creep, R is the gas constant, T is the absolute temperature, and A is a constant that takes into account such variables as microstructure and stacking fault or antiphase boundary energy. The values for n and Q depend on the operative deformation mechanisms within a given temperature and stress regime and thus, are useful indicators of deformation mode. Creep is most commonly controlled by diffusion; hence the value of Q for creep is often similar to that for diffusion Q_D. Therefore, knowledge of diffusion behavior also is desirable as an aid to understanding creep processes.

Diffusion data for NiAl have been compiled and discussed previously (Noebe, Bowman, and Nathal 1993; Miracle 1993). Unfortunately, no new experimental data have been generated for a number of years. Additional work is required to determine the activation energy and mechanisms of diffusion at lower temperatures because almost no data exist for diffusion in NiAl below 1200 K. From previous studies (Hancock and McDonnell 1971; Lutze-Birk and Jacobi 1975; Berkowitz, Jaumot, and Nix 1954), it appears that the activation energy for diffusion is a maximum at Ni-50Al, consistent with the diffusion coefficient minima at the same composition. Although there is considerable scatter among the various diffusion studies, critical analysis of the available data for NiAl indicates that the most likely range for Q_D is on the order of 250 to 300 kJ/mol.

Table III summarizes the stress exponents and activation energies for the high-temperature deformation of NiAl. The average value for the activation energy of creep is approximately 315 kJ/mol. However, the data in table III have not been corrected for the temperature dependence of the elastic modulus, which would reduce Q by 20 to 30 kJ/mol, thus bringing Q well within the range of data for bulk diffusion.

Dislocation creep in single-phase metals and alloys can usually be classified as one of two main types; class M, or pure metal creep, and class A, or alloy type behavior (Mohamed and Langdon 1974). Class M creep is characterized by glide being much faster than climb; thus creep is controlled by the rate of dislocation climb past substructural obstacles. Class A creep is often called viscous-glide-controlled creep because the glide of dislocations is restricted by solute atoms or perhaps by a high lattice friction stress because of long-range order. This reduced glide mobility is the limiting creep process, whereas climb can occur readily. These two types of behavior can be distinguished by several criteria including the stress exponent, the shape of the primary creep curve, the formation of a dislocation substructure, and the response of the material to stress or strain rate transients.

Figure 16 summarizes measured and interpolated creep data for binary NiAl at 1175 K. Most of the data fall within reasonable agreement, with no more than a factor of 5 difference in creep rate at a given stress level—except for the strengths reported by Vandervoort, Mukherjee, and Dorn (1966), which are abnormally weak for no known reason. The alloys in figure 16 also have similar stress exponents, about 4.5 to 6, except for a transition to a lower stress exponent at the lowest stress levels. Examination of the stress exponents in table III for materials with a wide variety of grain sizes, including single crystals, reveals that between 1100 to 1400 K, the values for n cluster between 5 and 7. Class A materials are usually characterized by a stress exponent of 3, whereas class M behavior is typically characterized by a stress exponent of 5. Although a stress exponent of 7 is higher than is characteristic for class M behavior, such high values have been observed in several class M materials (Ashby 1972). Observations of subgrain formation after high-temperature deformation (Kanne, Strutt, and Dodd 1969; Yang and Dodd 1973); operation of normal primary creep behavior under both constant load and constant crosshead speed tests (Strutt, Dodd, and Rowe 1970; Whittenberger 1987,1988); strain rate transient test results (Yaney and Nix 1988; Forbes et al. 1993); and strengthening via a reduction in grain size (Whittenberger 1988) are all consistent with class M behavior. Consequently, high-temperature creep in binary NiAl is apparently climb controlled over most stresses and temperatures.

Forbes et al. (1993) argue that creep deformation in single-crystal NiAl is a mixture of both class A and M behavior, with the relative proportions of each type dependent on crystal orientation and the stress/temperature regime. Both Forbes et al. (1993) and Vandervoort, Mukherjee, and Dorn (1966) show a gradual decrease in stress exponent, approaching $n \simeq 3$ at high temperatures (1400 to 1500 K), which is consistent with this idea. However, it remains to be determined whether the viscous glide contribution is significant in cases other than soft-orientation single crystals, where subgrain formation is suppressed because of the limited availability of slip systems.

At stresses that are too low for dislocation processes to be significant, time-dependent deformation also can occur by

TABLE III.—SUMMARY OF CREEP PARAMETERS FOR NiAl

Al content at.%	Grain size, μm	Temperature, K	Stress exponent, n	Activation energy for creep, Q, kJ/mol	Reference
48.25	5 to 9	1000 to 1400	6.0 to 7.5	313	Whittenberger (1988)
44 to 50.6	15 to 20	1100 to 1400	5.75	314	Whittenberger (1987)
50	12	1200 to 1300	6	350	Whittenberger et al. (1990)
50	450	1073 to 1318	10.2 to 4.6	283	Yang and Dodd (1973)
50	500	1173	4.7	----	Rudy and Sauthoff (1985)
50.4	1000	1075 to 1750	7.0 to 3.3	230 to 290	Vandervoort, Mukherjee, and Dorn (1966)
50	SX [123]	1023 to 1223	7.7 to 5.4	----	Hocking, Strutt, and Dodd (1971)
50	SX [multiple]	1023 to 1328	4.0 to 4.5	293	Bevk, Dodd, and Strutt (1973)
50	SX [001]	1000 to 1300	6	440	Whittenberger and Noebe (1991)
50	SX [001]	1123 to 1473	3 to 7	305	Forbes et al. (1993)
50	SX [223]	1123 to 1473	3 to 7	330	Forbes et al. (1993)

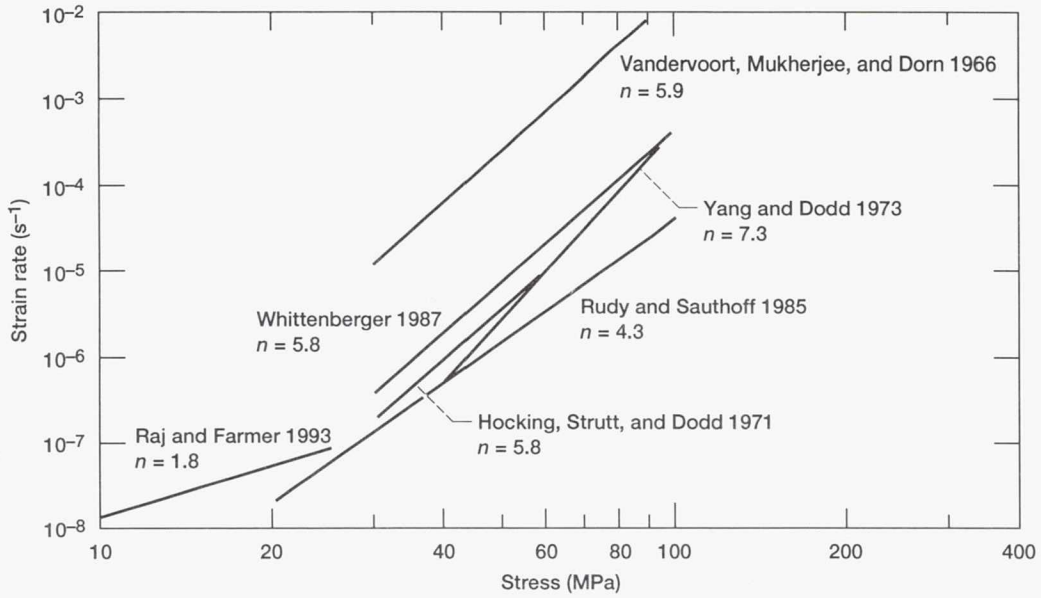

Figure 16.—Measured or interpolated creep behavior of near-stoichiometric NiAl at 1175 K.

stress-assisted vacancy flow. Creep by these diffusional mechanisms, such as Nabarro-Herring or Coble creep, is attributed solely to the movement of vacancies from sources to sinks, which are usually grain boundaries that have different orientations than that of the applied stress. These mechanisms are characterized by a stress exponent of $n = 1$ and a clear dependence of creep strength on grain size, with large-grained materials being more creep resistant.

Evidence for the operation of diffusional creep mechanisms in B2 alloys was reported by Rudy and Sauthoff (1985), who observed $n = 1$ for their experiments with a Ni-20Fe-50Al alloy. Some recent data at very low stress levels for NiAl revealed that the stress exponent was between 1.6 and 2.1 (Raj and Farmer 1993), which indicates the operation of a grain-boundary-assisted deformation mechanism. In addition, there is evidence of diffusional creep processes in binary NiAl at temperatures above 1300 K and at low strain rates, where grain growth during creep testing resulted in coarser grained material with higher strengths (Whittenberger 1987). Therefore, the limited data generated to date indicate that diffusional creep may occur in polycrystalline NiAl at $T > 1200$ K and at very low stresses.

One final point about the creep behavior of binary NiAl is worth noting. Unlike most NiAl properties, creep rate is roughly independent of stoichiometry for a broad range in composition, between about 45 and 51 at.% Al (Yang and Dodd 1973; Whittenberger 1987; Whittenberger, Kumar, and Mannan 1991a). The largest difference in creep rates within this range of compositions is about a factor of 5. Only at very low and high Al contents are nonstoichiometric alloys noticeably weaker (Whittenberger, Noebe, Cullers, Kumar and Mannan 1991; Whittenberger, Kumar, and Mannan 1991a). This loss in strength is most easily explained by the lower melting points of these compositions, which in turn implies a higher diffusivity. The diffusivity data for NiAl (Hancock and McDonnell 1971; Lutze-Birk and Jacobi 1975; Berkowitz, Jaumot, and Nix 1954) actually imply a more significant effect on properties than is observed. Nevertheless, these trends in strength as a function of stoichiometry are reversed from those observed at lower temperatures, where defect hardening predominates (Pascoe and Newey 1968b).

5.2 Design of Creep-Resistant NiAl-Based Alloys

As progressive alloying changes are made from pure Ni to a Ni-base superalloy, creep rate decreases by about 8 orders of magnitude. The formation of a second phase is one of the major reasons for this improvement (Nathal, Diaz, and Miner 1989). Comparable improvements in creep strength by similar alloying strategies are necessary for nickel aluminides to compete effectively with current superalloys. To measure progress in this direction, figures 17 and 18 compare the 1300 K creep strengths of NiAl-based materials (which were generated primarily in compression) to the tensile creep response of a first-generation, single-crystal superalloy (Nathal and Ebert 1985) and a range of polycrystalline superalloys typically used in engine applications, including IN100 and Udimet 700. The boxed regions in these figures represent the range in creep strengths observed for a given strengthening mechanism, whereas the angle of the box indicates the resulting stress exponents. More detailed comparisons of the various strengthening mechanisms in NiAl are given in a previous review (Nathal 1992).

Figure 17 summarizes the effects of alloying on the creep behavior of NiAl. The effects of solid-solution hardening by Fe, Nb, Ta, Ti, and Zr on creep strength were studied (Jung,

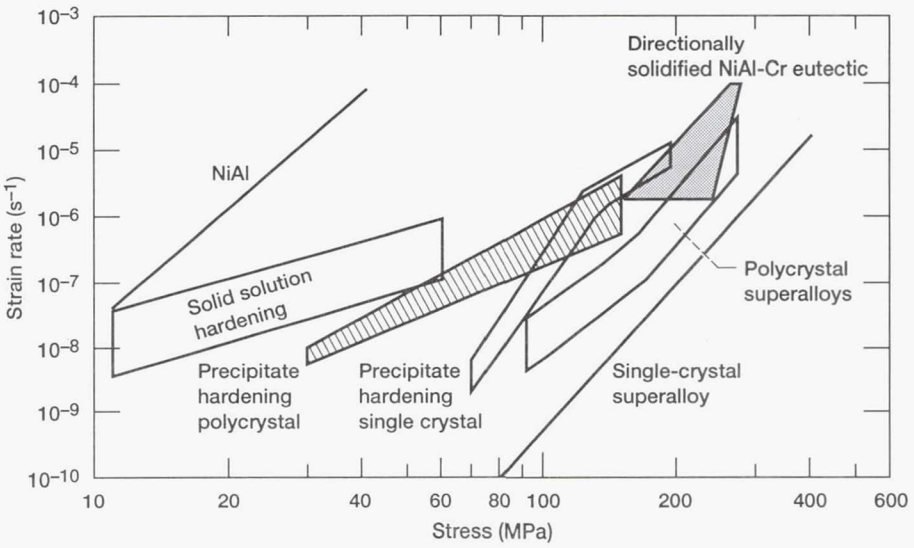

Figure 17.—Effects of alloying on the creep behavior of NiAl at 1300 K. Both solid-solution alloys and precipitation-hardened NiAl-based materials are included in the figure.

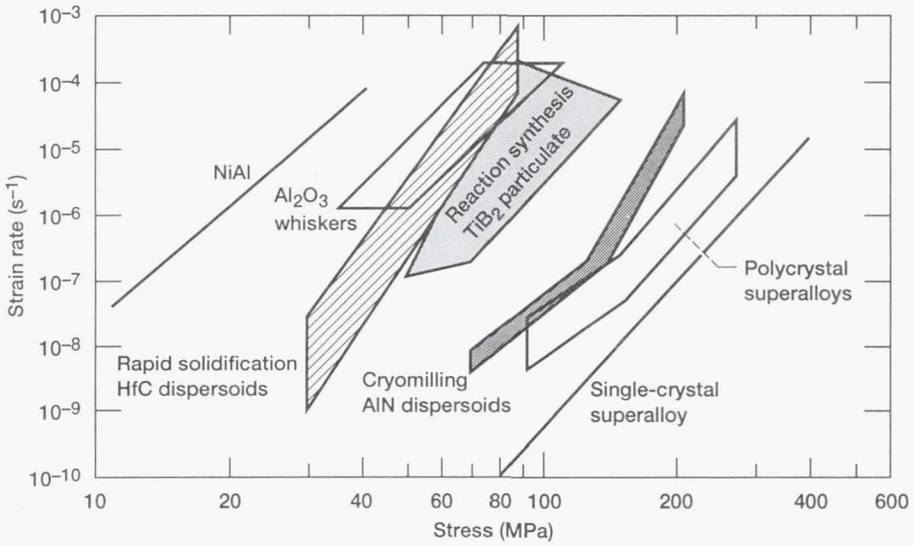

Figure 18.—Effect of composite strengthening and second-phase reinforcement on the creep behavior of NiAl at 1300 K.

Rudy, and Sauthoff 1987; Pathare 1988; Whittenberger et al. 1989; unpublished research by J.D. Whittenberger and R.D. Noebe, 1991, NASA Lewis Research Center, Cleveland, OH). All the solid-solution alloys were stronger than binary NiAl, but their stress exponents decreased to values near 3 to 4. Apparently, these solute additions altered the creep process in NiAl to a viscous drag mechanism, in a manner very similar to that which occurs when alloying elements are added to pure metals. In one recent study, a transition from class M to class A behavior was observed in the ternary B2 alloy Ni-20Fe-30Al as a function of applied stress (Raj, Locci, and Noebe 1992). This transition appears to be well described by current theories developed for disordered solid solutions (Mohamed and Langdon 1974). Although solid-solution hardening does improve creep strength over binary NiAl, it is inadequate by itself and must be used in combination with other strengthening mechanisms to compete with superalloys.

The use of precipitation hardening to significantly improve the creep strength of NiAl was first demonstrated by Polvani, Tzeng, and Strutt (1976). They added Ti to NiAl, forming a two-phase mixture of NiAl and the Heusler phase Ni_2AlTi, resulting in a substantial increase in creep strength. Additional Heusler phases and other intermetallic compounds such as Laves (e.g., NiAlX) can be formed with ternary additions such as Nb, Ta, Hf, Zr, and V. The range of creep properties observed for precipitation-hardened polycrystalline alloys (Polvani, Tzeng,

and Strutt 1976; Pathare 1988; Whittenberger et al. 1989) are shown in figure 17. These materials are reasonably strong, but the advantage diminishes when the data are extrapolated to low stresses because of the low stress exponent. It is not entirely clear why these alloys exhibit such low n values, because most creep-resistant, two-phase alloys exhibit significantly higher stress exponents than the matrix phase does. In most cases, the microstructures of the ternary alloys were probably not optimized. For example, if the second phase is too coarse, effective strengthening would not be expected. An equally valid explanation may be that the observed n values represent a superposition of several deformation mechanisms. By analogy to the superalloys, optimizing the creep strength requires a balance between the compositions of the two phases, the precipitate volume fraction, and the size and distribution of the precipitates.

One well-known strategy for improving creep strength is to eliminate grain boundaries by directional solidification. Yet surprisingly, binary NiAl, single crystals have little or no creep strength advantages over polycrystalline material (Whittenberger, Noebe, Cullers, Kumar, and Mannan 1991). However, a significant advantage in strength is obtained through single-crystal processing of alloyed NiAl. Figure 17 compares the creep response of the Heusler-containing NiAl alloy (containing 1 at.% Hf) in both polycrystalline (Whittenberger, Nathal, Raj, and Pathare 1991) and single-crystal form (Locci et al. 1993), the polycrystalline data falling within the band for precipitation hardening of polycrystals. The single-crystal version is not only stronger than the polycrystalline equivalent, but it displays a significantly higher stress exponent, presumably because grain boundary deformation mechanisms have been eliminated. Figure 19 summarizes the progress made in developing creep-resistant NiAl alloys (Darolia et al. 1992; Darolia 1993). Unlike figures 17 and 18, which rely heavily on compressive creep properties, figure 19 plots tensile rupture stress for single-crystal NiAl alloys versus the Larson-Miller parameter, which takes into account both time to failure and temperature. Through alloying strategies similar to the development of superalloys, NiAl alloys have been produced with greater than polycrystalline René 80 strength levels. The strength advantage of NiAl over superalloys is even more significant when the data are normalized with respect to density.

Anisotropy in creep strength is another factor that may be exploited with single crystals. Certain orientations may have higher creep strengths that could be used to advantage in applications such as turbine blades. During experiments with single-phase binary compounds at temperatures above approximately 1050 K, some investigators have observed significantly higher creep strengths for hard-orientation crystals (Strutt, Dodd, and Rowe 1970; Forbes et al. 1993). However, other investigators have not observed significant anisotropy (Pascoe and Newey 1968b; Whittenberger, Noebe, Cullers, Kumar, and Mannan 1991).

One reason for these discrepancies is the basic definition of strength used in the various studies (personal communication with K.R. Forbes, 1993, Stanford University, Stanford, CA). For example, above 1200 K the yield strengths of [001] single crystals, soft-orientation single crystals, and polycrystalline NiAl are all similar (fig. 3); but there is a large difference in strength at large strains because of differences in work hardening rates. At high temperatures, soft-orientation single crystals work soften appreciably, polycrystals reach a steady-state stress level just beyond the yield point, and hard-orientation single crystals strain harden considerably. Therefore, although the yield

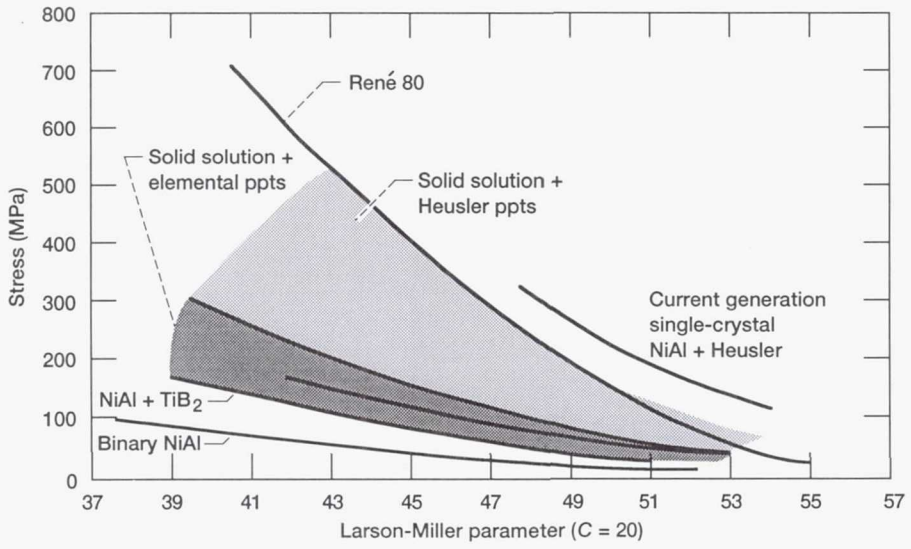

Figure 19.—Tensile stress rupture properties of single-crystal NiAl alloys and a NiAl/TiB_2 composite compared with superalloy René 80. The Larson-Miller parameter is calculated as $(T_R/1000)(\log t + 20)$, where T_R is the absolute temperature in Rankine and t is the time to rupture in hours (after Darolia et al. 1992 and Darolia 1993).

strength of all these forms of binary NiAl are nearly equivalent, the steady-state creep strengths determined at large strains (>10-percent) are significantly different. At 1300 K and a given stress level, the steady-state creep rate for polycrystalline NiAl is at least an order of magnitude lower than for [223]-oriented single crystals, and [001] single crystals have a minimum creep rate about an order of magnitude lower than that of polycrystalline NiAl (personal communication with K.R. Forbes, 1993, Stanford University, Stanford, CA). This difference in creep strength is due to the degree to which a dislocation substructure is formed in the various materials. Forbes et al. (1993) reported that a dislocation substructure formed during creep of hard-orientation single crystals but not during creep of soft crystals regardless of whether the samples were tested in tension or compression. The formation of a dislocation substructure along with the reduced mobility of <011> dislocations that operate in hard-orientation crystals can explain the increased creep strength of the hard-orientation NiAl single crystals over soft orientations or polycrystalline material (Forbes and Nix 1993).

A variation on single crystal processing that incorporates a second phase for strengthening is to form an in-situ composite by directionally solidifying eutectic alloys. In their early work, Walter and Cline (1970) showed that a eutectic consisting of α-Cr rods in a NiAl matrix has promising creep properties (fig. 17). However, good creep strength is only maintained as long as the Cr rods are continuous in nature—not just short fibers aligned parallel to the growth direction (Johnson et al. 1992). In addition, rod-type and lamellar eutectic microstructures can be produced in NiAl by directionally solidifying NiAl containing W, Mo, Re, V, NiAlNb, NiAlTa, or other intermetallic phases; and these microstructures may significantly increase the creep resistance of NiAl. For example, in NiAl/NiAlNb alloys, changing the processing from casting plus extrusion to directional solidification significantly improved both the creep strength and the stress exponent, even when the second phase was only partially aligned (Whittenberger, Westfall, and Nathal 1989; Whittenberger et al. 1992).

The effects of inert second phases (other than precipitates) on the creep strength of NiAl are summarized in figure 18. Rapid solidification, one method for fabricating two-component alloys, can produce very fine dispersions of second-phase particles, with diameters ranging from 20 to 50 nm. These particles usually resist coarsening because of their very low solubility in the matrix. For NiAl, pure elements, such as W and Mo, and various carbides or borides are candidates for this type of strategy. Experiments have determined that TiC and TiB_2 dispersoids (Whittenberger, Gaydosh, and Kumar 1990) have very little strengthening effect, but dispersions of HfB_2 and HfC resulted in considerable improvements in creep strength in comparison to binary NiAl (Whittenberger, Ray, Jha, and Draper 1991; Whittenberger, Ray, and Jha 1992). These studies also revealed that HfC-strengthened, coarse-grained NiAl was more creep resistant than the finer grained material.

The common mechanism for improved creep resistance of dispersion-strengthened alloys is related primarily to the interaction of the dispersoids with mobile dislocations and subgrain boundaries. However, it is probably not a coincidence that the two most effective dispersoids contained Hf—a very potent solid-solution strengthening agent. To date, the use of rapid solidification to dispersion strengthen NiAl has not provided sufficient creep resistance for NiAl to compete effectively with superalloys (fig. 18). However, its strength may be improved by optimizing the dispersoid volume fractions and devising the thermomechanical processing schedules needed to produce grain structures similar to those that have been proven successful in the oxide dispersion strengthening of Ni-base alloys.

An unusual but effective example of a creep-resistant composite is AlN dispersion-reinforced NiAl, produced by milling NiAl powder in liquid nitrogen followed by high-temperature consolidation (Whittenberger, Arzt, and Luton 1990a,b). This process produces very fine AlN dispersoids, on the order of 50 nm, at relatively high volume fractions of 10 vol % or greater. The particles are not uniformly distributed but clustered along prior particle boundaries surrounding particle-free areas. Creep strengths approaching those of superalloys were obtained with these composites (fig. 18). After correcting for density, the deformation resistance of a typical superalloy and NiAl/AlN are nearly equivalent. It is interesting to note that the consolidation process has relatively no effect on the strength of these materials, at least in compression. Properties of extruded versus hot isostatically pressed (HIP'ed) NiAl/AlN were roughly equivalent (Whittenberger, Arzt, and Luton 1990b). The reasons for the exceptional strength produced by this type of second-phase reinforcement are currently being investigated. Nevertheless, cryomilling of NiAl has proven to be a consistently reproducible method for generating NiAl/AlN composites with very high creep strength (Whittenberger and Luton 1992; Hebsur et al. 1993) as well as excellent oxidation resistance (Lowell, Barrett, and Whittenberger 1990).

Another approach to strengthening metals is the use of discontinuous reinforcements. These reinforcements are typically larger in size and present in higher concentrations than those found in dispersion-strengthened materials. One example is Al_2O_3 whisker-reinforced NiAl (Whittenberger, Mannan, and Kumar 1989; Whittenberger, Kumar, and Mannan 1991b). The whiskers, which had an average aspect ratio of approximately 7.5, were added by mechanical blending at volume fractions ranging from 0 to 25 vol %. Some improvement in creep resistance is seen in figure 18, but it is not very significant. The stress exponents of the NiAl/Al_2O_3 composites were about the same as that of the matrix material. This indicates that deformation is controlled by flow in the matrix, as predicted by several models of composite strengthening (Kelly and Street 1972). These models predict that creep strength may be further improved by increasing the aspect ratio of the whiskers. Because the aspect ratio of the whiskers was reduced during processing due to fracture (Whittenberger, Kumar, and Mannan 1991b), higher strength whiskers will also be needed. Controlling whisker distribution and alignment and limiting

whisker damage during processing are major concerns with this type of composite.

Another type of discontinuous, reinforced composite that has been characterized fairly extensively is NiAl containing 1-μm-diameter TiB_2 particles produced by an exothermic reaction process (Viswanadham et al. 1989; Wang and Arsenault 1990,1991). These composites have improved strength that scales with the amount of reinforcement (Whittenberger et al. 1990). In addition, the stress exponents are all high, indicating that the dislocation substructure was refined and stabilized by the second phase reinforcement. Evidence for this contention has been provided by transmission electron microscopy, where subgrain boundaries pinned by the particles, in combination with a high dislocation content within the subgrains, were characteristic of the deformation structure (Whittenberger et al. 1990). TiB_2-reinforced composites are stronger than Al_2O_3-whisker-containing materials but still fall short of the Ni-base superalloys (fig. 18). As an additional comparison, the tensile rupture strengths of a TiB_2-dispersed alloy (Kumar et al. 1992) are also included in figure 19. This gives a further indication of how far particulate-reinforced composites are from competing with superalloys or even single-crystal NiAl-based alloys.

Finally, tests of hybrid composites containing both TiB_2 particulates and Al_2O_3 whiskers have demonstrated that these strengthening mechanisms are additive (Whittenberger, Kumar, and Mannan 1991b). It should be noted, however, that combining creep-strengthening mechanisms is not always effective. For example, adding TiB_2 particles to a Heusler-phase-(Ni_2AlTi) reinforced NiAl alloy does not improve creep strength (Kumar and Whittenberger 1991).

Various strategies to improve the creep resistance of NiAl have been attempted, although none have been fully optimized. It is clear from these efforts that the poor creep strength exhibited by binary NiAl may be overcome by conventional metallurgical techniques. Of the processes investigated, both solid-solution strengthening and precipitation hardening are relatively ineffective when used with polycrystalline material; however, precipitation-hardened single crystals show extreme promise, exhibiting stress rupture properties superior to many superalloy systems. Rapid solidification combined with alloying has generally resulted in only small improvements in strength, whereas Al_2O_3 whiskers and TiB_2 particulates have provided larger, but still insufficient, advances in creep resistance. Finally, NiAl/AlN composites and alloyed single crystals exhibit some of the best creep properties to date, with specific strengths comparable to first-generation single-crystal superalloys.

6. Fatigue

In many structural applications, materials are subjected to repeated loading or vibration. In complex machinery, such as gas turbine engines, cyclic loading is compounded with the additional effects of creep at high temperatures and environment. Both creep processes and environment have been proven to adversely affect the fatigue behavior of most intermetallic systems studied previously (Stoloff, Smith, and Castagna 1993). Furthermore, even though fatigue is a complicated subject and a critical property for many applications, it is usually one of the last properties to be studied with a new material system. This was the case for NiAl, with fatigue studies beginning only since 1991. Fatigue investigations are a natural extension of the multitude of monotonic deformation studies performed on NiAl, which have led to a significant understanding of the deformation and fracture behavior of this material (section 3). The recent number of fatigue studies also indirectly indicates the maturity of this intermetallic system because substantial quantities of reproducible material are usually necessary for a detailed fatigue investigation. Both single-crystal and polycrystalline NiAl at room and elevated temperatures have been studied under zero-tension or fully reversed loading conditions.

Stress- and strain-controlled fatigue tests of single-crystal NiAl were performed on [001]-oriented Ni-49.9Al-0.1Mo crystals at room temperature and 1033 K (Bain, Field, and Lahrman 1991). At room temperature, the single-crystal NiAl failed elastically because of the high stress necessary for plastic flow in [001]-oriented crystals. At elevated temperatures, the crystals followed the expected Coffin-Manson strain life behavior, typical of conventional Ni-based superalloys, with fatigue lives very similar to those of polycrystalline NiAl (fig. 20).

Room-temperature, total-strain-controlled fatigue testing of soft-orientation single crystals revealed substantial cyclic ductility in [121]-oriented crystals (Smith et al. 1992). The samples hardened continuously during cycling for at least the first 400 cycles, generally reaching stresses 50 percent greater than the initial yield strength (Smith et al. 1992). Failure of these single-crystal NiAl specimens was attributed to the formation of cracks at slip extrusion-intrusions. This type of crack-initiation

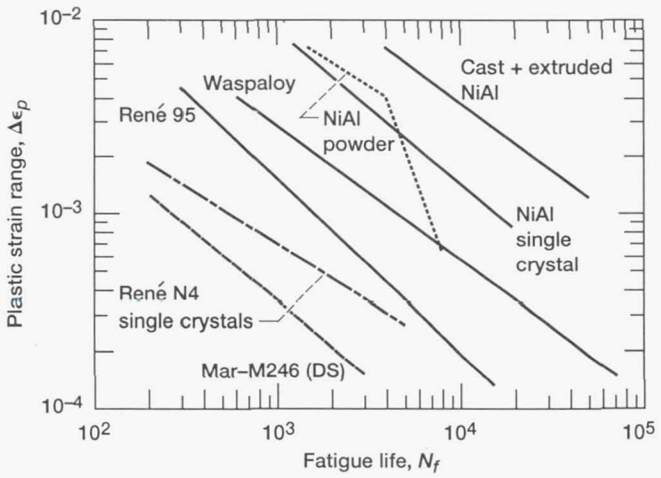

Figure 20.—Fatigue life at nominally 1000 K for NiAl in comparison to Ni-base superalloys and single-crystal NiAl on a plastic strain range basis (Lerch and Noebe 1994).

mechanism appears to be common to many intermetallic systems (Stoloff, Smith, and Castagna 1993).

High-cycle-fatigue (HCF) testing was performed on a high-strength, Hf-containing NiAl alloy with creep rupture properties equivalent to that of Rene'80 (Darolia 1993). At 1253 K the high cycle fatigue properties of the NiAl alloy were similar to those of the Ni-base superalloy. In addition, the material was not sensitive to surface finish because fatigue properties were not degraded when the alloy was tested in the as-electrodischarge-machined condition in comparison to electropolished samples. Preliminary tests indicate that the HCF behavior of this material at room temperature is also quite good (personal communication with R. Darolia, 1992, General Electric Aircraft Engines, Evendale, OH).

Low-cycle-fatigue (LCF) testing of polycrystalline NiAl has been performed at room temperature, near the monotonic BDTT, and at 1000 K. During room-temperature LCF testing, NiAl continuously work hardened during cyclic straining, eventually reaching stress levels that were around 60 percent greater than the monotonic fracture strength (Noebe and Lerch 1992; Edwards and Gibala 1993). The cyclic stress-strain response for NiAl was similar to that of body-centered cubic metals and other B2 alloys, and the fatigue life on a plastic strain range basis was considerably greater than that of comparable B2 intermetallics (Noebe and Lerch 1992). The plastic-strain-range/fatigue-life relation appears to be independent of grain size for cast and extruded NiAl but exhibits a much shallower slope (-0.14) than usually observed for metallic materials (-0.6) (Noebe and Lerch 1992; Edwards 1993). This shallow slope is representative of the brittle fracture behavior of NiAl at room temperature, with fracture initiating at prior defects in the material once a critical stress level was achieved (Lerch and Noebe 1993). In addition, high-cycle fatigue testing of hot-pressed flat sheet specimens of NiAl and NiAl/Al_2O_3 fiber composites was conducted at 0.3 Hz and R = 0 loading conditions under displacement control between prescribed stress ranges (Bowman 1992a). Consistent with other room-temperature studies, long fatigue lives were attained for NiAl when the stresses were kept just below the monotonic fracture stress of the samples. The fatigue tests on both the monolithic and composite samples were interrupted after 100 000 cycles without a measurable loss in compliance in either material.

The cyclic deformation behavior of NiAl was also investigated between 600 and 700 K, representing temperatures just above and below the monotonic BDTT of a powder-extruded alloy (Cullers and Antolovich 1992). Even though monotonic properties change dramatically over this temperature range (figs. 11 and 12), a more gradual transition in fatigue behavior was noted. Increasing the temperature from 600 to 700 K improved fatigue lives slightly and decreased stress response levels. However, the cyclic hardening behavior was similar over this temperature range as was the manner in which the dislocation structure developed. In this temperature range, the material work hardened significantly for the first few cycles, reached a plateau, and finally exhibited an additional region of work hardening very near the end of life. This behavior was traced to the dislocation structure that evolved during fatigue cycling (Cullers, Antolovich, and Noebe 1993). During the initial period of work hardening, the dislocation structure formed into a loose cellular array (fig. 21). These cells developed into well-aligned veins or walls of dense dislocation tangles leading to a period of stress saturation. This was followed, near the end of the sample's life, by a collapse of the vein structure leading to the second period of accelerated work hardening and failure of the sample.

LCF testing of polycrystalline NiAl has also been performed well above the monotonic BDTT (Lerch and Noebe 1994; Noebe and Lerch 1993). At 1000 K, both processing route and environment affected fatigue life. The fatigue lives of NiAl samples, produced by HIP'ing prealloyed powders, were about a factor of 3 less than those of cast and extruded NiAl because of the lower flow stress and thus, a lower crack driving force in the extruded material. An environmental effect was also observed. A factor of 3 increase in fatigue life occurred when HIP'ed powder samples were tested in vacuum instead of air. This increase in fatigue life is indicative of an environmentally assisted fatigue damage mechanism at elevated temperatures. At 1000 K, NiAl exhibits a typical Coffin-Manson strain life behavior; however, below a plastic strain range of about 0.3 percent, the fatigue life of HIP'ed NiAl is less than expected because of additional damage by creep cavitation processes (fig. 20). Consequently, the high-temperature fatigue behavior of NiAl is influenced by both environmental and creep processes. Yet, on a strain range basis, the fatigue lives of both single-crystal and polycrystalline NiAl are longer than those of conventional Ni-based superalloys at a nominal temperature of 1000 K (fig. 20). This advantage is due partly to the higher ductility of NiAl. The disadvantage is that the fatigue lives of binary NiAl would be shorter than those of Ni-based superalloys on a stress range basis because of the higher strength of superalloys at elevated temperatures (Lerch and Noebe 1993).

The poor LCF performance of the related B2 compounds Fe-40Al and Ni-20Fe-30Al (Hartfield-Wunsch and Gibala 1991) first raised concerns about the viability of any B2 alloy as a structural material because of fatigue considerations. However, initial results for both single-crystal and polycrystalline NiAl indicate that its fatigue life is generally equivalent or superior to other intermetallic compounds and other structural materials such as Ni-base superalloys. Consequently, fatigue behavior does not appear to be an area of immediate concern, though research will be continuing in this area for some time. Of particular interest will be fatigue studies on some of the stronger alloys and composites that tend to be less defect tolerant.

7. Environmental Resistance

The excellent oxidation resistance of NiAl-based materials is well known and has been exploited for many years in the

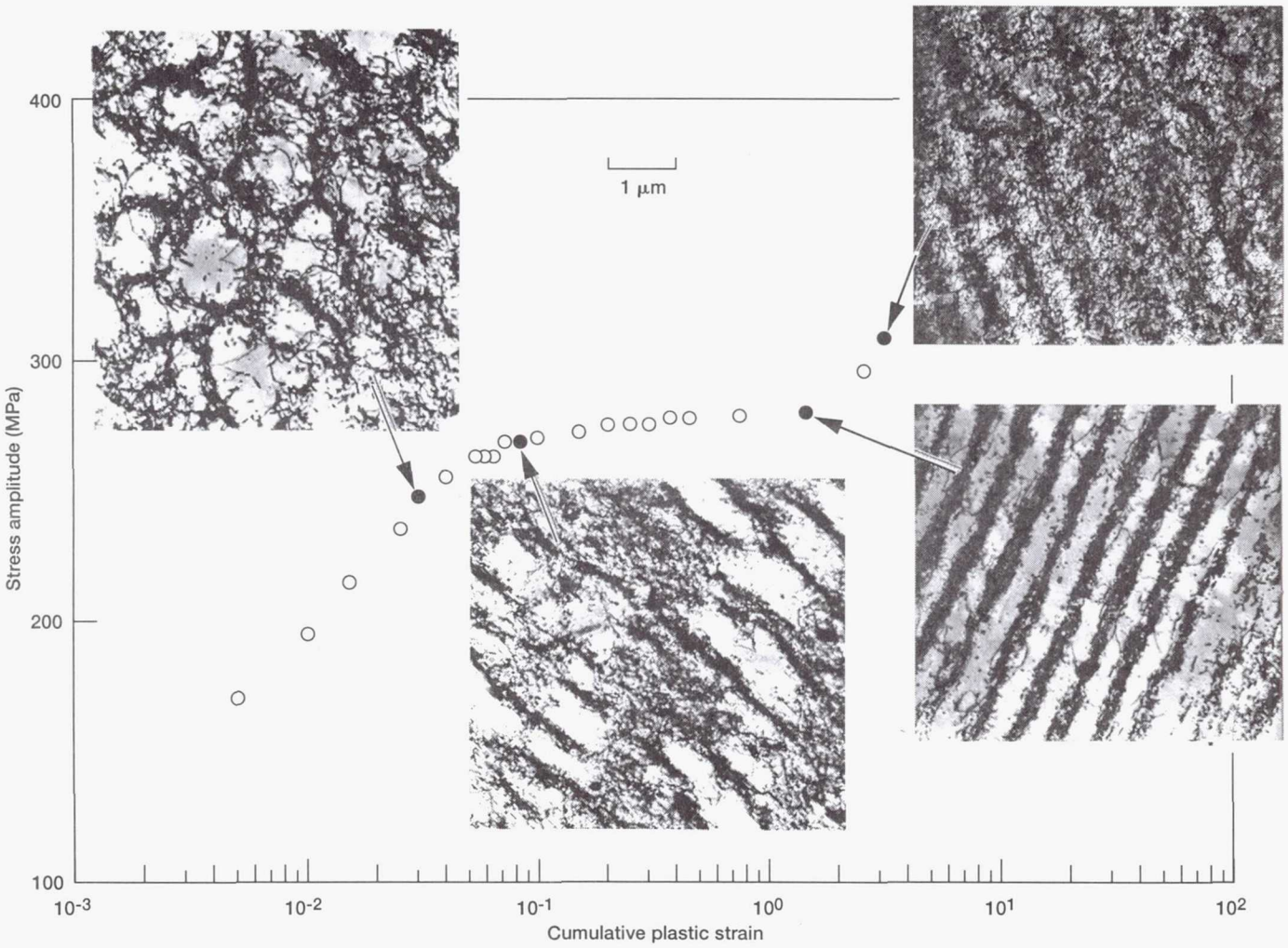

Figure 21.—Cyclic hardening curve for polycrystalline NiAl at 600 K and a plastic strain range, $\Delta\epsilon_p$, of 0.5 percent, and the dislocation microstructures observed at various stages of fatigue life (courtesy of C.L. Cullers).

form of coatings for Ni-base superalloys (Rhys-Jones 1989; Wood and Goldman 1987). The oxidation resistance of NiAl alloys is due to the easy formation and slow growth rate of protective Al_2O_3 scales. At low temperatures, γ-Al_2O_3 is the commonly observed oxide (Doychak, Smialek, and Mitchell 1989; Brumm and Grabke 1992). At temperatures near 1200 K, θ-Al_2O_3 appears to be the predominant oxide in mature scales, but at higher temperatures, α-Al_2O_3 is formed (Rybicki and Smialek 1989). Figure 22 compares the parabolic growth rate constants k_p for the higher temperature α-phase and the faster growing, lower temperature θ-phase Al_2O_3 scales. The growth rate of the lower temperature oxides, γ-Al_2O_3 and θ-Al_2O_3, are similar, but the growth rates are higher than that of α-Al_2O_3, such that oxidation at approximately 1200 K is faster than at 1300 K (Rybicki and Smialek 1989; Brumm and Grabke 1992).

At temperatures greater than 1300 K, $MoSi_2$ has better oxidation resistance because SiO_2 scales on $MoSi_2$ grow more slowly than Al_2O_3 scales grow on aluminide intermetallics (fig. 22) (Nesbitt and Lowell 1993). However, in the low-temperature range of 650 to 775 K, $MoSi_2$ is plagued by a rapid, catastrophic mode of oxidation known as "pest," which can quickly reduce a sample to a pile of powder (Chou and Nieh 1993). NiAl is not affected by a pesting reaction under ambient environments although it can be forced to undergo a mild pesting reaction by testing at very low partial pressures of oxygen (Grabke et al. 1991). Therefore, alumina-forming alloys such as NiAl exhibit the most oxidation-resistant behavior over the broadest range of temperatures in comparison to other metallic or intermetallic materials. NiAl alloys can be further protected at very high temperatures by the application of thermal barrier coatings (Miller and Doychak 1992).

Apparently, alloy stoichiometry has only a minor influence on isothermal oxidation rates of NiAl. Hutchings and Loretto (1978) found that increasing the Al level from 42 to 50 percent reduces the oxidation rate at 1173 K by an order of magnitude. More recent work (Doychak, Smialek, and Barrett 1989) shows that although oxidation rates differed by a factor of 10, the drop in rate was not proportional to Al level over the range of alloys studied. Instead, the oxidation rate at temperatures between 1273

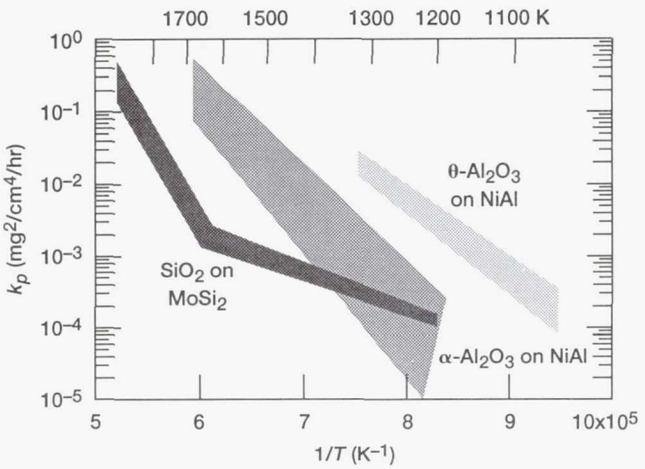

Figure 22.—Range of observed parabolic rate constants, k_p, for Al_2O_3 formation on NiAl and for SiO_2 formation on $MoSi_2$ as a function of temperature (Nesbitt and Lowell 1993).

and 1673 K increased by close to an order of magnitude after a 3-percent drop in Al content from the stoichiometric composition. Oxidation rates were then relatively constant with slight fluctuations for Ni-Al alloys containing 47 to 37 at.% Al.

Several studies have concentrated on the mechanisms of oxidation in NiAl in terms of mass transport phenomenon. Examination of tracer diffusion data (Young and DeWit 1986) and scale morphologies (Doychak, Smialek, and Mitchell 1989) indicates that the transition oxides grow primarily by outward cation diffusion. At higher temperatures, the mature α-Al_2O_3 oxide also grows initially by outward Al diffusion (Prescott et al. 1992) with the contribution of inward oxygen transport increasing during later stages of oxidation because of a strong influence from short circuit diffusion paths (Jedlinski and Borchardt 1991; Nicolas-Chaubet, Huntz, and Millot 1991). The oxidation behavior for NiAl is in contrast to that for MCrAl alloys, where inward-growing scales are typically formed (Reddy, Smialek, and Cooper 1982).

Cyclic oxidation testing between high and ambient temperatures is significantly more severe than isothermal oxidation and more closely approximates actual service conditions. During the cooling portion of the cycle, the difference in thermal expansion coefficients between metal and oxide produces high stresses at the oxide/metal interface that can lead to scale spallation. Spalling occurs randomly over the surface of the sample, exposing either fresh metal or fractured oxide scales to the next thermal cycle. Continued cycling causes repetitive selective oxidation of Al and, therefore, an overall loss of Al from the alloy. Cyclic lifetimes can be very short in comparison to those for isothermal conditions because the Al consumption rate is inversely proportional to the oxide thickness, and spalling keeps the oxide scale thin.

Three factors strongly affect the cyclic oxidation behavior of NiAl: temperature, alloy stoichiometry, and reactive element additions. Increased temperatures result in more rapid oxide growth and, therefore, a greater volume of oxide spalling during cooling (Nesbitt and Lowell 1993). Cyclic oxidation life decreases by about an order of magnitude for each 100-K increase in temperature above 1400 K (Doychak, Smialek, and Barrett 1989). Ni-Al alloys are also significantly more sensitive to stoichiometry under cyclic conditions than under isothermal tests. Ideally, for long-term cyclic conditions, NiAl alloys should contain at least 45 at.% Al. For even a few cycles, the composition should contain greater than 40 at.% Al to avoid transformation of the matrix to martensite and formation of a less protective Ni-containing oxide (Smialek and Lowell 1974; Doychak, Smialek, and Barrett 1989).

Finally, it is well known that rare-earth or oxygen-active dopants such as Y, Hf, Zr, Ce, and La have a very large and favorable effect on the cyclic oxidation resistance of MCrAl, NiAl, and superalloy materials (Smialek and Meier 1987). For example, the excellent cyclic oxidation resistance of NiAl compared with conventional oxidation-resistant alloys and other Al-forming intermetallics (fig. 23) is only achieved when reactive elements such as Zr are added. Such enhanced oxidation resistance of NiAl is achieved when approximately 0.1 at.% of the reactive element is in solution (Barrett 1988), or is added in the form of oxide dispersions, or is incorporated in the surface by ion implantation (Jedlinski and Mrowec 1987). These additions slightly decrease the isothermal oxide growth rate (Rybicki and Smialek 1989; Jedlinski and Mrowec 1987) by suppressing oxygen diffusion through the scale (Jedlinski, Borchardt, and Mrowec 1992). But the main benefit of these additions is a dramatic increase in scale adherence during cyclic oxidation testing (Doychak, Smialek, and Barrett 1989).

Oxide adherence has been attributed to several causes including oxide "pegging," elimination of voids at the

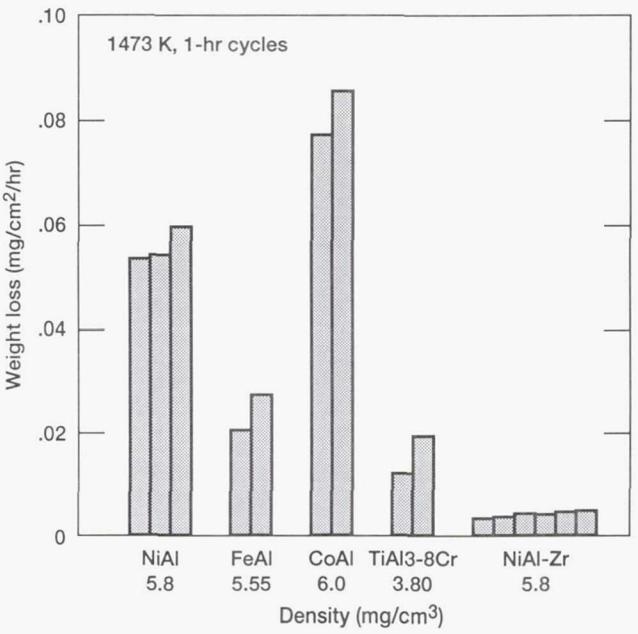

Figure 23.—Rates of weight loss due to cyclic oxidation at 1473 K for several Al_2O_3-forming alloys (Nesbitt and Lowell 1993).

interface, increased scale plasticity, and changes in the chemical bond between the oxide and metal (Smialek and Browning 1985). However, the most likely effect of reactive elemental additions is the role of these elements in preventing sulfur segregation to the oxide/metal interface as previously demonstrated in Ni-base superalloys (Smialek 1991; McVay et al. 1992). Sulphur segregation would reduce the surface energy, adversely reducing the scale adherence. Sulphur also prefers to segregate to free surfaces, favoring the formation of voids under the oxide scale and accelerating their growth to cavities (Grabke, Wiemer, and Viefhaus 1991).

The behavior of NiAl(Zr) alloys under isothermal and cyclic oxidation conditions has been sufficiently characterized that life prediction can be made with reasonable accuracy (Doychak, Smialek, and Barrett 1989; Nesbitt and Vinarcik 1991). Useful lives are usually defined as the time needed to obtain a given amount of metal recession, a given amount of weight change (typically 5 to 10 mg/cm^2), or a transition to a less protective oxide. In the case of NiAl, severe cyclic oxidation exposure eventually leads to Al depletion and subsequent formation of NiO and $NiAl_2O_4$, which can be used as a criterion to define life. Therefore, the Al reserve of an alloy, which is critical for extended oxidative life, makes stoichiometric alloys superior to Ni-rich materials.

Another environmental concern, hot corrosion due to molten sulfate deposits, has been studied because of the importance of this type of attack in marine, industrial, and aircraft gas turbine applications. This problem, which is most prominent at intermediate temperatures (900 to 1300 K), can result from several different mechanisms (Pettit and Giggins 1987). For example, molten deposits containing Na_2SO_4 can cause fluxing reactions that dissolve protective Al_2O_3 oxides. In addition, the formation of sulfides beneath the deposits, and subsequent oxidation of these sulfides, can be quite detrimental to surface integrity (Kaufman 1969).

Binary NiAl is not particularly resistant to hot corrosion, because the corrosion rate can far exceed the oxidation rate at equivalent temperatures (Ellis 1987; Godlewski et al. 1989). This occurs because Al depletion is much faster in sulfur-containing environments than in air, causing the less resistant Ni-containing oxides to form early during exposure. Chromium was found to increase the hot corrosion resistance of NiAl, and an additional improvement (albeit marginal) was noted when both Y and Cr were added to NiAl (McCarron, Lindblad, and Chatterji 1976). When Ni-Al was macroalloyed with Cr in sufficient quantity to form MCrAl-based alloys in the $\gamma + \gamma' + \beta$ phase field, hot corrosion resistance was very good (Kaufman 1969; Godlewski et al. 1989). However, Cr additions adversely affected the cyclic oxidation performance of NiAl alloys in air (Smeggil 1991; Grabke, Brumm, and Steinhorst 1992).

Overall, NiAl alloys have questionable sulphidation resistance and will probably need to be macroalloyed or coated if such conditions are encountered during use. NiAl alloys have good isothermal oxidation resistance. However, only when alloyed with reactive elements such as Zr does NiAl exhibit the exceptional cyclic oxidation resistance it is known for. NiAl(Zr) alloys exhibit long-term cyclic oxidation resistance to approximately 1500 K (Nesbitt and Lowell 1993), which exceeds the capabilities of essentially all other Al_2O_3-forming alloys.

8. NiAl-Fiber Composites

Although individual alloying strategies have successfully improved the ductility, fracture toughness, oxidation resistance, or creep strength of NiAl, no alloy composition has yet been developed which has an acceptable balance of properties in either polycrystalline or single-crystal form. Thus far, alloys that show significant improvements in high-temperature properties have lower toughness or ductility than binary NiAl. Similarly, when attempts are made to optimize low-temperature properties, creep strength is usually sacrificed. This dilemma is the driving force behind the research activities into fiber-reinforced NiAl-based composites, which are under increased scrutiny as a possible means for achieving a balance of properties that is presently unobtainable in monolithic NiAl.

Three categories of NiAl-based composites have received the majority of interest: (1) a NiAl matrix reinforced with continuous fibers of either W, Mo, or Al_2O_3, (2) a NiAl matrix containing a fine dispersion of TiB_2 or AlN particles, and (3) two-phase, in-situ NiAl composites. The mechanism for improving strength in continuous-fiber-reinforced composites differs from that in either the particulate or two-phase systems. In continuous-fiber composites, strengthening occurs when load is transferred from the relatively weak matrix to the high-strength fibers, rather than when the motion of dislocations is impeded as generally occurs in the other types of materials. The classification of a particular system as a "true" composite is often subjective, but for the purposes of this discussion, only artificial continuous-fiber-reinforced systems are considered because of their distinctive strengthening mechanism and unique problems.

To substantially improve strength in a fiber composite, the reinforcing fiber must possess high strength and have an elastic modulus significantly greater than that of the matrix. In addition, a strong bond must be present between the matrix and fiber to allow load transfer from the matrix to the fiber. Conversely, for materials where improved toughness is the primary goal, such as ceramics, a weak interface is desirable. In such cases, the matrix/fiber interface retards crack propagation by debonding in the wake of an advancing crack. Unfortunately, binary NiAl as a polycrystalline composite matrix material suffers from both low high-temperature strength and poor low-temperature toughness. Attempting to both strengthen and toughen NiAl by fiber reinforcement makes the task of engineering this composite system extremely challenging. Following the example of SiC/Ti aluminide matrix composites, an

intermediate level of bonding can provide a combination of strength, toughness, and fatigue crack growth resistance (Larsen, Revelos, and Gambone 1992). However, the bond strength in this system is low enough that transverse properties are a major concern.

The choice of reinforcing fiber for a NiAl-based composite is limited by the requirements of high elevated-temperature strength, high-modulus, low-density, environmental resistance, and compatibility with the matrix. The last requirement refers to mechanical suitability, similar coefficients of thermal expansion (CTE), and chemical compatibility with the matrix. In addition, the fiber must be readily available in quantities sufficient for developmental studies. At present, single-crystal Al_2O_3 fibers, typically 125 μm in diameter, are the best choice for meeting these requirements (Misra 1988; Noebe, Bowman, and Eldridge 1991). Polycrystalline Al_2O_3 fibers have been used to reinforce NiAl (Anton and Shah 1992), although the fibers suffer from a greater CTE mismatch with NiAl than single-crystal fibers, as well as a loss of creep strength at high temperatures. However, the polycrystalline fibers have such a small diameter (approximately 12 μm) that residual stresses in the matrix should be significantly reduced compared with those of the larger single-crystal Al_2O_3 fibers (Lu et al. 1991).

There are few other fiber systems that are available for use in metal or intermetallic matrix composites. Strengthening in combination with toughening has been observed in NiAl composites reinforced with W (Bowman 1992b) or Mo (Bowman et al. 1991). Because of greater ductility, the use of either W or Mo as a reinforcing fiber has successfully reduced the susceptibility of the fiber to processing-related strength loss. Therefore, even greater strength improvements have been noted in these systems than in NiAl/Al_2O_3 (fig. 24). These fibers are also chemically compatible with the matrix. They do, however, suffer from even greater CTE mismatch than the Al_2O_3 fibers do (α of NiAl = $16x10^{-6}$/K, Al_2O_3 = $9x10^{-6}$/K, Mo = $4.8x10^{-6}$/K, W = $4.5x10^{-6}$/K). In addition, because of their poor high-temperature oxidation resistance and high densities, W and Mo are not considered reasonable reinforcing candidates for NiAl-based aerospace materials.

SiC fibers have proven successful in Ti-based composites (Larsen, Revelos, and Gambone 1992) but are an unacceptable choice for NiAl because of the large CTE mismatch (α_{SiC} = $5.8x10^{-6}$/K) and severe chemical incompatibility at high temperatures (Chou and Nieh 1991). Because beryllides such as Nb_2Be_{17} have a CTE almost identical to that of NiAl, they would make a good reinforcing fiber; unfortunately they are neither chemically compatible with NiAl nor available in fiber form (Misra 1991).

Significant toughening has been observed in NiAl composites reinforced with stainless steel tubes (Nardone 1992). The stainless-steel-tube-reinforced system has demonstrated the proof-of-concept of using ductile reinforcements in a brittle matrix to improve toughness and tensile properties while maintaining a high fatigue limit (Nardone 1992; Bannister et al. 1992). Nevertheless, this particular system would not be suitable for high-temperature applications because of the extensive solubility of Fe in NiAl.

Because all other available continuous-fiber reinforcements have been eliminated for various reasons, single-crystal sapphire is presently the only potential fiber system for use with NiAl. Consequently, preliminary tensile, creep, fatigue, and cyclic oxidation properties for this system were generated (Bowman 1992a,b; Doychak et al. 1992; Jeng, Yang, and Amato 1992). Unfortunately, current composite processing schemes reduce fiber strength by 50 percent and decrease the fracture strain of the single-crystal Al_2O_3 fibers by about a factor of 4 (Draper, Gaydosh, and Chulya 1991; Draper, Locci, and Eldridge 1992). Such reductions in fiber properties limit the current strength of the composite to a level that the present generation of NiAl/Al_2O_3 composites do not compete with current high-temperature structural materials. The ultimate tensile strengths of the NiAl/Al_2O_3 composites tested by Jeng,

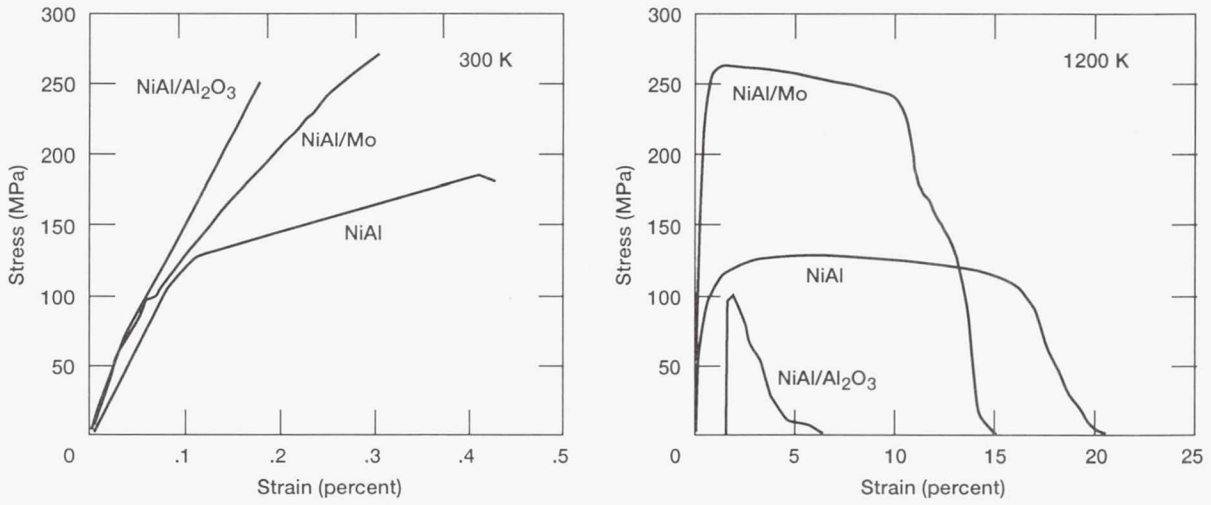

Figure 24.—Tensile stress-strain curves for NiAl, NiAl/Al_2O_3, and NiAl/Mo composites at 300 and 1200 K (Bowman 1992a).

Yang, and Amato (1992) and Bowman (1992a) were comparable to the strength of monolithic NiAl at both room and elevated temperatures. In addition, the tensile curves in figure 24 indicate that the toughness of NiAl/Al_2O_3 is less than that of monolithic NiAl. The reduced toughness or failure strain of the NiAl/Al_2O_3 composite can be attributed to the brittle nature of the fibers. Because of damage during processing, Al_2O_3 fibers have failure strains on the order of 0.18 percent in tension (Draper, Gaydosh, and Chulya 1991). In the case of NiAl-based composites, the relatively low matrix ductility is incapable of tolerating flaws that are created from the fiber failures. Consequently, the composite fails at the onset of fiber fracture. Maintenance of as-received fiber strength is essential for the success of these composites.

Preliminary results indicate that the uniaxial creep strength of NiAl/Al_2O_3 composites is quite good (Bowman 1992a). Creep strengths similar to NiAl(1Hf) single crystals have been measured at 1300 K. Also, NiAl/Al_2O_3 composites have excellent fatigue resistance as long as the applied strains during fatigue loading are below the fracture strains of the composite (Bowman 1992a).

Individually good cyclic oxidation resistance of the fiber and matrix does not necessarily guarantee an oxidation-resistant composite. When the bond strength between the NiAl and Al_2O_3 is weak, the cyclic oxidation of the composite is worse than for the matrix-only material because of oxidation along the matrix/fiber interface (Doychak et al. 1992). This is demonstrated in figure 25 where, for the first 150 cycles, the weight gain of the composite is much greater than for the unreinforced matrix because of additional oxidation along the fiber matrix interface. Shortly thereafter, the sample fails catastrophically. When the bond is strong, the oxidation resistance of the composite is comparable to that of the matrix-only material. Figure 25 also illustrates the importance of reactive element additions for achieving the best cyclic oxidation resistance in NiAl alloys. The oxidation resistance of a NiAl(Zr)/Al_2O_3 composite containing strongly bonded fibers is expected to be similar to that of NiAl(Zr); however, the composite does not survive thermal cycling because of the buildup of residual stresses in the more brittle Zr-doped matrix (Noebe, Bowman, and Eldridge 1991).

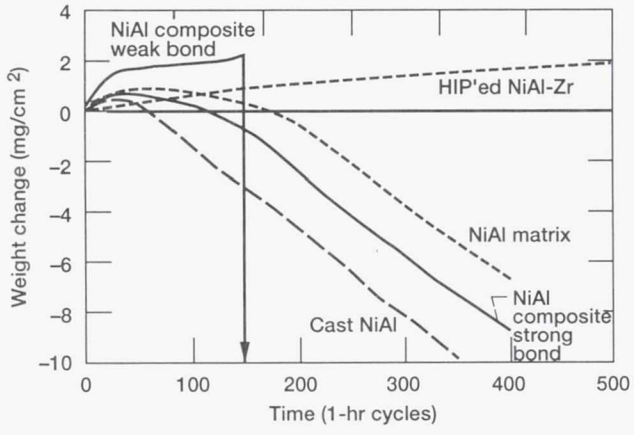

Figure 25.—Cyclic oxidation behavior of NiAl/Al_2O_3 composites with either strongly bonded or weakly bonded fibers in a comparison to various monolithic NiAl materials for 1-hr cycles at 1473 K (Bowman 1992a).

If processing-induced fiber strength degradation can be eliminated in this system, the primary obstacle to the use of Al_2O_3 fibers in NiAl will be the difference in the CTE between NiAl and c-axis-oriented, single-crystal Al_2O_3. This fiber/matrix CTE mismatch leads to the development of high residual stresses in the composite after various thermal excursions such as cooling from the processing consolidation temperature and subsequent thermal cycling. For a strongly bonded NiAl/Al_2O_3 system with 25 vol % fibers, an elastic-plastic model (unpublished research by S.M. Arnold, 1992, NASA Lewis Research Center, Cleveland, OH) predicts that the thermally generated residual stresses induced by cooling from the processing temperature will be 150 MPa axial, -175 MPa radial, and 200 MPa tangential, resulting in an effective stress of approximately 350 MPa at the fiber/matrix interface. Although some refinements in the current models are needed to account for creep and viscous flow, the results indicate that stresses in excess of the yield and fracture stresses of the matrix can be generated in this system. In qualitative agreement with the model, matrix cracking has been observed in strongly bonded NiAl/Al_2O_3 composites after only a few thermal cycles because of the inability of the matrix to accommodate the imposed strains (Bowman 1992a).

As a result, a substantial effort is under way to identify a suitable coating for the Al_2O_3 fibers to act as either a compliant or compensating layer. The compliant layer concept uses an interfacial layer that increases or maintains the ductility of the matrix/fiber interface but does not necessarily reduce the residual stresses within the system. A compensating fiber coating is designed to not only act as a compliant layer but also reduce the residual stresses by having a CTE that is higher than that of the matrix. To date, no single material has been identified that can meet either of these requirements while being chemically compatible with the constituent fiber and matrix.

Consequently, continuous-fiber composite technology in the NiAl system is a long way from maturity. The problem is twofold: (1) lack of an adequate fiber or processing technique that does not degrade fiber properties and (2) an unoptimized matrix. It is unlikely that a single type of fiber will be able to increase both high-temperature strength and low-temperature toughness of a NiAl matrix while still meeting all other property requirements. Instead, optimal alloying of NiAl will be necessary to solve one of these material deficiencies; then, a suitable fiber with a better CTE match can be used to overcome the remaining problem.

9. Processing and Fabrication

Compared with that of most intermetallics, the processing of NiAl is relatively easy in spite of a high melting temperature

and limited room-temperature ductility. Processing is greatly facilitated by a wide single-phase field, congruent melting point, single-phase microstructure, and high ductility above the BDTT. Therefore, NiAl can be routinely fabricated into polycrystalline, single-crystal, or composite form via a variety of processing routes. Numerous conventional processing techniques have been employed, including powder metallurgy (PM), casting and extrusion, directional solidification, and some less orthodox techniques such as mechanical alloying and reaction synthesis. Even though NiAl has a low fracture toughness at room temperature, machining complex geometries from the as-fabricated material is possible with standard techniques such as grinding, abrasive machining, and electrodischarge machining (EDM). Water-jet cutting is an ideal method for machining thin composite shapes that contain nonconductive fibers, such as Al_2O_3, which are not amenable to EDM.

9.1 Powder Metallurgy

In addition to being both economical and reproducible, powder metallurgy techniques may be used to fabricate shapes not readily possible by other techniques. The ability to obtain near net shape components significantly limits the amount of post-processing machining necessary. In addition, polycrystalline NiAl is usually fabricated via conventional PM techniques or the extrusion of small castings (table IV), and NiAl-based composites are fabricated almost exclusively by PM-related processes at the present time.

Usually, NiAl powder processing takes advantage of prealloyed powders that are gas or vacuum atomized in helium or argon. Several commercial vendors using pilot plant facilities routinely produce high-quality, low-interstitial, spherical NiAl powder in heats of 20 to 45 kg, which sell for about $45.00/kg. A greater demand for powder in the future should drive the cost down as larger heats are produced. Because of the increased chemical uniformity of the final product, prealloyed powders are preferred to material that is reaction synthesized and milled. Cold compaction of the resulting NiAl powders to high densities is not feasible because of the inherent brittleness of the intermetallic. Instead, the prealloyed powders are typically consolidated by extrusion, HIP, vacuum hot pressing, thermal spray techniques, or some combination of these (Noebe and Locci 1990; German and Iacocca 1993).

Although powder processing has several advantages, PM techniques are susceptible to problems with bulk composition or elevated impurity levels. The most common impurity found in powder-processed material is oxygen. Because small powders have large surface-area-to-volume ratios, oxygen contamination presents a concern, although the effect of interstitial oxygen on the mechanical properties of NiAl is probably not a serious problem (Noebe and Garg 1994). In addition, the oxide scales on the powder particles result in prior particle boundaries after consolidation and can be potential sites for failure initiation. Extrusion of NiAl powder breaks up these boundaries into fine oxide particles (Zeller, Noebe, and Locci 1990), thus reducing their impact on mechanical properties. Prior particle boundaries would be of greater concern in HIP'ed, hot-pressed, or thermally sprayed NiAl materials. Interstitials such as C, N, and S are typically present at the same levels in prealloyed NiAl powders as in wrought castings of NiAl (Bowman et al. 1992), although a "dirty" consolidation atmosphere can elevate the level of these impurities (Pickens et al. 1989).

Of equal or more concern is the issue of stoichiometry. High-temperature atomization and thermal spray processes can change

TABLE IV.—EFFECT OF PROCESSING ON ROOM-TEMPERATURE TENSILE PROPERTIES OF POLYCRYSTALLINE NiAl

Al content at.%	Process	Grain size, μm	Yield stress, MPa	Ultimate tensile strength, MPa	Ductility, percent	Reference
49.4	PM + hot press	20	------	476	0.5	Singleton, Wallace, and Miller (1966)
50.6	PM + extrude	5	370	405	0.8	Noebe et al. (1991)
50.6	PM + extrude	10 to 33	290 to 350[a]	------	0	Bowman et al. (1992)
49.6	PM + hot press	35	120	175	0.42	Bowman (1992a)
50.0	As-cast	150	------	100	0	Grala (1960)
49.0	Cast + extrude	5 to 140	------	234 to 538	0	Schulson (1982)
50.5	Cast + extrude	----	167 to 193	≈220	3.5 to 4.8	Rozner and Wasilewski (1966)
49.4	Cast + extrude	11 to 16	------	490	0	Hahn and Vedula (1989)
50.3	Cast + extrude	11 to 16	245	335	2.1	Hahn and Vedula (1989)
50.0	Cast + extrude	30	154	229	2.2	George and Liu (1990)
50.3	Cast + extrude	13 to 270	≈110	200 to 300	0.5 to 2.3	Nagpal and Baker (1990b)
50.0	Cast + extrude	40	175	229	0.45	Margevicius and Lewandowski (1991)
50.0	Cast + extrude	18	180	257	1.4	Noebe and Behbehani (1992)

[a]Compressive yield stress.

the final composition of NiAl if one constituent, such as Al, is evaporated preferentially (German and Iacocca 1993). Therefore, although powder processing offers many advantages, it is very easy to upset the stoichiometry of the powder or to introduce higher impurity levels during intermediate or final powder consolidation steps, resulting in a material with a higher yield stress and a greater tendency for completely brittle behavior. However, room-temperature tensile ductility can be obtained from powder-extruded or even hot-pressed NiAl powders (table IV), although tensile ductility is generally achieved more consistently from extruded ingots because the chemistry is more easily and reliably controlled.

As indicated in table IV, NiAl has been produced by extrusion of either powder or cast material encased in steel cans. In powder extrusion, both densification and deformation occur in one step with a very short process cycle time (Roberts and Ferguson 1991). Although the number of slip systems in NiAl does not allow for generalized plasticity in polycrystalline material at room temperature (Ball and Smallman 1966b), considerable reductions in area without cracking are possible by extrusion because of additional elevated-temperature deformation mechanisms and the hydrostatic compressive stress on the intermetallic due the presence of a canning material. During extrusion of NiAl, the cross-sectional area of the material is typically reduced from 7:1 to 16:1 at temperatures between 1100 to 1400 K, resulting in grain sizes ranging from 3 to 100 μm. Lower extrusion temperatures result in finer grain sizes that scale linearly with the extrusion temperature (Zeller, Noebe, and Locci 1990). Most extruded NiAl alloys have a recrystallized and equiaxed grain structure with a weak <111> fiber texture (Khadkikar, Michal, and Vedula 1990), although extrusion of NiAl at temperatures less than about 1100 K produces a partially recrystallized material with a preferred <110> orientation (Bieler et al. 1992). The relation between processing variables, resulting microstructure, and mechanical properties for extruded NiAl alloys has been reviewed previously (Baker and Nagpal 1993).

Consolidation of NiAl powders by techniques other than extrusion has also been studied. Powder rolling, which has been demonstrated as a viable consolidation process, produces a strong <111> texture in the plane of the sheet (K. Bowman et al. 1993). The parameters for densifying NiAl powders by HIP and by uniaxial deformation have been studied experimentally as well as by modeling and are, therefore, relatively well understood (Panda, Lagraff, and Raj 1988; Wright, Knibloe, and Noebe 1991). Finally, less conventional consolidation techniques such as reactive hot pressing and powder injection molding have been investigated (Alman and Stoloff 1991). Reactive hot pressing of elemental powders is preferably performed by adding prealloyed NiAl powder to the compact to dilute the exothermic reaction. However, complete consolidation is achieved only when the reactive-sintered compact is HIP'ed to eliminate porosity.

9.2 Single Crystals

Melt processing of stoichiometric single crystals is, in principle, relatively easy because of the congruent melting temperature and high ordering energy of NiAl. The high melting point does, however, push conventional furnace and crucible materials to their limit. Because the melting point of NiAl is near 1955 K (Walston and Darolia 1993), furnace temperatures are nearly 300 K higher than those used to produce superalloys. Mold and core reactivity as well as structural integrity are already serious concerns in the production of single-crystal superalloys. Such concerns are magnified in NiAl single-crystal production because higher temperatures are required. Mold reactivity issues were first observed during a study of Zr and Hf additions to NiAl single crystals (Locci and Noebe 1989; Locci et al. 1991). During transmission electron microscope analysis of these alloys, an unexpected G-phase ($Ni_{16}X_6Si_7$, X = Hf or Zr) was observed. Because Si was not an intentional alloying addition, Locci et al. determined that the contamination originated from the mold material used during the directional solidification process. Si contamination of commercially produced single crystals is still a problem, though the effect of Si on mechanical properties has not been discerned (Hack, Brzeski, and Darolia 1992).

In spite of the high temperatures involved, NiAl single crystals have been successfully produced by a Bridgman melt processing technique, originally in only small quantities used primarily in slip system studies (McDonnell et al. 1967). The commercial development of NiAl single crystals is presently being led by General Electric Aircraft Engines (GEAE) in an attempt to achieve the high-temperature creep strengths necessary to compete with current superalloys. Using a modified Bridgman process, single crystals measuring 10.2 by 2.5 by 3.8 cm have been routinely produced from binary NiAl as well as from more highly alloyed compositions (Darolia et al. 1992). These ingots have been used to characterize the physical and mechanical properties of single-crystal NiAl and NiAl alloys in an effort to identify a suitable composition for turbine blade applications.

In addition to the Bridgman technique, melt processes such as the Czochralski and edge-defined, film-fed growth process have been used successfully to produce NiAl single crystals and eutectics (Goldman 1993). Large NiAl single crystals can also be grown by containerless float zone technology. This procedure has an advantage over other melt processing techniques because no mold is involved. In addition, zone refining a chemical system open to the atmosphere can be used as a method to further purify the ingots (Reviere, Oliver, and Bruns 1989). Binary NiAl alloys with low Si and very low levels of interstitial elements have been produced by this process (Johnson et al. 1993).

Although these techniques are adequate for producing ingots for characterization, the fabrication of actual single-crystal

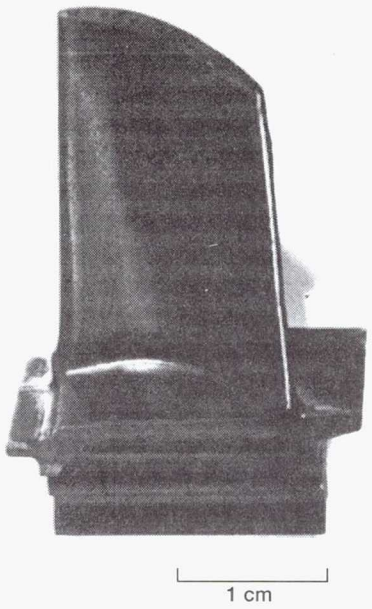

Figure 26.—Small, high-pressure turbine blade machined from a single-crystal NiAl ingot (courtesy of R. Darolia, General Electric Aircraft Engines, Evendale, OH).

turbine blades is more involved. Starting with single-crystal ingots and using a combination of EDM, electrochemical machining, and grinding processes, GEAE has successfully fabricated small single-crystal turbine blades (fig. 26) and vanes (Darolia 1991). More complicated, single-crystal blade designs that contain intricate internal cooling passages would require sophisticated core technology. However, the cracking that can occur as the molten NiAl solidifies around the ceramic core is a serious concern. Such core-related problems are a major source of low yields in superalloys and are expected to be worse with NiAl because of its lower ductility and toughness.

To produce complex, thin-walled NiAl alloy turbine airfoils, GEAE considered an alternative approach from that used with superalloys (Darolia 1991). The new approach involves machining internal cooling passages into each half of a single-crystal preform that has been split by wire-EDM. The two halves are then bonded back together before final machining of the airfoil contours. Initial results with NiAl (Darolia 1993) show that single-crystal bond joints, with properties equivalent to the base metal without forming a grain boundary, may be possible. Also, diffusion brazing of NiAl using self-generated filler metal has been used successfully to bond polycrystalline NiAl alloys (Moore and Kalinowski 1993) and would work even better with single-crystal components. Therefore, the fabrication of intricate turbine blades from single-crystal NiAl seems completely feasible. The major hurdle is identifying the proper alloy composition.

9.3 Continuous-Fiber Composites

Fabrication techniques for continuous-fiber-reinforced NiAl are being investigated by several research groups. Possible processing routes include the powder-cloth process (Pickens et al. 1989), foil/fiber or tape casting, thermal spray processes (Kern, Kaczmarek, and Janczak 1992), and pressure casting (Nourbakhsh et al. 1991). Of these techniques, powder-cloth has been used most often for generating NiAl matrix composites for mechanical property characterization. In the powder-cloth process, the matrix material is processed into flexible clothlike sheets by combining matrix powders with a fugitive organic binder. Likewise, fiber mats are produced by winding the fibers on a drum and applying another organic binder. The composite panel is assembled by stacking alternating layers of matrix cloth and fiber mats. This assemblage is consolidated by vacuum hot pressing to drive off the binders followed by HIP to ensure complete densification of the composite. One interesting feature of the powder-cloth technique is that by altering the binders, or by eliminating them completely, either a strong or weak matrix/fiber bond can be created in the NiAl/Al_2O_3 system (Bowman 1992a). This offers a convenient method for investigating the effect of strong versus weak interfaces on the mechanical properties of the composite without altering the constituents or coating the fibers.

In tape casting, a binder/powder slurry is spread as a thin sheet over the fiber mats. These matrix/fiber mats are then consolidated in a manner similar to the powder-cloth process. In foil/fiber production, alternating layers of thin foils of matrix material and mats of the reinforcing fiber are consolidated. Alternatively, the fibers can be placed within grooves machined into the thin foils—no binders are necessary with this technique. The foil/fiber process has not been attempted with NiAl because very thin sheets of matrix material are not readily available. During thermal spray processing, matrix/fiber mats are fabricated by depositing the matrix material onto fiber mats by either plasma or arc-spray techniques. The matrix/fiber mats are then consolidated in the normal fashion. Noebe and Locci (1990) present an overview of these processes.

All the fabrication techniques mentioned above usually result in some damage of the sapphire fibers, reducing the composite strength. Fiber damage can consist of either fiber fragmentation or surface roughening, which severely degrades the fracture stress of brittle fibers such as Al_2O_3. In addition, consolidation can be challenging when large volume fractions of fibers are used because of the difficulty in promoting material flow between the small interfiber regions. At a critical fiber volume fraction, the interfiber spacing becomes so small that the composite cannot be completely densified at reasonable temperatures and times. In addition, with fabrication techniques that require volatile binders, trapped gases and incomplete binder burn-off can elevate impurity levels. A major drawback to the thermal spray techniques is that during matrix

deposition the high-speed molten matrix droplets can severely damage the fiber on impact. Molten metal infiltration, which is physically less damaging to the fiber than other processes, is one of the few techniques that is suitable for use with fine-diameter fibers; however, it comes with its own set of problems. These include inadequate control of fiber spacing, incomplete infiltration of the fibers, improper wetting of the fibers, or severe reaction between the fiber and matrix.

Without adequate control, these processing problems can be aggravated to a point where the composite properties are inferior to those of the monolithic alloy (German and Iacocca 1993). Consequently, development of continuous-fiber-reinforced composites is trailing that of other types of NiAl-based materials. Fortunately, intense interest in composite materials should ensure continued improvements in this area.

9.4 General Considerations

Although NiAl processing is generally straightforward and relatively easy, it is still difficult to yield reproducible mechanical properties. As discussed in previous sections, many intrinsic low-temperature properties of NiAl are extremely sensitive to metallurgical variables such as stoichiometry, interstitial content, lattice defects, and solute concentrations. This sensitivity indicates that processing parameters, such as charge composition and cooling rate, are critical to mechanical properties. Imprecise control over processing parameters, which can lead to a wide range of material properties, has been a major contributor to the disparity in the mechanical behavior of nominally identical materials reported over the past several decades. For instance, although yield stress is one of the most common mechanical properties, it is one of the most inconsistent properties reported for NiAl (table IV).

Part of the problem is that after processing, the material can vary from the target composition by as much as ±1 at.% Al. Chemistry variations can arise from inaccuracies in the initial charge or from changes in chemistry that occur during processing, such as vaporization of Al. What is equally frustrating is that chemical analyses for major constituents such as Ni and Al are usually no more precise than ±0.5 at.% (Whittenberger and Luton 1992). In a preliminary study in which identical NiAl samples were sent to several chemical laboratories and research facilities, an almost 1 at.% range in Al content was reported by the various groups (unpublished research by D.F. Johnson and R.D. Noebe, 1993, NASA Lewis Research Center, Cleveland, OH). Yet, the properties of Ni-50Al compared with Ni-49Al or Ni-51Al are as different as a pure metal is to a solid-solution alloy. Minor deviations from stoichiometry have a direct effect on the lattice parameter, thermodynamic properties, diffusion, and mechanical properties such as yield stress, fracture stress, and ductility. For example, an alloy that is 1 at.% Ni-rich exhibits a yield stress 120 MPa greater than stoichiometric NiAl, whereas a Ni-51Al alloy has a yield stress nearly 350 MPa greater than that of Ni-50Al. Because routine chemical analyses cannot generally detect variations of 0.5 at.% for major elements, undetectable deviations from stoichiometry can contribute to apparent discrepancies in the properties of nominally identical materials. Detecting trace metallic impurities is even more difficult, though these impurities also can have an overwhelming effect on properties.

In addition to the bulk chemistry, trace levels of nonmetallic impurities such as C can profoundly affect the properties of NiAl alloys. Impurities such as C dramatically increase the flow stress of NiAl alloys (George and Liu 1990) and possibly degrade properties such as fracture toughness (Hack, Brzeski, and Darolia 1992). Also, very minute amounts of S are probably responsible for degrading cyclic oxidation resistance (Smialek and Browning 1985). In many cases, the concentration of interstitials necessary to significantly affect properties is less than the resolution of analysis techniques. Concerns over accuracy in interstitial level measurements were recently confirmed in a round-robin chemical analyses program. Using a variety of techniques but identical samples, eleven laboratories measured C, S, O, and N in directionally solidified NiAl (Parker, Johnstone, and Oligee 1991). The measured composition differed considerably from group to group. For example, the range in reported C levels varied from 12 to 335 ppm. Because the estimated hardening rate of C in NiAl is about 1750 MPa/at.% (fig. 5), the possible range in flow stress due to such a compositional variation is 200 MPa. As with bulk chemistries, dramatic variations in properties may be observed in alloys that have impurity levels that are identical within analytical resolution.

Therefore, although a substantial body of data exists for NiAl, most studies do not report processing parameters or chemistry in sufficient detail to allow for meaningful comparisons. Such problems have placed a premium on stringent control over processing to ensure the consistency necessary to successfully study this material. As the effect of processing variables on properties and improvements in process technology emerge, a more consistent view of the properties of NiAl will appear. This has been evident in recent years from the consistent room-temperature tensile ductilities obtained from cast and extruded NiAl alloys (table IV).

10. Concluding Remarks

Our knowledge of the behavior of NiAl has come a long way since the first exploratory studies of the late 1950's and early 1960's. Most of this understanding and progress have come about in only the last few years, with more papers published on NiAl in the last 3 years than during the entire previous history of this material. At this currently intense rate of research, some information presented in this report may be out of date by the time it is published. Yet, all the previous work on NiAl lays a solid foundation for future studies so that we can build upon

lessons of the past. One of the most critical of these lessons is to never underestimate the effect of processing and chemistry on properties.

We also know that the environmental durability of NiAl alloys, which is very good, is so well understood that it can be reliably predicted or modeled. The creep strength of NiAl can be improved to levels equivalent to Ni-base superalloys through alloying combined with single-crystal processing or through compositing. Fatigue behavior even at this early stage of investigation appears to be better than expected, and the inherent fracture toughness and ductility of single crystals may be much higher than originally believed.

This optimistic outlook needs to be tempered by the reality that impact behavior, which may be a formidable problem, has not yet been addressed. Also, the poor low-temperature ductility and toughness of most NiAl alloys still need to be dealt with. Nevertheless, with the significant research effort being invested in NiAl, it is only a matter of time until this intermetallic material is used in some practical application or spinoff. However, some degree of patience is necessary and justified. For instance, Ni-base superalloys and Al-Li alloys for aerospace applications were developed over a period of several decades at an intensity greater than what NiAl is presently experiencing.

Acknowledgments

The authors acknowledge the useful discussions on NiAl that have occurred over the years with Ron Gibala, Dan Whittenberger, Ram Darolia, Jim Cotton, and the many others who have worked in this area.

References

Alman, D.E., and Stoloff, N.S. 1991. Powder Fabrication of Monolithic and Composite NiAl. Int. J. Powder Metal., vol. 27, no. 1, pp. 29–41.

Anton, D.L., and Shah, D.M. 1992. Mechanical Evaluation of FP Alumina Reinforced NiAl Composites. Intermetallic Matrix Composites II, D.B. Miracle et al., eds., (MRS Symposia Proceedings, Vol. 273), MRS, Pittsburgh, PA, pp. 157–164.

Ashby, M.F. 1972. A First Report on Deformation-Mechanism Maps. Acta Metall., vol. 20, pp. 887–897.

Bain, K.R., Field, R.D., and Lahrman, D.F. 1991. Fatigue Behavior of NiAl Single Crystals. Presented at the 1991 TMS Fall Meeting, Oct. 21, Cincinnati, OH.

Baker, I., and Nagpal, P. 1993. Processing of Iron and Nickel Aluminides via Hot Extrusion. Processing and Fabrication of Advanced Materials for High Temperature Applications, T.S. Srivatsan and R.A. Ravi, eds., The Minerals, Metals and Materials Society, Warrendale, PA.

Baker, I., Nagpal, P., Liu, F., and Munroe, P.R. 1991. The Effect of Grain Size on the Yield Strength of FeAl and NiAl Alloys. Acta Metall. Mater., vol. 39, pp. 1637–1644.

Baker, I., and Schulson, E.M. 1984. The Structure of Extruded NiAl. Metall. Trans. A., vol. 15A, pp. 1129–1136.

Ball, A., and Smallman, R.E. 1966a. The Deformation Properties and Electron Microscopy Studies of the Intermetallic Compound NiAl. Acta Metall., vol. 14, pp. 1349–1355.

Ball, A., and Smallman, R.E. 1966b. The Operative Slip System and General Plasticity of NiAl-II. Acta Metall., vol. 14, pp. 1517–1526.

Bannister, M.K., Spearing, S.M., Lofvander, J.P.A., and De Graef, M. 1992. Fatigue of Extruded Steel/NiAl Composites. Intermetallic Matrix Composites II, D.B. Miracle et al., eds., (MRS Symposia Proceedings, Vol. 273), MRS, Pittsburgh, PA, pp. 177–182.

Barrett, C.A. 1988. Effect of 0.1 at.% Zirconium on the Cyclic Oxidation Behavior of ß-NiAl. Oxid. Met., vol. 30, pp. 361–390.

Berkowitz, A.E., Jaumot, F.E., and Nix, F.C. 1954. Diffusion of Co^{60} in Some Ni-Al Alloys Containing Excess Vacancies. Phys. Rev., vol. 95, pp. 1185–1189.

Bevk, J., Dodd, R.A., and Strutt, P.R. 1973. The Orientation Dependence of Deformation Mode and Structure in Stoichiometric NiAl Single Crystals Deformed by High Temperature Steady-State Creep. Metall. Trans., vol. 4, pp. 159–166.

Bieler, T.R., Noebe, R.D., Whittenberger, J.D., and Luton, M.J. 1992. Extrusion Textures in NiAl and Reaction Milled NiAl/AlN Composites. Intermetallic Matrix Composites II, D.B. Miracle et al., eds., (MRS Symposia Proceedings, Vol. 273), MRS, Pittsburgh, PA, pp. 165–170.

Bowman, K.J., Noebe, R.D., Jenny, J.R., and Kim, S.T. 1993. Texture in Hot-Worked B2-Structure Aluminides. Mater. Sci. Eng. A., vol. A160, pp. 201–208.

Bowman, R.R. 1992a. Influence of Interfacial Characteristics on the Mechanical Properties of Continuous Fiber Reinforced NiAl Composites. Intermetallic Matrix Composites II, D.B. Miracle et al., eds., (MRS Symposia Proceedings, Vol. 273), MRS, Pittsburgh, PA, pp. 145–155.

Bowman, R.R. 1992b. Influence of Interfacial Bond Strength on the Mechanical Properties of Continuous Fiber Reinforced NiAl Composites. HITEMP Review—1992: Advanced High Temperature Engine Materials Technology Program, NASA CP–10104, pp. 38–1 to 38–15.

Bowman, R.R., Noebe, R.D., and Darolia, R. 1989. Mechanical Properties and Deformation Mechanisms of NiAl. HITEMP Review—1989: Advanced High Temperature Engine Materials Technology Program, NASA CP–10039, pp. 47–1 to 47–15.

Bowman, R.R., Noebe, R.D., Doychak, J., Crandall, K.S., and Locci, I.E. 1991. Effect of Interfacial Properties on the Behavior of NiAl Based Composites. HITEMP Review—1991: Advanced High Temperature Engine Materials Technology Program, NASA CP–10082, pp. 43–1 to 43–14.

Bowman, R.R., Noebe, R.D., Raj, S.V., and Locci, I.E. 1992. Correlation of Deformation Mechanisms With the Tensile and Compressive Behavior of NiAl and NiAl(Zr) Intermetallic Alloys. Metall. Trans. A., vol. 23A, pp. 1493–1508.

Bradley, A.J., and Taylor, A. 1937. An X-ray Analysis of the Nickel-Aluminum System. Proc. R. Soc. (London), vol. A159, pp. 66–72.

Brumm, M.W., and Grabke, H.J. 1992. Oxidation Behavior of NiAl-I. Phase Transformations in the Alumina Scale During Oxidation of NiAl and NiAl-Cr Alloys. Corros. Sci., vol. 33, pp. 1677–1690.

Brzeski, J.M., Hack, J.E., Darolia, R., and Field, R.D. 1993. Strain Aging Embrittlement of the Ordered Intermetallic Compound NiAl. Mater. Sci. Eng., vol. A170, pp. 11-18.

Castro, G.R., Isern, H., Schneider, U., Stocker, M., and Wandelt, K. 1991. Two-Dimensional Phase Transition of Adsorbed Xenon on NiAl(110) and Al(110). J. Vac. Sci. Technol. A, vol. 9, pp. 1676–1679.

Chaki, T.K. 1991. Mechanism of Boron-Induced Strengthening of Grain Boundaries in Ni_3Al. Philos. Mag. Lett., vol. 63, pp. 123–126.

Chakrabarti, D.J. 1977. Phase Stability in Ternary Systems of Transition Elements With Aluminum. Metall. Trans. B, vol. 8B, pp. 121–123.

Chakravorty, S., and Wayman, C.M. 1976. The Thermoelastic Martensitic Transformation in ß'Ni-Al Alloys: I. Crystallography and Morphology. Metall. Trans. A, vol. 7A, pp. 555–568.

Chambers, S.A., and Loebs, V.A. 1990. Schottky Barrier Height and Thermal Stability of the NiAl/n-Ge/GaAs(001) Interface. J. Vac. Sci. Technol A, vol. 8, pp. 2074–2078.

Chan, K.S. 1990a. Theoretical Analysis of Grain Size Effects on Tensile Ductility. Scr. Metall. Mater., vol. 24, pp. 1725–1730.

Chan, K.S. 1990b. Fracture and Toughening Mechanisms in an Alpha-2 Titanium Aluminide Alloy. Metall. Trans. A, vol. 21A, pp. 2687–2699.

Chang, K.-M., Darolia, R., and Lipsitt, H.A. 1992. Cleavage Fracture in B2 Aluminides. Acta Metall. Mater., vol. 40, pp. 2727–2737.

Chou, T.C., and Nieh, T.G 1991. Interfacial Reactions of SiC with NiAl. Scr. Metall. Mater., vol. 25, pp. 2059–2064.

Chou, T.C., and Nieh, T.G. 1993. Mechanism of $MoSi_2$ Pest During Low Temperature Oxidation. J. Mater. Res., vol. 8, pp. 214–226.

Cooper, M.J. 1963. An Investigation of the Ordering of the Phases CoAl and NiAl. Philos. Mag., vol. 8, pp. 805–810.

Cotton, J.D. 1991. The Influence of Chromium on Structure and Mechanical Properties of B2 Nickel Aluminide Alloys. Ph.D. Thesis, The University of Florida, Gainesville, FL. (Also NASA CR–189124, 1992.)

Cotton, J.D., Kaufman, M.J., and Noebe, R.D. 1991. Constitution of Pseudobinary Hypoeutectic ß-NiAl + α-V Alloys. Scr. Metall. Mater., vol. 25, pp. 1827–1832.

Cotton, J.D., Noebe, R.D., and Kaufman, M.J. 1993a. Chromium-Bearing NiAl Intermetallic Alloys: Part I. Microstructure and Mechanical Properties. Intermetallics, vol. 1, pp. 3–20.

Cotton, J.D., Noebe, R.D., and Kaufman, M.J. 1993b. Chromium-Bearing NiAl Intermetallic Alloys: Part II. Slip Systems. Intermetallics, vol. 1, pp. 117–126.

Cotton, J.D., Noebe, R.D., and Kaufman, M.J. 1993c. NiAl-Rich Portion of the NiAl-Cr Pseudobinary Eutectic System. J. Phase Equil., vol. 14, no. 5., pp. 579–582.

Cotton, J.D., Noebe, R.D., and Kaufman, M.J. 1993d. Ternary Alloying Effects In Polycrystalline ß-NiAl. International Symposium on Structural Intermetallics, R. Darolia et al., eds., The Minerals, Metals and Materials Society, Warrendale, PA, pp. 513–522.

Cottrell, A.H. 1958. Theory of Brittle Fracture in Steel and Similar Metals. Trans. Metall. Soc. AIME, vol. 212, pp. 192–205.

Crimp, M.A., and Vedula, K. 1991. Room-Temperature Deformation of Single-Crystal B2 Fe-Al Alloys: the Effect of Stoichiometry and Cooling Rate. Philos. Mag. A, vol. 63, pp. 559–570.

Cullers, C.L, and Antolovich, S.D. 1992. Low Cycle Fatigue Behavior of NiAl Deformed Near the Brittle-to-Ductile Transition Temperature. Superalloys 1992, S.D. Antolovich et al., eds., The Minerals, Metals and Materials Society, Warrendale, PA, pp. 351–359.

Cullers, C.L., Antolovich, S.D., and Noebe, R.D. 1993. Deformation Behavior of Polycrystalline NiAl Cyclically Deformed Near the Brittle-to-Ductile Transition Temperature. High Temperature Ordered Intermetallic Alloys V, I. Baker et al., eds., (MRS Symposia Proceedings, Vol. 288), MRS, Pittsburgh, PA, pp. 531–536.

Darolia, R. 1991. NiAl Alloys for High-Temperature Structural Applications. J. Met., vol. 43, no. 3, pp. 44–49.

Darolia, R. 1993. Structural Applications of NiAl. International Symposium on Structural Intermetallics, R. Darolia et al., eds., The Minerals, Metals and Materials Society, Warrendale, PA, pp. 495–504.

Darolia, R., Chang, K.-M., and Hack, J.E. 1993. Observation of High Index {511} Type Fracture Planes and Their Influence on Toughness in NiAl Single-Crystals. Intermetallics, vol. 1, pp. 65–78.

Darolia, R., Lahrman, D., and Field, R.D. 1992. The Effect of Iron, Gallium and Molybdenum on the Room Temperature Tensile Ductility of NiAl. Scr. Metall. Mater, vol. 26, pp. 1007–1012.

Darolia, R., Lahrman, D.F., Field, R.D., Dobbs, J.R., Chan, K.M., Goldman, E.H., and Konitzer, D.G. 1992. Overview of NiAl Alloys For High Temperature Applications. Ordered Intermetallics—Physical Metallurgy and Mechanical Behavior, C.T. Liu et al., eds., Kluwer Academic Publishers, Dordrecht, Netherlands, pp. 679–698.

Darolia, R., Lahrman, D.F., Field, R.D., and Freeman, A.J. 1989. Alloy Modeling and Experimental Correlation for Ductility Enhancement in NiAl. High Temperature Ordered Intermetallic Alloys III, C.T. Liu et al., eds., (MRS Symposia Proceedings, Vol. 133), MRS, Pittsburgh, PA, pp. 113–118.

DeMarco, H.K., and Ardell, A.J. 1993. Mechanical Behavior of Monocrystaline NiAl Using a Miniaturized Disk-Bend Test. High Temperature Ordered Intermetallic Alloys V, I. Baker et al., eds., (MRS Symposia Proceedings, Vol. 288), MRS, Pittsburgh, PA, pp. 641–646.

Dollar, M., Dymek S., Hwang, S.J., and Nash P. 1992. The Occurrence of <110> Slip in NiAl. Scr. Metall. Mater., vol. 26, pp. 29–34.

Doychak, J. 1992. Metal- and Intermetallic-Matrix Composites for Aerospace Propulsion and Power Systems. J. Met., vol. 44, no. 6, pp. 46–51.

Doychak, J., Nesbitt, J.A., Noebe, R.D., and Bowman, R.R. 1992. Oxidation of Al_2O_3 Continuous Fiber-Reinforced/NiAl Composites. Oxid. Met., vol. 38, pp. 45–72.

Doychak, J., Smialek, J.L, and Barrett, C.A. 1989. The Oxidation of Ni-Rich Ni-Al Intermetallics. Oxidation of High Temperature Intermetallics, T. Grobstein and J. Doychak, eds., The Minerals, Metals and Materials Society, Warrendale, PA, pp. 41–55.

Doychak, J., Smialek, J.L., and Mitchell, T.E. 1989. Transient Oxidation of Single-Crystal ß-NiAl. Metall. Trans. A, vol. A20, pp. 499–518.

Draper, S.L., Gaydosh, D.J., and Chulya, A. 1991. Tensile Behavior of Alumina-Reinforced FeAl and FeCrAl. HITEMP Review—1991: Advanced High Temperature Engine Materials Technology Program, NASA CP–10104, pp. 42–1 to 42–14.

Draper, S.L., Locci, I.E., and Eldridge, J.I. 1992. Al_2O_3 Fiber Strength Degradation in MMC's and IMC's. HITEMP Review—1992: Advanced High Temperature Engine Materials Technology Program, NASA CP–10104, pp. 17–1 to 17–13.

Edwards, K.M. 1993. Low-Cycle Fatigue Behavior of Polycrystalline NiAl at Room Temperature. M.S. Thesis, The University of Michigan, Ann Arbor, MI.

Edwards, K.M., and Gibala, R. 1993. Low-Cycle Fatigue Behavior of Polycrystalline NiAl at Room Temperature. High Temperature Ordered Intermetallic Alloys V, I. Baker et al., eds., (MRS Symposia Proceedings, Vol. 288), MRS, Pittsburgh, PA, pp. 665–670.

Ellis, D.L. 1987. Hot Corrosion of the B2 Nickel Aluminides. M.S. Thesis, Case Western Reserve University, Cleveland, OH.

Field, R.D., Lahrman, D.F., and Darolia, R. 1991a. Room Temperature Deformation in "Soft" Orientation NiAl Single Crystals. High Temperature Ordered Intermetallic Alloys IV, L. Johnson et al., eds., (MRS Symposia Proceedings, Vol. 213), MRS, Pittsburgh, PA, pp. 255–260.

Field, R.D., Lahrman, D.F., and Darolia, R. 1991b. Slip Systems in <001> Oriented NiAl Single Crystals. Acta Metall. Mater., vol. 39, pp. 2951–2959.

Field, R.D., Lahrman, D.F., and Darolia, R. 1991c. The Effect of Alloying on Slip Systems in <001> Oriented NiAl Single Crystals. Acta Metall. Mater., vol. 39, pp. 2961–2969.

Field, R.D., Lahrman, D.F., and Darolia, R. 1993. A Mechanistic Study of the Microalloying Effect in NiAl Base Alloys. High Temperature Ordered Intermetallic Alloys V, I. Baker et al., eds., (MRS Symposia Proceedings, Vol. 288), MRS, Pittsburgh, PA, pp. 423–428.

Fleischer, R.L. 1993. Solid Solution Strengthening of Intermetallic Compounds. High Temperature Ordered Intermetallic Alloys V, I. Baker et al., eds., (MRS Symposia Proceedings, Vol. 288), MRS, Pittsburgh, PA, pp. 165–170.

Forbes, K.R., Glatzel, U., Darolia, R., and Nix, W.D. 1993. High Temperature Deformation of Single Crystals of NiAl. High Temperature Ordered Intermetallic Alloys V, I. Baker et al., eds., (MRS Symposia Proceedings, Vol. 288), MRS, Pittsburgh, PA, pp. 45–58.

Forbes, K.R., and Nix, W.D. 1993. Mobility and Substructure Controlled Creep Deformation of [100] Oriented NiAl Crystals. To be published in the Proceedings of the 5th International Conference on Creep and Fracture of Engineering Materials and Alloys, Swansea, Wales.

Franchy, R., Wuttig, M., and Ibach, H. 1987. The Adsorption of Sulfur, Carbon Monoxide and Oxygen in NiAl(111). Surf. Sci., vol. 189–190, pp. 438–447.

Fraser, H.L., Smallman, R.E., and Loretto, M.H. 1973. The Plastic Deformation of NiAl Single Crystals Between 300 °K and 1050 °K: I. Experimental Evidence on the Role of Kinking and Uniform Deformation in Crystals Compressed Along <001>. Philos. Mag., vol. 28, pp. 651–665.

Gandhi, C., and Ashby, M.F. 1979. Fracture-Mechanism Maps for Materials Which Cleave: F.C.C., B.C.C. and H.C.P. Metals and Ceramics. Acta Metall., vol. 27, pp. 1565–1602.

George, E.P., and Liu, C.T. 1990. Brittle Fracture and Grain Boundary Chemstry of Micro-Alloyed NiAl. J. Mater. Res., vol. 5, pp. 754–762.

George, E.P., Liu, C.T., and Pope, D.P. 1992. Environmental Embrittlement: The Major Cause of Room-Temperature Brittleness in Polycrystalline Ni_3Al. Scr. Metall. Mater., vol. 27, pp. 365–370.

Georgopoulos, P., and Cohen, J.B. 1977. The Defect Structure and Debye Waller Factors vs. Composition in ß$Ni_{1\pm x}Al_{1\pm x}$. Scr. Metall., vol. 11, pp. 147–150.

German, R.M., and Iacocca, R.G. 1993. Powder Metallurgy of Intermetallics. Processing and Fabrication of Advanced Materials for High Temperature Applications, T.S. Srivatsan and R.A. Ravi, eds., The Minerals, Metals and Materials Society, Warrendale, PA.

Godlewski, K., Godlewski, E., Mrowec, S., and Danielewski, M. 1989. Sulphide Corrosion of Pure and Chromium-Modified, ß-NiAl Intermetallic Compound at High Temperatures. Mater. Sci. Eng., vol. A120, pp. 105–109.

Goldman, E.H. 1993. Single Crystal Processing of Intermetallics for Structural Applications. High Temperature Ordered Intermetallic Alloys V, I. Baker et al., eds., (MRS Symposia Proceedings, Vol. 288), MRS, Pittsburgh, PA, pp. 83–94.

Grabke, H.J., Brumm, M., and Steinhorst, M. 1992. Development of Oxidation Resistant High Temperature Intermetallics. Mater. Sci. Technol., vol. 8, pp. 339–344.

Grabke, H.J., Steinhorst, M., Brumm, M., and Wiemer, D. 1991. Oxidation and Intergranular Disintegration of the Aluminides NiAl and $NbAl_3$ and Phases in the System Nb-Ni-Al. Oxid. Met., vol. 35, pp. 199–222.

Grabke, H.J., Wiemer, D., and Viefhaus, H. 1991. Segregation of Sulfur During Growth of Oxide Scales. Appl. Surf. Sci., vol. 47, no. 3, pp. 243–250.

Graham, R.B. 1984. The Effect of Temperature, Composition and Grain Size on the Mechanical Properties of NiAl. M.E. Thesis, Dartmouth College, Hanover, NH.

Grala, E.M. 1960. Investigations of NiAl and Ni_3Al. Mechanical Properties of Intermetallic Compounds, J.H. Westbrook, ed., New York: John Wiley & Sons, Inc., New York, pp. 358–402.

Groves, G.W., and Kelly, A. 1969. Change of Shape Due to Dislocation Climb. Philos. Mag., vol. 19, pp. 977–986.

Guha, S., Munroe, P.R., and Baker, I. 1991. Room Temperature Deformation Behavior of Multiphase Ni-20at.%Al-30at.%Fe and its Constituent Phases. Mater. Sci. Eng. A, vol. A131, pp. 27–37.

Guseva, L.N. 1951. On the Nature of the ß-phase in the System Ni-Al. Dokaldy Akad. Nauk. U.S.S.R., vol. 77, pp. 415–418.

Hack, J.E., Brzeski, J.M., and Darolia, R. 1992. Evidence of Inherent Ductility in Single Crystals of the Ordered Intermetallic Compound NiAl. Scr. Metall. Mater., vol. 27, pp. 1259–1263.

Hahn, K.H., and Vedula, K. 1989. Room Temperature Tensile Ductility in Polycrystalline B2 NiAl. Scr. Metall., vol. 23, pp. 7–12.

Hancock, G.F., and McDonnell, B.R. 1971. Diffusion in the Intermetallic Compound NiAl. Phys. Status Solidi., vol. 4, pp. 143–150.

Harmouche, M.R., and Wolfenden, A. 1987. Temperature and Composition Dependence of Young's Modulus in Polycrystalline B2 Ni-Al. J. Test. Eval., vol. 15, pp. 101–104.

Hartfield-Wunsch, S.E., and Gibala, R. 1991. Cyclic Deformation of B2 Aluminides. High Temperature Ordered Intermetallic Alloys IV, L. Johnson et al., eds., (MRS Symposia Proceedings, Vol. 213), MRS, Pittsburgh, PA, pp. 575–580.

Hebsur, M.G., Whittenberger, J.D., Dickerson, R.M., and Aikin, B.J.M. 1993. Microstructure/Property Relations in AlN and Al_2O_3 Particulate Strengthened NiAl. High Temperature Ordered Intermetallic Alloys V, I. Baker et al., eds., (MRS Symposia Proceedings, Vol. 288), MRS, Pittsburgh, PA, pp. 1111–1116.

Henig, E.-T., and Lukas, H.L. 1975. Kalorimetrische Bestimmung der Bildungsenthalpie und die Beschrzeibung der Fehlordnung der Geordneten ß-Phase $(Ni,Cu)_{1-x}Al_x$. Z. Metallk., vol. 66, pp. 98–106.

Hocking, L.A., Strutt, P.R., and Dodd, R.A. 1971. Comparison of Steady-State Compression Creep Behavior in Stoichiometric CoAl and NiAl Single Crystals Between 850 and 1050 °C. Inst. Met. J., vol. 99, pp. 98–101.

Hong, T., and Freeman, A.J. 1991. Effect of Antiphase Boundaries on the Electronic Structure and Bonding Character of Intermetallic Systems: NiAl. Phys. Rev. B, vol. 43, pp. 6446–6458.

Hutchings, R., and Loretto, M.H. 1978. Compositional Dependence of Oxidation Rates of NiAl and CoAl. Metall. Sci., vol. 12, pp. 503–510.

Jedlinski, J., and Borchardt, G. 1991. On the Oxidation Mechanism of Alumina Formers. Oxid. Met., vol. 36, pp. 317–337.

Jedlinski, J., Borchardt, G., and Mrowec, S. 1992. Transport Properties of Alumina Scales on the ß-NiAl Intermetallic. Solid State Ionics, vol. 50, pp. 67–74.

Jedlinski, J., and Mrowec, S. 1987. The Influence of Implanted Yttrium on the Oxidation Behavior of ß-NiAl. Mater. Sci. Eng., vol. 87, pp. 281–287.

Jeng, S.M., Yang, J.-M., and Amato, R.M. 1992. Mechanical Properties and Deformation Mechanisms of an Al_2O_3 Fiber-Reinforced NiAl Matrix Composite. Intermetallic Matrix Composites II, D.B. Miracle et al., eds., (MRS Symposia Proceedings, Vol. 273), MRS, Pittsburgh, PA, pp. 217–225.

Johnson, D.R., Joslin, S.M., Oliver, B.F., Noebe, R.D., and Whittenberger, J.D. 1992. Intermetallic/Metallic Polyphase In-Situ Composites. Intermetallic Matrix Composites II, D.B. Miracle et al., eds., (MRS Symposia Proceedings, Vol. 273), MRS, Pittsburgh, PA, pp. 87–92.

Johnson, D.R., Joslin, S.M., Oliver, B.F., Noebe, R.D., and Whittenberger, J.D. 1993. High-Purity NiAl Single Crystals and Composites by Containerless Automated Processing. First International Conference on Processing Materials for Properties, ed. H. Henein and T. Oki, eds., The Minerals, Metals and Materials Society, Warrendale, PA, pp. 865–870.

Joo, G.C., Kalman, Z., Tsakalakos, T., and Chen, S.P. 1992. On the Growth of NiAl Intermetallics on III–V Semiconductors. NanoStruct. Mater., vol. 1, pp. 213–218.

Jung, I., Rudy, M., and Sauthoff, G. 1987. Creep in Ternary B2 Aluminides and Other Intermetallic Phases. High Temperature Ordered Intermetallic Alloys II, N.S. Stoloff et al., eds., (MRS Symposia Proceedings, Vol. 81), MRS, Pittsburgh, PA, pp. 263–274.

Kanne, W.R., Strutt, P.R., and Dodd, R.A. 1969. Nature of Slip Line Formation During Creep in Stoichiometric NiAl at Temperatures Between 475° and 775° C. Trans. Metall. Soc. AIME, vol. 245, pp. 1259–1267.

Kaufman, M. 1969. Hot Corrosion in Nickel, Cobalt and Nickel-Aluminide-Base Alloys. Trans. ASM, vol. 62, pp. 590–606.

Kelly, A., and Street, K.N. 1972. Creep of Discontinuous Fibre Composites II. Theory for the Steady State. Proc. R. Soc. London A., vol. 328, no. 1573, pp. 283–293.

Kern, H., Kaczmarek, R., and Janczak, J. 1992. Thermally Sprayed Fiber-Reinforced MMCs. J. Therm. Spray Technol., vol. 1, no. 2, pp. 137–142.

Khadkikar, P.S., Michal, G.M., and Vedula, K. 1990. Preferred Orientations in Extruded Nickel and Iron Aluminides. Metall. Trans. A., vol. 21A, pp. 279–288.

Kim, J.T. 1990. On the Slip Behavior and Surface Film Effects in B2 Ordered NiAl Single Crystals. Ph.D. Thesis, University of Michigan, Ann Arbor,MI.

Kim, J.T., and Gibala, R. 1991. Slip Transition in [001] Oriented NiAl at High Temperatures. High Temperature Ordered Intermetallic Alloys IV, L. Johnson, ed., (MRS Symposia Proceedings, Vol. 213), MRS, Pittsburgh, PA, pp. 261–266.

Kostrubanic, J., Koss, D.A., Locci, I.E., and Nathal, M. 1991. On Improving the Fracture Toughness of a NiAl-Based Alloy by Mechanical Alloying. High Temperature Ordered Intermetallic Alloys IV, L. Johnson et al., eds., (MRS Symposia Proceedings, Vol. 213), MRS, Pittsburgh, PA, pp. 679–684.

Kumar, K.S., Darolia, R., Lahrman, D.F., and Mannan, S.K. 1992. Tensile Creep Response of an NiAl-TiB_2 Particulate Composite. Scr. Metall. Mater., vol. 26, pp. 1001–1006.

Kumar, K.S., Mannan, S.K., and Viswanadham, R.K. 1992. Fracture Toughness of NiAl and NiAl-Based Composites. Acta Metall. Mater., vol. 40, pp. 1201–1222.

Kumar, K.S., and Whittenberger, J.D. 1991. Intermetallic Matrix Composites via XD^{TM} Synthesis. Proceedings of the International Symposium on Intermetallic Compounds—Structure and Mechanical Properties, O. Izumi, ed., Japan Institute of Metals, Sendai, Japan, pp. 927–934.

Lahrman, D.F., Field, R.D., and Darolia, R. 1991. The Effect of Strain Rate on the Mechanical Properties of Single Crystal NiAl. High Temperature Ordered Intermetallic Alloys IV, L. Johnson et al., eds., (MRS Symposia Proceedings, Vol. 213), MRS, Pittsburgh, PA, pp. 603–607.

Lahrman, D.F., Field, R.D., and Darolia, R. 1993a. Effect of Crystallographic Orientation on the Mechanical Properties of a NiAl+Fe Alloy. High Temperature Ordered Intermetallic Alloys V, I. Baker et al., eds., (MRS Symposia Proceedings, Vol. 288), MRS, Pittsburgh, PA, pp. 679–684.

Lahrman, D.F., Field, R.D., and Darolia, R. 1993b. Evaluation of Environmental Effects on the Room Temperature Tensile Properties of Single Crystal Stoichiometric NiAl and NiAl Alloys. Scr. Metall. Mater., vol. 28, pp. 709–714.

Larsen, J.M., Revelos, W.C., and Gambone, M.L. 1992. An Overview of Potential Titanium Aluminide Composites in Aerospace Applications. Intermetallic Matrix Composites II, D.B. Miracle et al., eds., (MRS Symposia Proceedings, Vol. 273), MRS, Pittsburgh, PA, pp. 3–16.

Law, C.C., and Blackburn, M.J. 1987. Rapidly Solidified Lightweight Durable Disk Material. Final Technical Report AFWAL–TR–87–4102, Pratt and Whitney Aircraft Co., West Palm Beach, FL.

Lerch, B.A., and Noebe, R.D. 1994. Low-Cycle Fatigue Behavior of Polycrystalline NiAl at 1000 K. Metall. Trans. A., vol. 25A, pp. 309–319.

Lerch, B.A., and Noebe, R.D. 1993. Low Cycle Fatigue Behavior of Polycrystalline NiAl at 300 and 1000 K. NASA TM–105987.

Lloyd, C.H., and Loretto, M.H. 1970. Dislocations in Extruded ß'-NiAl. Phys. Status Solidi., vol. 39, pp. 163–170.

Locci, I.E., Dickerson, R., Bowman, R., Whittenberger, D., and Nathal, M.V. 1993. Microstructure and Mechanical Properties of Cast, Homogenized and Aged NiAl Single Crystal Containing Hf. High Temperature Ordered Intermetallic Alloys V, I. Baker et al., eds., (MRS Symposia Proceedings, Vol. 288), MRS, Pittsburgh, PA, pp. 686–692.

Locci, I.E., and Noebe, R.D. 1989. Characterization of Second Phase Particles in NiAl-Containing Trace Additions of Zr. Proceedings of the 47th Annual Meeting of the Electron Microscopy Society of America, G.W. Bailey, ed., San Francisco Press, Inc., San Francisco, CA, pp. 308–309.

Locci, I.E., Noebe, R.D., Bowman, R.R., Miner, R.V., Nathal, M.V., and Darolia, R. 1991. Microstructure and Mechanical Properties of a Single Crystal NiAl Alloy With Zr or Hf Rich G-Phase Precipitates. High Temperature Ordered Intermetallic Alloys IV, L. Johnson et al., eds., (MRS Symposia Proceedings, Vol. 213), MRS, Pittsburgh, PA, pp. 1013–1018.

Locci, I.E., Noebe, R.D., Moser, J.A., Lee, D.S., and Nathal, M. 1989. Processing and Microstructure of Melt Spun NiAl Alloys. High Temperature Ordered Intermetallic Alloys III, C.T. Liu et al., eds., (MRS Symposia Proceedings, Vol. 133), MRS, Pittsburgh, PA, pp. 639–646.

Loretto, M.H., and Wasilewski, R.J. 1971. Slip Systems in NiAl Single Crystals at 300 °K and 77 °K. Philos. Mag., vol. 23, pp. 1311–1328.

Lowell, C.E., Barrett, C.A., and Whittenberger, J.D. 1990. Cyclic Oxidation Resistance of a Reaction Milled NiAl-AlN Composite. Intermetallic Matrix Composites, D.L. Anton et al., eds., (MRS Symposia Proceedings, Vol. 194), MRS, Pittsburgh, PA, pp. 355–360.

Lu, T.C., Yang, J., Suo, Z., Evans, A.G., Hecht, R. and Mehrabian, R. 1991. Matrix Cracking in Intermetallic Composites Caused by Thermal Expansion Mismatch. Acta Metall. Mater., vol. 39, pp. 1883–1890.

Lutze-Birk, A., and Jacobi, H. 1975. Diffusion of ^{114m}In in NiAl. Scr. Metall., vol. 9, pp. 761–765.

Margevicius, R.W., and Lewandowski, J.J. 1991. The Effects of Hydrostatic Pressure on the Mechanical Behavior of NiAl. Scr. Metall. Mater., vol. 25, pp. 2017–2022.

Margevicius, R.W., and Lewandowski, J.J. 1993. Pressure-Induced Dislocations and Subsequent Flow in NiAl. Acta Metall. Mater., vol. 41, pp. 485–496.

Mason, D.P., Van Aken, D.C., Noebe, R.D., Locci, I.E., and King, K.L. 1991. Microstructure and Mechanical Properties of Near Eutectic ß-NiAl Plus α-Re Alloys Produced by Rapid Solidification and Extrusion. High Temperature Ordered Intermetallic Alloys IV, L. Johnson et al., eds., (MRS Symposia Proceedings, Vol. 213), MRS, Pittsburgh, PA, pp. 1033–1038.

Matsugi, K., Wenman, D.W., and Stoloff, N.S. 1992. Observation of the Brittle to Ductile Transition Temperature in the Iron Microalloyed Polycrystalline NiAl Intermetallic Compound. Scr. Metall. Mater., vol. 27, pp. 1633–1638.

McCarron, R.L., Lindblad, R.L., and Chatterji, D. 1976. Environmental Resistance of Pure and Alloyed γ'–Ni_3Al and ß-NiAl. Corrosion, vol. 32, pp. 476–481.

McDonnell, B.R., Pascoe, R.T., Hancock, G.F., and Newey, C.W.A. 1967. The Growth of Single Crystals of the Intermediate Phases NiAl and Ni_3Al. J. Mater. Sci., vol. 2, pp. 365–370.

McVay, R.V., Williams, P., Meier, G.H., Pettit, F.S., and Smialek, J.L. 1992. Oxidation of Low Sulfur Single Crystal Nickel-Base Superalloys. Superalloys 1992, S.D. Antolovich et al., eds., The Minerals, Metals and Materials Society, Warrendale, PA, pp. 807–816.

Miller, R.A., and Doychak, J. 1992. Plasma-Sprayed Ceramic Thermal Barrier Coatings for Smooth Intermetallic Alloys. J. Therm. Spray Technol., vol. 1, no. 3, pp. 211–214.

Mills, M.J., Daw, M.S., Foiles, S.M., and Miracle, D.B. 1993. HRTEM Observation and EAM Calculation of Dislocation Cores in NiAl. High Temperature Ordered Intermetallic Alloys V, I. Baker et al., eds., (MRS Symposia Proceedings, Vol. 288), MRS, Pittsburgh, PA, pp. 257–262.

Mills, M.J., and Miracle, D.B. 1993. The Structure of a<100> and a<110> Dislocation Cores in NiAl. Acta Metall. Mater., vol. 41, pp. 85–95.

Miracle, D.B. 1991. Deformation in NiAl Bicrystals. Acta Metall. Mater., vol. 39, pp. 1457–1468.

Miracle, D.B. 1993. The Physical and Mechanical Properties of NiAl. Acta Metall. Mater., vol. 41, pp. 649–684.

Miracle, D.B., Russell, S., and Law, C.C. 1989. Slip System Modification in NiAl. High Temperature Ordered Intermetallic Alloys III, C.T. Liu et al., eds., (MRS Symposia Proceedings, Vol. 133), MRS, Pittsburgh, PA, pp. 225–230.

Misra, A.K. 1988. Thermodynamic Analysis of Compatibility of Several Reinforcement Materials With Beta Phase NiAl Alloys. NASA CR–4171.

Misra, A.K. 1991. Preliminary Studies on NiAl/Nb_2Be_{17} Reaction and Effectiveness of BeO as an Interfacial Barrier. Metall. Trans. A., vol. 22A, pp. 2535–2538.

Misra, A., Noebe, R.D., and Gibala, R. 1993. The Role of Interfaces in the Room Temperature Mechanical Behavior of Directionally Solidified ß+γ'-$Ni_{70}Al_{30}$ and ß+(γ+γ')-$Ni_{50}Fe_{30}Al_{20}$ Alloys. High Temperature Ordered Intermetallic Alloys V, I. Baker et al., eds., (MRS Symposia Proceedings, Vol. 288), MRS, Pittsburgh, PA, pp. 483–488.

Mohamed, F.A., and Langdon, T.G. 1974. The Transition from Dislocation Climb to Viscous Glide in Creep of Solid Solution Alloys. Act Metall., vol. 22, pp. 779–788.

Moore, T.J., and Kalinowski, M. 1993. Diffusion Brazing NiAl With Self-Generated Filler Metal. High Temperature Ordered Intermetallic Alloys V, I. Baker et al., eds., (MRS Symposia Proceedings, Vol. 288), MRS, Pittsburgh, PA, pp. 1173–1178.

Moose, C.A. 1991. Interfacial Shear Studies of Sapphire Fiber-Reinforced Nickel Aluminide Matrix Composites. M.S. Thesis, Pennsylvania State University, University Park, PA.

Nagpal, P., and Baker, I. 1990a. Effect of Cooling Rate on Hardness of FeAl and NiAl. Metall. Trans. A, vol. 21A, pp. 2281–2282.

Nagpal, P., and Baker, I. 1990b. The Effect of Grain Size on the Room-Temperature Ductility of NiAl. Scr. Metall. Mater., vol. 24, pp. 2381–2384.

Nagpal, P., and Baker, I. 1991. Room Temperature Fracture of FeAl and NiAl. Mater. Character., vol. 27, pp. 167–173.

Nagpal, P., and Baker, I. 1992. Dislocation Arrangements in Polycrystalline NiAl After Room Temperature Deformation. J. Mater. Lett., vol. 11, pp. 1209–1210.

Nagpal, P., Baker, I., Liu, F., and Munroe, P.R. 1991. Room Temperature Strength and Fracture of FeAl and NiAl. High Temperature Ordered Intermetallic Alloys IV, L. Johnson et al., eds., (MRS Symposia Proceedings, Vol. 213), MRS, Pittsburgh, PA, pp. 533–538.

Nardone, V.C. 1992. Fracture Behavior of Stainless Steel-Toughened NiAl Composite Plate. Metall. Trans. A., vol. 23A, pp. 563–572.

Nathal, M.V. 1992. Creep Deformation of B2 Aluminides. Ordered Metallics—Physical Metallurgy and Mechanical Behavior, C.T. Liu et al., eds., Kluwer Academic Publishers, Dordrecht, Netherlands, pp. 541–563.

Nathal, M.V., Diaz, J.O., and Miner, R.V. 1989. High Temperature Creep Behavior of Single Crystal Gamma Prime and Gamma Prime Alloys. High Temperature Ordered Intermetallic Alloys III, C.T. Liu et al., eds., (MRS Symposia Proceedings, Vol. 133), MRS, Pittsburgh, PA, pp. 269–274.

Nathal, M.V., and Ebert, L.J. 1985. Elevated Temperature Creep-Rupture Behavior of the Single Crystal Nickel-Base Superalloy NASAIR 100. Metall. Trans. A., vol. 16A, pp. 427–439.

Nesbitt, J.A., and Lowell, C.E. 1993, High Temperature Oxidation of Intermetallics. High Temperature Ordered Intermetallic Alloys V, I. Baker et al., eds., (MRS Symposia Proceedings, Vol. 288), MRS, Pittsburgh, PA, pp. 107–118.

Nesbitt, J.A., and Vinarcik, E.J. 1991. Predicting the Oxidative Lifetime of ß NiAl-Zr Alloys. Damage and Oxidation Protection in High Temperature Composites, G.K. Haritos and O.O. Ochoa, eds., The American Society of Mechanical Engineers, New York, pp. 9–22.

Nicolas-Chaubet, D., Huntz, A.M., and Millot, F. 1991. Electrochemical Method for the Investigation of Transport Properties of Alumina Scales Formed by Oxidation. Part II: Scale Formed on a ß-NiAl Alloy. J. Mater. Sci., vol. 26, pp. 6119–6126.

Noebe, R.D. 1994. The Effect of Various Metallurgical Parameters on the Flow and Fracture Behavior of Polycrystalline NiAl Near the Brittle-to-Ductile Transition. Ph.D. Thesis, The University of Michigan, Ann Arbor, MI. (Also NASA TM–016534, 1994.)

Noebe, R.D., and Behbehani, M.K. 1992. The Effect of Microalloying Additions on the Tensile Properties of Polycrystalline NiAl. Scr. Metall. Mater., vol. 27, pp. 1795–1800.

Noebe, R.D., Bowman, R.R, Cullers, C.L., and Raj, S.V. 1990. Flow and Fracture Behavior of Binary NiAl With Prospects for Future Alloy Development. HITEMP Review—1990: Advanced High Temperature Engine Materials Technology Program, NASA CP–10051, pp. 20–1 to 20–19.

Noebe, R.D., Bowman, R.R, Cullers, C.L., and Raj, S.V. 1991. Flow and Fracture Behavior of NiAl in Relation to the Brittle-to-Ductile Transition Temperature. High Temperature Ordered Intermetallic Alloys IV, L. Johnson et al., eds., (MRS Symposia Proceedings, Vol. 213), MRS, Pittsburgh, PA, pp. 589–596.

Noebe, R.D., Bowman, R.R., and Eldridge, J.I. 1991. Initial Evaluation of Continuous Fiber Reinforced NiAl Composites. Intermetallic Matrix Composites, D.L. Anton et al., eds., (MRS Symposia Proceedings, Vol. 194), MRS, Pittsburgh, PA, pp. 323–331.

Noebe, R.D., Bowman, R.R., Locci, I.E., and Raj, S.V. 1989. Effect of Zr Additions on the Microstructure and Mechanical Behavior of NiAl. HITEMP Review—1989: Advanced High Temperature Engine Materials Technology Program. NASA CP–10039, pp. 48–1 to 48–15.

Noebe, R.D., Bowman, R.R., and Nathal, M.V. 1993. Review of the Physical and Mechanical Properties of the B2 Compound NiAl. Inter. Mater. Rev., vol. 38, pp. 193–232. (Also, NASA TM–105598, April 1992.)

Noebe, R.D., Cullers, C.L., and Bowman, R.R. 1992. The Effect of Strain Rate and Temperature on the Tensile Properties of NiAl. J. Mater. Res., vol. 7, pp. 605–612.

Noebe, R.D., and Garg, A. 1994. Characterization of Nitrogen-Doped NiAl. Metall. Mater, vol. 30, pp. 815–820.

Noebe, R.D., and Gibala, R. 1986. Surface Oxide Softening of Single Crystal NiAl. Scr. Metall., vol. 20, pp. 1635–1639.

Noebe, R.D., and Lerch, B.A. 1992. Room Temperature Cyclic Deformation Behavior of Cast and Extruded NiAl. Scr. Metall. Mater., vol. 27, pp. 1161–1166.

Noebe, R.D., and Lerch, B.A. 1993. Low Cycle Fatigue Behavior of Polycrystalline NiAl at 1000 K. High Temperature Ordered Intermetallic Alloys V, I. Baker et al., eds., (MRS Symposia Proceedings, Vol. 288), MRS, Pittsburgh, PA, pp. 743–748.

Noebe, R.D., and Locci, I.E. 1990. Metal Matrix Composites, Rapid Solidification. International Encyclopedia of Composites, Vol. 3, S.M. Lee, ed., VCH Publishers, Inc., New York, pp. 294–313.

Noebe, R.D., Misra, A., and Gibala, R. 1991. Plastic Flow and Fracture of B2 NiAl-Based Intermetallic Alloys Containing a Ductile Second Phase. Iron Steel Inst. Japan. Int., vol. 31, pp. 1172–1185.

Nourbakhsh, S., Sahin, O., Rhee, W.H., and Margolin, H. 1991, Pressure Casting of a Zirconia-Toughened Alumina Fiber-Reinforced NiAl Composite. Metall. Trans. A., vol. 22A, pp. 3059–3064.

Panda, P.C., Lagraff, J., and Raj, R. 1988. Shear Deformation and Compaction of Nickel Aluminide Powders at Elevated Temperatures. Acta Metall., vol. 36, pp. 1929–1939.

Parker, D.J., Johnstone, W.H., and Oligee, R.M. 1991. Determining Carbon, Sulfur, Oxygen, and Nitrogen in NiAl—Assessment of Techniques Through Interlaboratory Chemical Analysis Round Robin. General Electric Technical Memorandum, TM–91–451, Evendale, OH.

Pascoe, R.T., and Newey, C.W.A. 1968a. Deformation Modes of the Intermediate Phase NiAl. Phys. Status Solidi., vol. 29, pp. 357–366.

Pascoe, R.T., and Newey, C.W.A. 1968b. The Mechanical Behavior of the Intermediate Phase NiAl. Metal. Sci. J., vol. 2, pp. 138–143.

Pathare, V.M. 1988. Processing, Physical Metallurgy and Creep of NiAl+Ta and NiAl+Nb Alloys. Ph.D. Thesis, Case Western Reserve University, Cleveland, OH. (Also, NASA CR–182113, 1988.)

Patrick, D.K., Chang, K.-M., Miracle, D.B., and Lipsitt, H.A. 1991. Burgers Vector Transition in Fe-Al-Ni Alloys. High Temperature Ordered Intermetallic Alloys IV, L. Johnson et al., eds., (MRS Symposia Proceedings, Vol. 213), MRS, Pittsburgh, PA, pp. 267–272.

Pettit, F.S., and Giggins, G.S. 1987. Hot Corrosion. Superalloys II, C.T. Sims, N.S. Stoloff, and W.C. Hagel, eds., John Wiley & Sons, Inc., New York, pp. 327–358.

Pickens, J.W., Noebe, R.D., Watson, G.K., Brindley, P.K., and Draper, S.L. 1989. Fabrication of Intermetallic Matrix Composites by the Powder Cloth Process. NASA TM–102060.

Polvani, R.S., Tzeng, W.S., and Strutt, P.R. 1976. High Temperature Creep in a Semi-Coherent NiAl-Ni_2AlTi Alloy. Metall. Trans. A., vol. 7A, pp. 33–40.

Prescott, R., Mitchell, D.F., Sproule, G.I., and Graham, M.J. 1992. Transport in α-Al_2O_3 Scales on Fe-Al and Ni-Al Alloys at 1100 °C. Solid State Ionics, vol. 53, pp. 229–237.

Raj, S.V., and Farmer, S.C. 1993. Observation of a New Creep Regime in Polycrystalline Ni-50(at.%)Al Intermetallic Alloy. High Temperature Ordered Intermetallic Alloys V, I. Baker et al., eds., (MRS Symposia Proceedings, Vol. 288), MRS, Pittsburgh, PA, pp. 647–652.

Raj, S.V., Locci, I.E., and Noebe, R.D. 1992. Deformation Behavior of a Ni-30Al-20Fe-0.05Zr Intermetallic Alloy in the Temperature Range 300 to 1300 K. Metall. Trans. A, vol. 23A, pp. 1705–1718.

Reddy, K.P.R., Smialek, J.L., and Cooper, A.R. 1982. ^{18}O Tracer Studies of Al_2O_3 Scale Formation on NiCrAl Alloys. Oxid. Met., vol. 17, pp. 429–449.

Reuss, S., and Vehoff, H. 1990a. Temperature Dependence of the Fracture Toughness of Single Phase and Two Phase Intermetallics. Scr. Metall. Mater., vol. 24, pp. 1021–1026.

Reuss, S., and Vehoff, H. (as reported by G. Sauthoff) 1990b. Mechanical Properties of Intermetallics at High Temperatures. High Temperature Aluminides and Intermetallics, S.H. Whang et al., eds., The Minerals, Metals and Materials Society, Warrendale, PA, p. 344.

Reviere, R.D., Oliver, B.F., and Bruns, D.D. 1989. Computer Controlled Containerless Processing of High Temperature Intermetallic Compounds. Mater. Manuf. Proc., vol. 4, no. 1, pp. 103–131.

Rhys-Jones, T.N. 1989. Coatings for Blade and Vane Applications in Gas Turbines. Corr. Sci., vol. 29, pp. 623–646.

Rigney, J.D., and Lewandowski, J.J. 1992a. Fracture Toughness of Monolithic Nickel Aluminide Intermetallics. Mater. Sci. Eng., vol. A149, pp. 143–151.

Rigney, J.D., and Lewandowski, J.J. 1992b. Effects of Reinforcement Size and Distribution on Fracture Toughness of Composite Nickel Aluminide Intermetallics. Mater. Sci. Eng., vol. A158, pp. 31–45.

Roberts, P.R., and Ferguson, B.L. 1991. Extrusion of Metal Powders. Int. Mater. Rev., vol. 36, pp. 62–79.

Rozner, A.G., and Wasilewski, R.J. 1966. Tensile Properties of NiAl and NiTi. J. Inst. Met., vol. 94, pp. 169–175.

Rudy, M., and Sauthoff, G. 1985. Creep Behavior of the Ordered Intermetallic (Fe,Ni)Al Phase. High Temperature Ordered Intermetallic Alloys, C.C. Koch et al., eds., (MRS Symposia Proceedings, Vol. 39), MRS, Pittsburgh, PA, pp. 327–333.

Rusovic, N., and Warlimont, H. 1977. The Elastic Behavior of $ß_2$-NiAl. Phys. Stat. Solidi., (A), vol. 44, pp. 609–619.

Rusovic, N., and Warlimont, H. 1979. Young's Modulus of $ß_2$-NiAl Alloys. Phys. Stat. Solidi., (A), vol. 53, pp. 283–288.

Russell, S.M., Law, C.C., Blackburn, M.J., Clapp, P.C., and Pease, D.M. 1989. Lightweight Disk Alloy Development. Report PWA–FR–19577–8, Pratt & Whitney, West Palm Beach, FL.

Russell, S.M., Law, C.C., Blackburn, M.J., Clapp, P.C., and Pease, D.M. 1991. Lightweight Disk Alloy Development. Report PWA–FR–21413, Pratt & Whitney, West Palm Beach, FL.

Rybicki, G.C., and Smialek, J.L. 1989. Effect of the θ-α-Al_2O_3 Transformation on the Oxidation Behavior of ß-NiAl+Zr. Oxid. Met., vol. 31, pp. 275–304.

Sands, T. 1988. Stability and Epitaxy of NiAl and Related Intermetallic Films on III-V Compound Semiconductors. Appl. Phys. Lett., vol. 52, pp. 197–199.

Schneibel, J.H., Jenkins, M.G., and Maziasz, P.J. 1993. Crack Propagation in NiAl and FeAl. High Temperature Ordered Intermetallic Alloys V, I. Baker et al., eds., (MRS Symposia Proceedings, Vol. 288), MRS, Pittsburgh, PA, pp. 549–554.

Schulson, E.M. 1981. Comments on the Brittle to Ductile Transition of Long-Range Ordered Alloys. Res. Mech. Lett., vol. 1, pp. 111–114.

Schulson, E.M. 1982. The Strength and Ductility of Polycrystalline NiAl in Tension. COSAM (Conservation of Strategic Aerospace Materials) Program Overview, J.R. Stephens, ed., NASA TM–83006, pp. 175–182.

Schulson, E.M. 1985. The Effects of Grain Size on the Flow and Fracture of Long-Range Ordered Alloys. High Temperature Ordered Intermetallic Alloys, C.C. Koch et al., eds., (MRS Symposia Proceedings, Vol. 39), MRS, Pittsburgh, PA, pp. 193–204.

Schulson, E.M., and Barker, D.R. 1983. A Brittle to Ductile Transition in NiAl of a Critical Grain Size. Scr. Metall., vol. 17, pp. 519–522.

Singleton, M.F., Murray, J.L., and Nash, P. 1986. NiAl. Binary Alloy Phase Diagrams, T.B. Massalski, ed., American Society for Metals, Metals Park, OH, pp. 140–143.

Smeggil, J.G. 1991. The Effect of Chromium on the High Temperature Oxidation Resistance of Ni:Al. Surf. Coat. Technol., vol. 46, pp. 143–153.

Smialek, J.L. 1991. The Effect of Sulfur Content on Al_2O_3 Scale Adhesion. Microscopy of Oxidation, M.J. Bennett and G.W. Lorimer, eds., The Institute of Metals, London, UK, pp. 258–270.

Smialek, J.L., and Browning, R. 1985. Current Viewpoints on Oxide Adherence Mechanisms. NASA TM–87168.

Smialek, J.L., and Lowell, C.E. 1974. Effects of Diffusion on Aluminum Depletion and Degradation of NiAl Coatings, J. Electrochem. Soc., vol. 121, pp. 800–805.

Smialek, J.L., and Meier, G.H. 1987. High-Temperature Oxidation. Superalloys II, C.T. Sims, N.S. Stoloff, and W.C. Hagel, eds., John Wiley & Sons, Inc., New York, pp. 293–326.

Smith, T.R., Kallingal, C.G., Rajan, K., and Stoloff, N.S. 1992. Strain-Controlled Fatigue of NiAl Crystals at Room Temperature. Scr. Metall. Mater., vol. 27, pp. 1389–1393.

Stephens, J.T. 1988. High Temperature Metal Matrix Composites for Future Aerospace Systems. AIAA Paper 88–3059.

Stoloff, N.S., Smith, T.R., and Castagna, A. 1993. Fatigue Behavior of Intermetallic Compounds and Their Composites. High Temperature Ordered Intermetallic Alloys V, I. Baker et al., eds., (MRS Symposia Proceedings, Vol. 288), MRS, Pittsburgh, PA, pp. 59–70.

Strutt, P.R., Dodd, R.A., and Rowe, G.M. 1970. Creep in Stoichiometric Beta-NiAl. Strength of Metals and Alloys, Vol. III, ASM International, Metals Park, OH, pp. 1057–1061.

Subramanian, P.R., Mendiratta, M.G., Miracle, D.B., and Dimiduk, D.M. 1990. Microstructures and Mechanical Properties of NiAl+Mo In-Situ Eutectic Composites. Intermetallic Matrix Composites, D.L. Anton et al., eds., (MRS Symposia Proceedings, Vol. 194), MRS, Pittsburgh, PA, pp. 147–154.

Takasugi, T., Kishino, J., and Hanada, S. 1993. Anomalous Elongation Behavior of Stoichiometric NiAl Single Crystals at Intermediate Temperatures. Acta Metall. Mater., vol. 41, pp. 1009–1020.

Takasugi, T., Watanabe, S., and Hanada, S. 1992. The Temperature and Orientation Dependence of Tensile Deformation and Fracture in NiAl Single Crystals. Mater. Sci. Eng., vol. A149, pp. 183–193.

Taylor, A., and Doyle, N.J. 1972. Further Studies on the Nickel-Aluminum System. I. The ß-NiAl and δ-Ni_2Al_3 Phase Fields. J. Appl. Cryst., vol. 5, pp. 201–209.

Vandervoort, R.R., Mukherjee, A.K., and Dorn, J.E. 1966. Elevated-Temperature Deformation Mechanisms in ß′-NiAl. Trans. ASM, vol. 59, pp. 930–944.

Vedula, K., and Khadkikar, P.S. 1990. Effect of Stoichiometry on Low Temperature Mechanical Properties. High Temperature Aluminides and Intermetallics, S.H. Whang et al., eds., The Minerals, Metals and Materials Society, Warrendale, PA, pp. 197–217.

Vehoff, H. 1993. Fracture and Toughness of Intermetallics. High Temperature Ordered Intermetallic Alloys V, I. Baker et al., eds., (MRS Symposia Proceedings, Vol. 288), MRS, Pittsburgh, PA, pp. 71–82.

Veyssiere, P., and Noebe, R.D. 1992. Weak-Beam Study of <111> Superlattice Dislocations in NiAl. Philos. Mag., vol. 65, pp. 1–13.

Viswanadham, R.K., Mannan, S.K., Kumar, K.S., and Wolfenden, A. 1989. Elastic Modulus of NiAl-TiB_2 Composites in the Temperature Range 300 to 1273 K. J. Mater. Sci. Lett., vol. 8, pp. 409–410.

Vitek, V., and Chen, S.P. 1991. Modeling of Grain Boundary Structure and Properties in Intermetallic Compounds. Scr. Metall. Mater., vol. 25, pp. 1237–1242.

Wachtell, R.L. 1952. An Investigation of Various Properties of NiAl. WADC TR 52–291.

Walston, W.S., and Darolia, R. 1993. Effect of Alloying on Physical Properties of NiAl. High Temperature Ordered Intermetallic Alloys V, I. Baker et al., eds., (MRS Symposia Proceedings, Vol. 288), MRS, Pittsburgh, PA, pp. 237–242.

Walter, J.L., and Cline, H.E. 1970. The Effect of Solidification Rate on Structure and High Temperature Strength of the Eutectic NiAl-Cr. Metall. Trans., vol. 1, pp. 1221–1229.

Wang, L., and Arsenault, R.J. 1990. Microstructure of TiB_2-NiAl. Mater. Sci. Eng., vol. A127, pp. 91–98.

Wang, L., and Arsenault, R.J. 1991. Interfaces in XD Processed TiB_2/NiAl Composites. Metall. Trans. A, vol. 22A, pp. 3013–3018.

Wasilewski, R.J. 1966. Elastic Constants and Young's Modulus of NiAl. Trans. Metall. Soc. AIME, vol. 36, pp. 455–457.

Wasilewski, R.J., Butler, S.R., and Hanlon, J.E. 1967. Plastic Deformation of Single-Crystal NiAl. Trans. Metall. Soc. AIME, vol. 239, pp. 1357–1364.

Weaver, M.L., Kaufman, M.J., and Noebe, R.D. 1993. The Effects of Alloy Purity on the Mechanical Behavior of Soft Oriented NiAl Single Crystals. Scr. Metall. Mater., vol. 29, pp. 1113–1118.

Whittenberger, J.D. 1987. Effect of Composition and Grain Size on Slow Plastic Flow Properties of NiAl Between 1200 to 1400 K. J. Mater. Sci., vol. 22, pp. 394–402.

Whittenberger, J.D. 1988. The Influence of Grain Size and Composition on 1000 to 1400 K Slow Plastic Flow Properties of NiAl. J. Mater. Sci., vol. 23, pp. 235–240.

Whittenberger, J.D., Arzt, E., and Luton, M.J. 1990a. Preliminary Investigation of a NiAl Composite Prepared by Cryomilling. J. Mater. Res., vol. 5, pp. 271–277.

Whittenberger, J.D., Arzt, E., and Luton, M.J. 1990b. 1300 K Compressive Properties of a Reaction Milled NiAl-AlN Composite. J. Mater. Res., vol. 5, pp. 2819–2827.

Whittenberger, J.D., Gaydosh, D.J., and Kumar, K.S. 1990. 1300 K Compressive Properties of Several Dispersion Strengthened NiAl Materials. J. Mater. Sci., vol. 25, pp. 2771–2776.

Whittenberger, J.D., Kumar, K.S., and Mannan, S.K. 1991a. 1000 to 1300 K Slow Plastic Compression Properties of Al-Deficient NiAl. J. Mater. Sci., vol. 26, pp. 2015–2022.

Whittenberger, J.D., Kumar, K.S., and Mannan, S.K. 1991b. 1200 and 1300 K Slow Plastic Compression Properties of Ni-50Al Composites. Mater. High Temp., vol. 9, pp. 3–12.

Whittenberger, J.D., and Luton, M.J. 1992. Elevated Temperature Compressive Properties of Reaction Milled NiAl-AlN and Zr-doped NiAl-AlN Composites. J. Mater. Res., vol. 7, pp. 2724–2732.

Whittenberger, J.D., Mannan, S.K., and Kumar, K.S. 1989. 1100 to 1300 K Slow Plastic Compression Properties of Ni-38.5Al Composites. Scr. Metall., vol. 23, pp. 2055–2060.

Whittenberger, J.D., Nathal, M.V., Raj, S.V., and Pathare, V.M. 1991. Slow Strain Rate 1200–1400 K Compressive Properties of NiAl-Hf. Mater. Lett., vol. 11, pp. 267–272.

Whittenberger, J.D., Noebe, R.D., Cullers, C.L., Kumar, K.S., and Mannan, S.K. 1991. 1000 to 1200 K Time-Dependent Compressive Deformation of Single-Crystalline and Polycrystalline B2 Ni-40Al. Metal. Trans. A, vol.22A, pp. 1595–1607.

Whittenberger, J.D., Ray, R., and Jha, S.C. 1992. Influence of Grain Size on the Creep Behavior of HfC–Dispersed NiAl. Mater. Sci. Eng., vol. A151, pp. 137–146.

Whittenberger, J.D., Ray. R., Jha, S.C., and Draper, S. 1991. 1000–1300 K Slow Strain Rate Properties of NiAl Containing Dispersed TiB_2 and HfB_2. Mater. Sci. Eng., vol. A138, pp. 83–93.

Whittenberger, J.D., Reviere, R., Noebe, R.D., and Oliver, B.F. 1992. Compressive Strength of Directionally Solidified NiAl-NiAlNb Intermetallics at 1200 and 1300 K. Scr. Metall. Mater., vol. 26, pp. 987–992.

Whittenberger, J.D., Viswanadham, R.K., Mannan, S.K., and Kumar, K.S. 1989. 1200 to 1400 K Slow Strain Rate Compressive Behavior of Small Grain Size NiAl/Ni_2AlTi Alloys and NiAl/Ni_2AlTi-TiB_2 Composites. J. Mater. Res., vol. 4, pp. 1164–1171.

Whittenberger, J.D., Viswanadham, R.K., Mannan, S.K., and Sprissler, B. 1990. Elevated Temperature Slow Plastic Deformation of NiAl-TiB_2 Particulate Composites at 1200 and 1300 K. J. Mater. Sci., vol. 25, pp. 35–44.

Whittenberger, J.D., Westfall, L.J., and Nathal, M.V. 1989. Compressive Strength of a B2 Matrix NiAl-Nb Intermetallic at 1200 and 1300 K. Scr. Metall., vol. 23, pp. 2127–2130.

Wood, D.L., Grenoble, H.E., and Westbrook, J.H. 1960–1964. Effect of Basic Physical Parameters on Engineering Properties of Intermetallic Compounds. Report WADD TR–60–184, Pts. I–VII, Wright-Patterson AFB, OH.

Wood, J.H., and Goldman, E.H. 1987. Protective Coatings. Superalloys II, C.T. Sims, N.S. Stoloff, and W.C. Hagel, eds., John Wiley & Sons, New York, pp. 359–384.

Wright, R.N., Knibloe, J.R., and Noebe, R.D. 1991. Consolidation of NiAl Powders Using Hot Isostatic Pressing. Mater. Sci. Eng., vol. A141, pp. 79–83.

Wunderlich, W., Machon, L., and Sauthoff, G. 1992. Dislocation Analysis at Crack Tips at Phase Boundaries in an Intermetallic NiAl-NbNiAl Alloy. Z. Metallkd., vol. 83, pp. 679–684.

Yaney, D.L., and Nix, W.D. 1988. Mechanisms at Elevated-Temperature Deformation in the B2 Aluminides NiAl and CoAl. J. Mater. Sci., vol. 23, pp. 3088–3098.

Yang, W.J., and Dodd, R.A. 1973), Steady-State Creep and Associated Microstructures in Stoichiometric and Non-Stoichiometric Polycrystalline NiAl. Metall. Sci. J., vol. 7, pp. 41–47.

Young, E.W.A., and DeWit, J.H.W. 1986. The Use of ^{18}O Tracer and Rutherford Backscattering Spectrometry to Study the Oxidation Mechanism of NiAl. Solid State Ionics, vol. 16, pp. 39–46.

Zeller, M.V., Noebe, R.D., and Locci, I.E. 1990. Grain Boundary Segregation Studies of NiAl and NiAl(Zr) Using Auger Electron Spectroscopy. HITEMP Review—1990: Advanced High Temperature Engine Materials Technology Program, NASA CP–10051, pp. 21–1 to 21–17.

REPORT DOCUMENTATION PAGE

Form Approved
OMB No. 0704-0188

1. AGENCY USE ONLY (*Leave blank*)	2. REPORT DATE	3. REPORT TYPE AND DATES COVERED
	April 1994	Technical Paper

4. TITLE AND SUBTITLE

Physical and Mechanical Metallurgy of NiAl

5. FUNDING NUMBERS

WU–510–01–50

6. AUTHOR(S)

Ronald D. Noebe, Randy R. Bowman, and Michael V. Nathal

7. PERFORMING ORGANIZATION NAME(S) AND ADDRESS(ES)

National Aeronautics and Space Administration
Lewis Research Center
Cleveland, Ohio 44135–3191

8. PERFORMING ORGANIZATION REPORT NUMBER

E–7713

9. SPONSORING/MONITORING AGENCY NAME(S) AND ADDRESS(ES)

National Aeronautics and Space Administration
Washington, D.C. 20546–0001

10. SPONSORING/MONITORING AGENCY REPORT NUMBER

NASA TP–3398

11. SUPPLEMENTARY NOTES

Ronald D. Noebe, Randy R. Bowman, and Michael V. Nathal, NASA Lewis Research Center. Chapter from Physical Metallurgy and Processing of Intermetallic Compounds edited by N.S. Stoloff and V.K. Sikka to be published by Van Nostrand Reinhold, New York, NY. Responsible person, Ronald D. Noebe, organization code 5180, (216) 433–2093.

12a. DISTRIBUTION/AVAILABILITY STATEMENT

Unclassified - Unlimited
Subject Category 26

12b. DISTRIBUTION CODE

13. ABSTRACT ***(Maximum 200 words)***

Considerable research has been performed on NiAl over the last decade, with an exponential increase in effort occurring over the last few years. This is due to interest in this material for electronic, catalytic, coating, and especially high-temperature structural applications. This report uses this wealth of new information to develop a complete description of the properties and processing of NiAl and NiAl-based materials. Emphasis is placed on the controlling fracture and deformation mechanisms of single and polycrystalline NiAl and its alloys over the entire range of temperatures for which data are available. Creep, fatigue, and environmental resistance of this material are discussed. In addition, issues surrounding alloy design, development of NiAl-based composites, and materials processing are addressed.

14. SUBJECT TERMS	15. NUMBER OF PAGES
Review; NiAl; Physical properties; Mechanical properties; Fatigue; Creep; Oxidation; Composites	44
	16. PRICE CODE: A03

17. SECURITY CLASSIFICATION OF REPORT	18. SECURITY CLASSIFICATION OF THIS PAGE	19. SECURITY CLASSIFICATION OF ABSTRACT	20. LIMITATION OF ABSTRACT
Unclassified	Unclassified	Unclassified	